The Generation and Characterization of the *Nrl*$^{-/-}$;*Ccdc136*$^{+/-}$ Mouse Line to Investigate Cone Photoreceptor Transplantation in Adult Mouse Retinas

Sheila Smiley

A thesis submitted to the
Faculty of Graduate and Postdoctoral Studies
in partial fulfillment of the requirements for the
M.Sc. program in Cellular and Molecular Medicine

Department of Cellular and Molecular Medicine
Faculty of Medicine
University of Ottawa
The Ottawa Hospital Research Institute
Ottawa, Ontario

ABSTRACT

Human vision is heavily dependent on cone photoreceptor function and irreversible loss of these cells, caused by retinal degenerative diseases, results in deterioration of central, high acuity vision. Here, I characterized coiled-coil domain containing 136 (Ccdc136) as a cone marker. *Ccdc136*$^{-/-}$ mice were generated and examined using immunohistochemical and electrophysiological analyses. To investigate cone transplantation, the mice were crossed onto a cone-only neural retina leucine zipper knockout (*Nrl*$^{-/-}$) background generating *Nrl*$^{-/-}$*;Ccdc136*$^{+/-}$ donor mice. *Ccdc136*$^{-/-}$ mice expressed GFP in cone but not rod photoreceptors. *Nrl*$^{-/-}$*;Ccdc136*$^{+/-}$ donor mice had an enriched population of GFP+ cones and showed enhanced cone function, identical to *Nrl*$^{-/-}$ mice. After transplantation, *Nrl*$^{-/-}$*;Ccdc136*$^{+/-}$ cells migrated successfully into adult recipient retinas. Morphology of integrated cells improved with younger donor age with some integrated cells expressing cone markers. In conclusion, the *Nrl*$^{-/-}$*;Ccdc136*$^{+/-}$ mouse is an appropriate strain to investigate cone photoreceptor transplantation. Future studies aim to improve integration rates to assess vision rescue in degenerated retinas.

ACKNOWLEDGEMENTS

I would like to extend my sincere gratitude to my supervisor, Dr. Valerie A. Wallace, for giving me the opportunity to be a part of this project, for her guidance and support, and for her insightful teachings. It has been a truly enriching experience. I would also like Dr. William Staines and Dr. William Stanford for taking time from their busy schedules to serve on my committee and for their valuable feedback and suggestions. Additionally, I would like to thank our collaborators, Dr. Catherine Tsilfidis and Adam Baker for helping me develop my surgical technique for subretinal injections. As well, I would like to thank Dr. Yves Sauvé at the University of Alberta for his help in running electroretinograms. In particular, I thank all my colleagues from the Wallace lab for their support, advice and enlightening discussions. I would especially like to thank Chantal Mazerrolle, Sherry Thurig, and Dr. Alan Mears, whose expertise, technical assistance, and patience was greatly appreciated. Finally, I would like to thank my parents, Sam and Marie Smiley, and my sisters, Sally Monsour and Sandy Smiley (and Eli Monsour who is like a sister to me), for their continuous love, support, and encouragement which has enabled me to persevere through this endeavour.

TABLE OF CONTENTS

LIST OF TABLES

LIST OF FIGURES

ABBREVIATIONS

AAV	Adeno-associated virus
AMD	Age-related macular degeneration
ATP	Adenosine triphosphate
bp	Base pair
BrdU	Bromodeoxyuridine
BSA	Bovine serum albumin
Ccdc136	Coiled-coil domain containing 136
cGMP	Cyclic guanine monophosphate
ChR2	Channelrhodopsin-2
CNG	Cyclic nucleotide-gated cation channel
DNA	Deoxyribonucleic acid
DIG	Digoxigenin
CAr	Cone arrestin
Crx	Cone-rod homeobox
E	Embryonic day
EBSS	Earle's balanced salt solution
EDTA	Ethylenediaminetetraacetic acid
EGFP	Enhanced green fluorescent protein
ERG	Electroretinograph
ES cells	Embryonic stem cells
EtOH	Ethanol
FACS	Fluorescence-activated cell sorting
FBS	Fetal bovine serum
GCL	Ganglion cell layer
GFP	Green fluorescent protein
GMP	Guanine monophosphate
IHC	Immunohistochemisty
INL	Inner nuclear layer
IPL	Inner plexiform layer
IS	Inner segments
KO	Knock-out
LCA	Leber's congenital amaurosis
LGN	Lateral geniculate nucleus
L opsin	Longwave opsin
M opsin	Medium wave opsin
MABT	Maleic acid buffer containing Tween-20
mRNA	Messenger ribonucleic acid
mTOR	Mammalian target of rapamycin
NAG6	Nasopharyngeal carcinoma-associated gene 6
NFL	Nerve fibre layer
Nr2e3	Nuclear receptor subfamily 2, group E, Member 3
Nrl	Neural retina leucine zipper
OCT	Optimal cutting temperature
ONL	Outer nuclear layer

OPL	Outer plexiform layer
OS	Outer segments
Otx	Orthodenticle homeobox
P	Postnatal day
PBS	Phosphate buffered saline
PCR	Polymerase chain reaction
PDE6	Phosophodiesterase 6
PFA	Paraformaldehyde
PKC	Protein kinase C
PNA	Peanut agglutinin
RdCVF	Rod-derived cone viability factor
Rho	Rhodopsin
RNA	Ribonucleic acid
RORβ	Retinoid-related orphan nuclear receptor
RP	Retinitis pigmentosa
RPC	Retinal progenitor cell
RPE	Retinal pigmented epithelium
SEM	Standard error of the mean
S opsin	Shortwave opsin
TRβ2	Thyroid hormone receptor β2
Tris	Tris(hydroxymethyl)aminomethane
VEGF-A	Vascular endothelial growth factor A

Chapter 1. Introduction

1.1 The retina

The retina is the light-sensitive neural tissue that lies along the posterior region inside the eye (Figure 1.1 A). Light enters through the cornea and lens and makes its way to the back of the eye where it strikes the outer segments of the photoreceptors in the retina. Millions of these cells are responsible for converting light into nerve impulses that are sent down the optic nerve to the visual cortex in the brain, where the information is processed into vision.

1.1.1 Structure of the retina

The neural retina is a laminar structure comprised of six different neuronal cell types and one type of glial cell (Figure 1.1 B). The cells are organized into three cellular layers: the outer nuclear layer (ONL), the inner nuclear layer (INL), and the ganglion cell layer (GCL). From the apical side, abutting the retinal pigment epithelium (RPE), is the ONL, which is comprised of the cell bodies of rod and cone photoreceptors. Their outer segments (OS) extend into the subretinal space where they are enveloped by the processes of the RPE. The INL is located basal to the ONL, and is made up of bipolar cells, horizontal cells and amacrine cells. The cell bodies of Müller glia, a type of radial glial cell, are also located in the INL and their processes span the retina. On the basal side, adjacent to the vitreous humour that fills the eye cavity, is the ganglion cell layer (GCL). This layer is comprised of ganglion cells and displaced amacrine cells (Wallace, 2011). The axons of ganglion cells form the nerve fibre layer (NFL), which runs along the inner face of the retina, and exits the eye as a thick bundle called the optic nerve. The axons extend into the brain, terminating in the lateral geniculate nucleus (LGN) in the

thalamus (Marieb & Hoehn, 2007). Neurons in the LGN then relay the received signal to the primary visual cortex for processing into vision.

The nuclear layers of the retina are separated by plexiform layers, which contain neuronal synapses. The outer plexiform layer (OPL) is located between the ONL and INL. The axons of rods and cones extend into the OPL where they form synapses called rod spherules and cone pedicles, respectively, with the dendrites of bipolar cells or horizontal cells. The inner plexiform layer (IPL) is located between the INL and GCL and contains the synapses between bipolar cell axons and ganglion cell dendrites and amacrine cell processes.

Located at the apical surface of the neural retina is the RPE, a single layer of cuboidal, pigmented epithelial cells. These cells form a part of the blood/retina barrier, acting as a barrier from the fenestrated capillaries in the underlying choroid (Bok, 1993). One of the main functions of these pigmented cells is to absorb light striking the back of the eye to reduce light scattering (Strauss, 2011). However, the RPE plays many other roles in maintaining retinal cells. It provides structural support by enveloping the outer segments of photoreceptors through their apical microvilli. It also plays a role in phagocytosis of photoreceptor outer segments, to renew the cells after constant photo-oxidative damage. As an epithelial barrier, it controls ion homeostasis, and transports nutrients, water and metabolites between the retina and the blood. Finally, it plays an important role in the visual cycle by re-isomerising all-*trans* retinal to 11-*cis* retinal to be delivered to photoreceptors and used in initiation of the visual transduction cascade (Strauss, 2005).

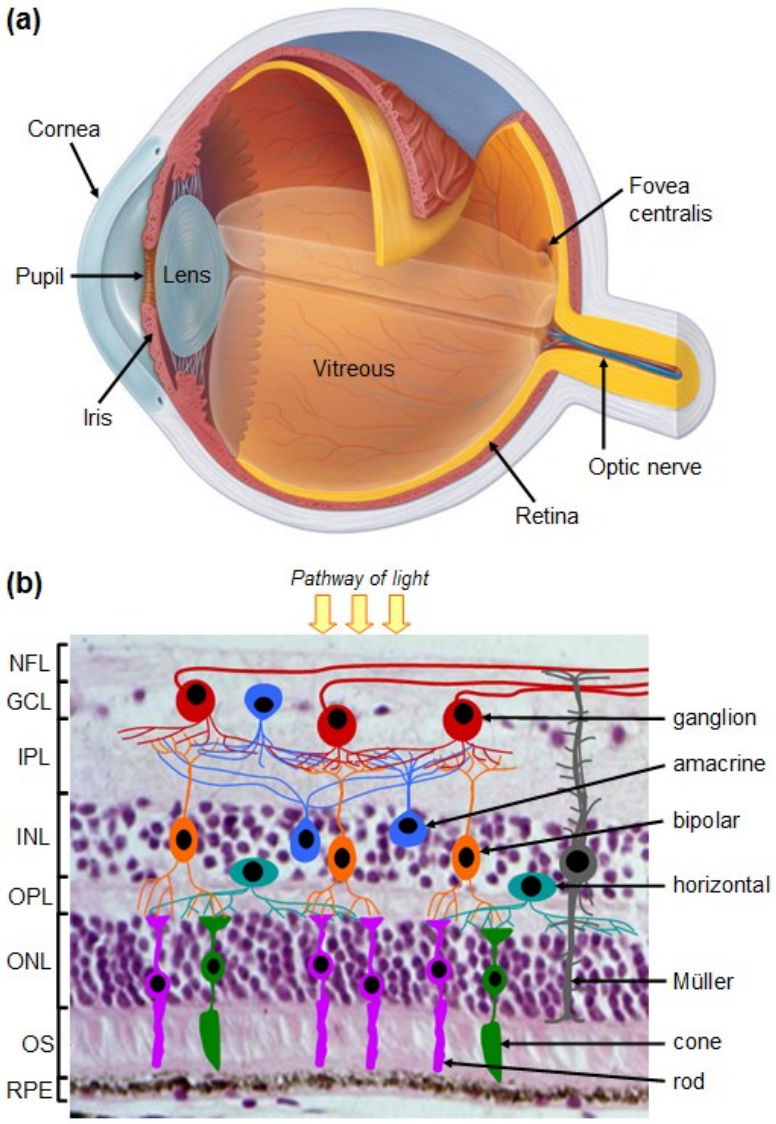

Figure 1.1 Basic anatomy of the vertebrate eye and retina. (A) Schematic of the eye indicating its major structures. (B) Photomicrograph of the retina with schematic showing the relative positions of photoreceptors, bipolar cells, horizontal cells, amacrine cells, ganglion cells, and Müller glia. The cell bodies of the neurons and glia are organized into three layers: the ganglion cell layer (GCL), the inner nuclear layer (INL), the outer nuclear layer (ONL) with the inner and outer plexiform layers located between. The retinal pigment epithelium is located apical to the neural retina. Abbreviations: IPL, inner plexiform layer; NFL, neural fibre layer; OPL, outer plexiform layer; OS, outer segments; RPE, retinal pigment epithelium. Reproduced from Bassett & Wallace (2012) with the permission of Copyright Clearance Center on behalf of Elsevier.

1.1.2 Photoreceptors

Photoreceptors are the specialized light-sensitive neurons of the retina that mediate phototransduction. There are two types of photoreceptors in the ONL, rods and cones. The retina also contains melanopsin-positive photosensitive ganglion cells, located in the INL, which are involved in pupillary reflexes in bright light and maintaining circadian rhythm (Foster et al., 1991). However, these cells are very rare will not be considered further here.

1.1.2.1 Photoreceptor structure

Rods and cones have separate roles in vision and have different distributions within the retina. However, both have the same general structure (Figure 1.2). Two processes extend from the cell bodies, a basal axon or inner fibre and an apical outer process. The outer process consists of a proximal inner segment (IS) and a distal peripheral outer segment (OS) joined together by a cilium (Figure 1.2). The IS contain many mitochondria to provide ATP for the cell's sodium-potassium pumps.

The OS are the photoreceptive regions of the cell and contain the protein components that mediate phototransduction (see Section 1.1.2.2). The OS membrane is folded into discs to maximize surface area for trapping light (Marieb & Hoehn, 2007). These discs are generated at the proximal part of the OS, where the membrane at the cilium evaginates and invaginates (Steinberg et al., 1980). As these new discs are generated, they displace existing discs apically towards the RPE. Then older discs at the distal end of the OS are pinched off and phagocytosed by the RPE cells (Young, 1971, 1976). The continual shedding of discs and phagocytosis allows for renewal of these

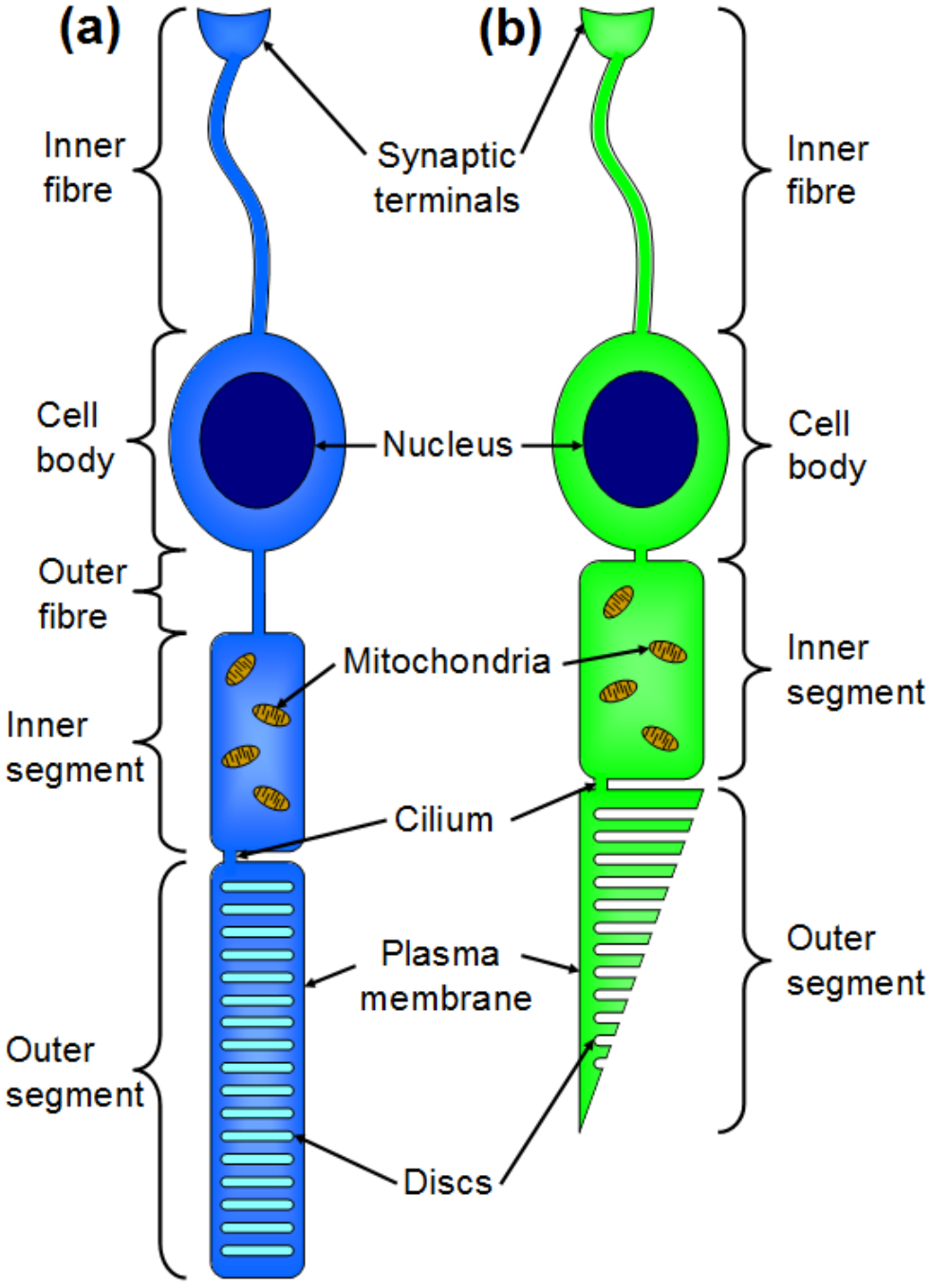

Figure 1.2 Basic structure of (a) rod and (b) cone photoreceptors.

sensitive portions of the photoreceptor after constant exposure to photo-oxidative damage.

The OS in cone photoreceptors are short and conical-shaped, giving rise to their name, with the IS joining directly to the cell body. Cone cell bodies are situated in a row closest to the apical edge of the ONL (Kolb, 2011). Meanwhile, rod photoreceptors have long rod-shaped OS. The IS of rods connect the cell bodies by an outer fibre. These cells make up the remainder of the ONL. Another difference between cones and rods is that the discs in rods are discontinuous, sitting separately in a stack. Conversely, the discs in cones are continuous with the plasma membrane, meaning they are directly exposed to the extra-cellular space.

1.1.2.2 Phototransduction

Photoreceptors are able to sense and react to light via visual pigments, opsins, embedded in the membrane of their OS. There are four types of opsins: rhodopsin (present only in rods) and cone-restricted longwave (L), medium wave (M) and shortwave (S) opsins. All opsins bind a molecule of retinal, a vitamin A derivative that is synthesized in the RPE. Retinal exists as two isomers. The 11-*cis* form of the molecule, which has a bent shape, is incorporated into the visual pigments. Phototransduction is initiated when photons of light are absorbed by opsins triggering a rapid series of steps where opsin-conjugated 11-cis retinal undergoes a conformational switch to the all-*trans* isomer and is released from opsin (Figure 1.3). The breakdown of the visual pigment is referred to as bleaching. In rods, one of the intermediate forms generated during bleaching is the activated state of rhodopsin, metarhodopsin II (Rho*). Activation of

opsin triggers a cascade of events that are summarized in Figure 1.4, highlighting the sequence of events that takes place in rods.

Metarhopsin II is responsible for activating hundreds of molecules of the heterotrimeric G-protein, transducin ($T_{\alpha\beta\gamma}$). Activation promotes the exchange of GDP bound to the α subunit, T_{α}, to be exchanged for GTP, allowing the α subunit (T_{α}*) to dissociate from $T_{\beta\gamma}$. T_{α}* binds and activates phosphodiesterase 6 (PDE6). PDE6 is responsible for hydrolyzing cyclic GMP (cGMP) to GMP, thereby reducing cGMP concentration inside the OS. In the dark, cGMP levels are high (because PDE6 is inactive), allowing cGMP to bind to Na^{+}/Ca^{2+} ion (CNG) channels and maintain their open conformation. Thus, in the dark, cations freely enter the photoreceptor in a "dark current" that depolarizes the cell. The transmembrane potential, or dark potential, is about -40mV (Marieb & Hoehn, 2007). During this state, voltage-gated calcium channels at the synaptic terminals are kept open and there is release of the neurotransmitter glutamate to receptive bipolar cells. Light-induced PDE6 activation (PDE6*) and cGMP break down results in CNG channels closing and reduction of cation influx. The photoreceptors develop a hyperpolarizing receptor potential of about -70mV and calcium channels at the synapse close inhibiting neurotransmitter release.

The "switching off" or inhibition of neurotransmitter release during light conditions makes photoreceptors unique. Typically, neurons release neurotransmitters in response to a stimulus. Conversely, light stimulus inhibits release of glutamate in photoreceptors. This "switch off" activates the next cells in the visual pathway, bipolar cells. Without glutamate, bipolar cells depolarize and release their own neurotransmitter

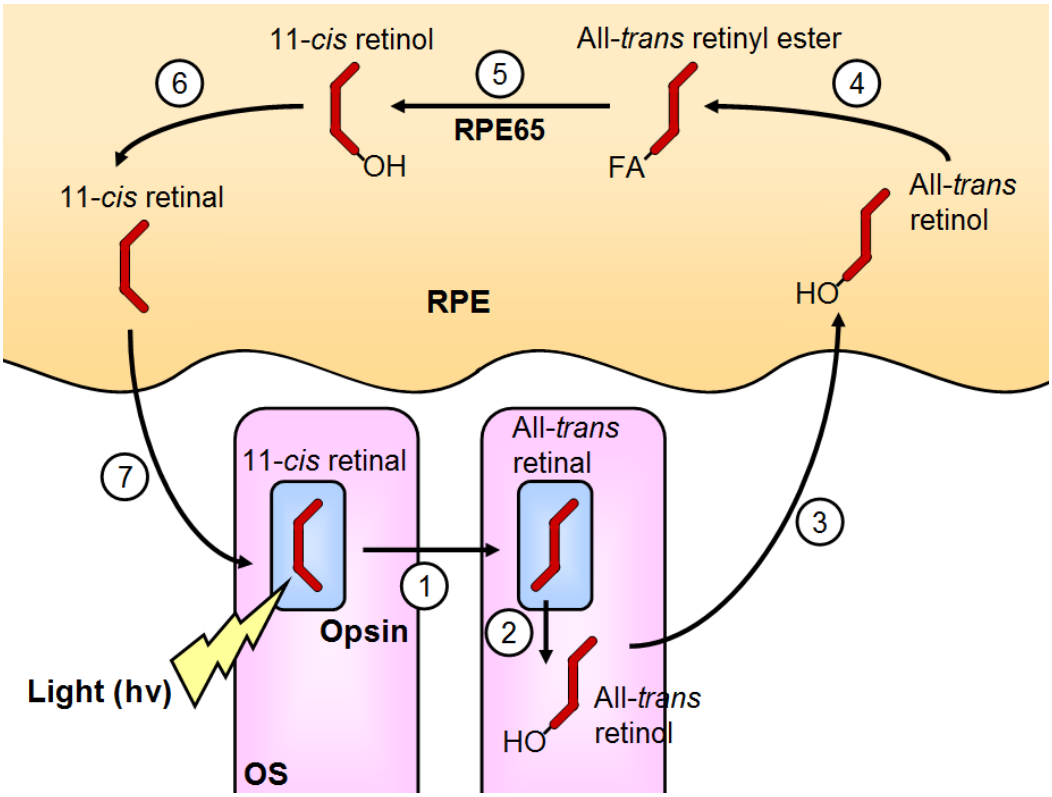

Figure 1.3 Schematic representation of the visual cycle. (1) Vision begins when light (hv) causes photoisomerization of 11-*cis* retinal to all-*trans* retinal, activating the opsin to which it is conjugated. (2) All-*trans* retinal is released from the opsin and reduced to all-*trans* retinol. (3) The all-*trans* retinol is exported from the rod outer segment to the RPE. (4) Here, all-*trans* retinol is metabolized to produce all-*trans* retinyl esters. (5) RPE65 is the key enzyme that catalyzes the conversion of all-*trans* retinyl ester to 11-*cis* retinol. (6) 11-*cis* retinol is enzymatically reduced to 11-*cis* retinal, (7) which is then transported back to the photoreceptor OS where it recombines with opsin. Abbreviations: OS, outer segments; RPE, retinal pigment epithelium (Wright et al., 2010)

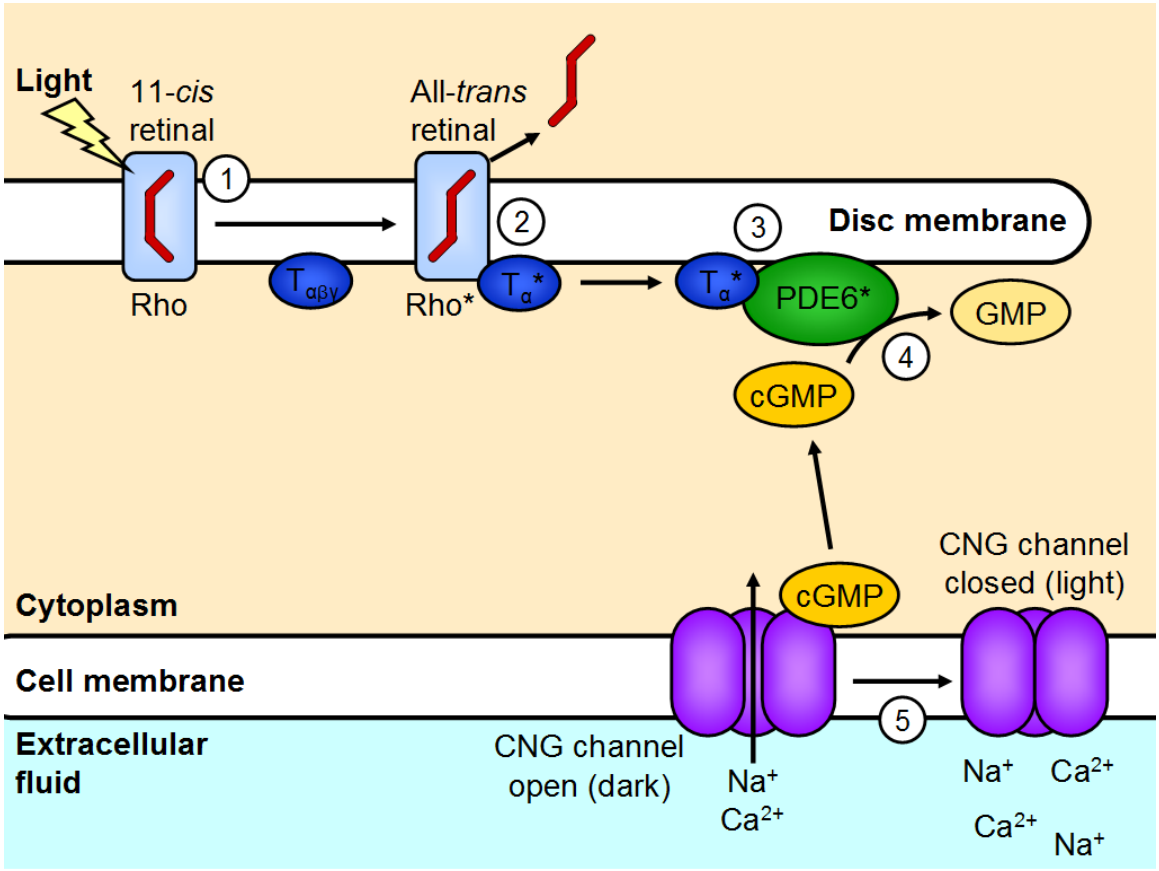

Figure 1.4 Schematic of the phototransduction cascade in rods. (1) Light strikes the visual pigment, rhodopsin (Rho), causing a conformational change of 11-*cis* retinal to all-*trans* retinal activating rhodopsin (Rho*). All-*trans* retinal is released and transported to the RPE for conversion back to 11-*cis* retinal. (2) Rho* makes repeated contacts with transducin ($T_{\alpha\beta\gamma}$) molecules. Rho* activates transducin (T_α*), causing the T_α to dissociate from $T_{\beta\gamma}$. (3) T_α* binds and activates phosphodiesterase 6 (PDE6*). (4) PDE6* hydrolyzes cGMP to GMP. (5) Levels of cytosolic cGMP fall drastically and can no longer bind and hold open CNG channels. CNG channels close preventing influx of Na^+ and Ca^{2+}. The cascade is the same in cones, except rhodopsin is replaced by cone-specific opsins (Fu & Yau, 2007).

to receptive ganglion cells. Consequently, ganglion cells generate an action potential, which relays the information to the brain.

Another key difference between rods and cones is their connectivity with other retinal cells and the way they transmit a signal through the retina. All photoreceptors synapse directly to a bipolar cell, which then relays the signal to ganglion cells. However, rod photoreceptors will converge together to form a pathway, with 15 to 30 rods connecting to a single rod bipolar cell. Furthermore, rod bipolar cells do not directly synapse with ganglion cells. They instead connect to amacrine cells in the IPL and the amacrine cells spread out rod information before converging on ganglion cells (Kolb, 2011). This results in up to one hundred rods relaying information to a single ganglion cell. Because the information must be processed collectively by the visual cortex, this means that rod vision provides low visual acuity.

On the other hand, the cone pathway is more direct. Usually one or a few cone photoreceptors will connect directly to a cone bipolar cell, then to a ganglion cell. This allows for more detailed, high-resolution vision, meaning cones are responsible for our high visual acuity (Marieb & Hoehn, 2007). Beyond the photoreceptor-bipolar-ganglion cell pathway, horizontal cells also provide lateral connections to help integrate and regulate the input of many photoreceptors cells. They synapse at the OPL with many cone cells covering a wide spatial field. A subset of horizontal cells synapses with both cones and rods. This allows for increase in spatial resolution and contrast.

1.1.2.3 Stimulation of photoreceptors

Rods and cones both respond to light in similar ways through the biochemical events that take place during phototransduction. However, the photoreceptors differ in the

wavelengths of light that initially stimulate them. Rhodopsin responds to light optimally at a wavelength around 498nm (Bowmaker & Dartnall, 1980). Consequently, their visual response is perceived in grey tones. Rods also have a low threshold for activation. They are extremely sensitive to light and will react in dim-light conditions to a single photon (Marieb & Hoehn, 2007). This allows them to mediate our night time or scotopic vision.

Humans have three types of cones: long wave (L) or red cones, medium wave (M) or green cones, and short wave (S) or blue cones. Depending on the subtype of cone, their opsins absorb light maximally at long wavelengths of red light (564nm), medium wavelengths of green light (534nm) or short wavelengths of blue light (420nm) (Bowmaker & Dartnall, 1980). Cones also have a far greater threshold for activation, requiring higher intensity light than rods to react. Therefore, cone photoreceptors are responsible for our day time colour vision or photopic vision.

1.1.2.4 Photoreceptor distribution

In the mammalian retina, rods greatly outnumber cone photoreceptors. In humans, the rod-to-cone ratio is roughly 20 to 1, with approximately 120 million rods versus only 6 million cones (Osterberg, 1935). However the distributions and densities of rods and cones throughout the retina are not constant. At the centre of the human retina, located behind the lens, is the macula (Figure 1.1 A). The macula contains the fovea centralis or fovea. Within the fovea is the foveal pit, a region consisting of approximately 20,000 cones packed in a hexagonal mosaic (Curcio et al., 1990). The foveal pit is surrounded by a belt called the parafovea and an outer perifoveal region. Cone density decreases in the parafoveal belt and is even lower in the surrounding perifovea. In the peripheral retina,

cone density is very low with rods being the most abundant photoreceptor. Cones appear to be evenly distributed surrounded by rings of rods (Kolb, 2011).

1.1.3 Retinal development

The eye originates as an outgrowth of the anterior part of the neural tube, in the posterior region of the forebrain. During embryonic development, the neuroectoderm evaginates to form two bilateral vesicles. The peripheral portion of these protrusions form a bulb called the optic vesicle. Meanwhile, the proximal portion elongates and forms the optic stalk, ultimately becoming the optic nerve (Figure 1.5A). The optic vesicle develops into a double-walled optic cup, where the outer layer becomes the RPE and the inner layer becomes the neural retina (Fuhrmann et al., 2000).

The retina begins as a single layer of proliferating retinal progenitor cells (RPCs), called the neuroepithelium. Lineage tracing studies have shown that RPCs are multipotent (Turner & Cepko, 1987; Turner et al., 1990; Wetts & Fraser, 1988); a single RPC can generate any the different retinal cell types. All of the different retinal cells develop in a chronological and overlapping sequence (Young, 1985) (Figure 1.5B). Maintaining a large enough pool of proliferating RPCs over the course of retinal development is important so that precise proportions of all the different retinal cell types are generated. In vertebrates, ganglion cells are the first post-mitotic cells to be generated. Soon afterwards, cone photoreceptors, horizontal cells, and a portion of amacrine cells begin differentiation in succession, during embryonic development. Bipolar cells, Müller glia and the remaining amacrine cells are generated postnatally. Rod photoreceptors are generated during the span of embryonic to postnatal development. Figure 1.5 provides a

summary of the key transcription factors that regulate retinal cell proliferation and differentiation.

1.1.3.1 Photoreceptor development

Photoreceptor production occurs over a wide temporal span. Proliferating RPCs exit mitosis to become committed rod or cone photoreceptor precursors. These post-mitotic precursors take weeks or months to mature into a functional photoreceptor (Swaroop et al., 2010). In humans, post-mitotic cone and rod precursors are born at about fetal week 8 to 10. Soon afterwards, expression of photoreceptor genes for phototransduction and morphogenesis takes place. For example, opsins transcripts can be detected at fetal week 15 (Hendrickson et al., 2008). However, photoreceptors remain immature at birth and maturation, such as axon and outer segment growth and synapse formation occurs postnatally.

There are several transcription factors that have well known roles in directing differentiation of precursors into rods or cones. These include the homeobox protein, OTX2, and cone-rod homeobox protein, CRX, which are both expressed early in photoreceptor precursors. These two transcription factors are essential in regulating photoreceptor lineage. *Otx2*- and *Crx*-deficient mice both show severe degeneration of photoreceptors (Furukawa et al., 1999; Koike et al., 2007; Nishida et al., 2003). Neural retina leucine zipper protein (Nrl) is a transcription factor that is essential and sufficient to specify rod photoreceptor fate (Mitton et al., 2000). Photoreceptor cell-specific nuclear receptor (NR2E3) also acts to direct precursors to a rod cell fate, but it cannot substitute for Nrl. Nr2e3 inhibits cone gene expression and acts with Nrl and Crx to promote expression of rod genes. Retinoid-related orphan nuclear receptor (RORβ) regulates rod

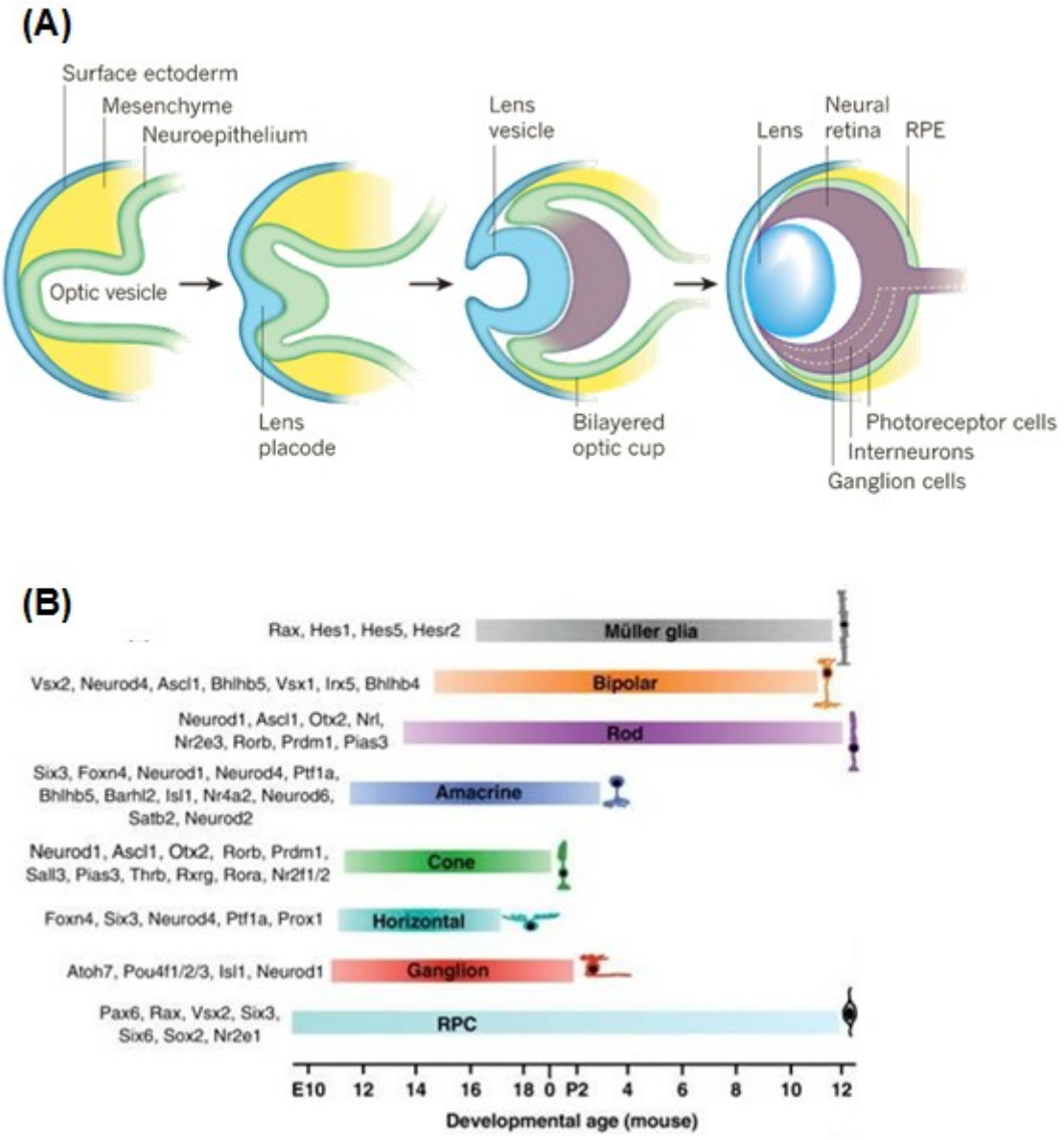

Figure 1.5 Development of the retina. (A) Eye organogenesis in vertebrates. Optic vesicle formation from evagination of the neural tube during embryonic development. A double-walled optic cup forms where the outer layer becomes the RPE (green) and the inner layer becomes the neural retina (purple). Reproduced from Ali & Sowden (2011) with the permission of Copyright Clearance Center on behalf of Nature Publishing Group. (B) Temporal development and transcriptional regulation of retinal cells in mice. Reproduced from Bassett & Wallace (2012) with the permission of Copyright Clearance Center on behalf of Elsevier.

and cone development. It is necessary for generation of rods and for the proper formation of OS in S cones (Jia et al., 2009). Finally, thyroid hormone receptor β2 (TRβ2) is necessary for M cone differentiation (Lu et al., 2009).

1.2 Visual impairment

Visual impairment is a significant limitation of functional vision resulting from disease, trauma or a congenital conditions (Arditi & Rosenthal, 1998). Many of the leading causes of visual impairment are age-related, including cataract, glaucoma, age-related macular degeneration (AMD), corneal opacification and diabetic retinopathy. Worldwide, cataract is the leading cause of visual impairment, accounting for 47.9% of cases of blindness (WHO, 2014). However, cataract and corneal opacification are commonly treated by surgery in developed countries. In Canada, the leading causes of blindness arise from retinal degenerative diseases (FFB, 2014).

Damage to the light-sensitive retina results in vision loss. This damage may be caused by acute injury, such as penetrating eye trauma or a blunt trauma to the head, which can lead to retinal detachment. More commonly, damage is caused by chronic conditions. Complications from diabetes (diabetic retinopathy) can damage the blood vessels in the eyes, leading to blurred vision. Increased intraocular pressure is one mechanism to account for the ganglion cell and axon degeneration that is associated with glaucoma.

1.2.1 Retinal degenerative diseases

Retinal degenerative diseases encompass a group of disorders all causing progressive photoreceptor cell death (Figure 1.6). Like other types of neurons, photoreceptors are post mitotic and cannot be replaced if destroyed or damaged, thus

photoreceptor loss leads to irreversible vision loss. The most prevalent of these diseases is AMD, which is the leading cause of blindness in Canada (National Coalition for Vision Health, 2007). Retinitis pigmentosa (RP) and other inherited retinal degenerative diseases affect one in 3500 people in Canada (FFB, 2014).

1.2.1.1 Age-related macular degeneration

In North America, AMD is the leading cause of blindness in people 60 years of age or older. While there are many risk factors for developing AMD, including smoking, exposure to sunlight, and hypertension, the biggest risk factor is age. Prevalence of AMD increases with age; it is observed in 10% of individuals aged 66 to 74 years old and increases to nearly 30% in individuals over 75 years old (The National Coalition for Vision Health, 2007). AMD affects the macula, the central area of the retina containing the fovea centralis. While this region comprises only four percent of the entire retina, this area of the eye has the highest density of cones and is responsible for our colour vision and our high visual acuity (Hageman, 2011). Thus, macular degeneration causes both loss of central vision and ability to see fine details. While AMD patients retain peripheral vision, they lose ability to read, recognize faces, and drive.

There are two forms of AMD: nonexudative or "dry" AMD and exudative or "wet" AMD. Nonexudative AMD is the more common and less severe form of the disease and is associated with large accumulations of drusen. Drusen are deposits of extracellular material, such as proteins and lipids that may damage the retina by interfering with the transfer of nutrients and oxygen between the RPE and underlying blood vessels (Pauleikhoff et al., 1990). The exudative form of AMD is less common, occurring in about 10 to 15% of patients, but this type causes more severe, rapid

deterioration of vision (Sunness, 1999). Wet AMD involves choroidal neovascularization, which is the abnormal growth of blood vessels from the underlying choroid layer into subretinal space. Fibrovascular scarring and leakage of blood and fluid lead to photoreceptor damage and vision loss (Fine et al., 2000). Visual deterioration occurs over several months, usually beginning with central vision loss in one eye and often progressing to bilateral vision loss (Abugreen et al., 2003).

1.2.1.2 Retinitis pigmentosa

Retinitis pigmentosa (RP) is a group of hereditary, degenerative diseases that are characterized by loss of peripheral rod photoreceptors. RP is the most common inherited retinal degeneration, affecting about 1.5 million people worldwide (Shintani et al., 2009). Disease onset is variable, ranging from infancy to adulthood and degeneration is not stable or consistent (Boughman et al., 1980; Haim, 2002). At the early stages, patients often experience nyctalopia, or night vision problems, where their vision is limited in the dark because rod photoreceptors have degenerated leaving cone photoreceptors, which need bright light for stimulation. Due to the progressive degeneration of the peripheral visual field, patients also often experience tunnel vision, seeing with the central cone photoreceptors that remain functional. As the disease progresses and rods degenerate further, cone viability is also compromised affecting central vision and ultimately resulting in complete vision loss (Farrar et al., 2002).

To date, 44 genes that cause RP have been identified (Hartong et al., 2006; Marc et al., 2003). RP genes often encode for proteins involved in photoreceptor structure, the phototransduction cascade or the visual cycle. RP is primarily inherited as an autosomal-recessive trait (50 to 60% of cases). RP can also be inherited as an autosomal-dominant

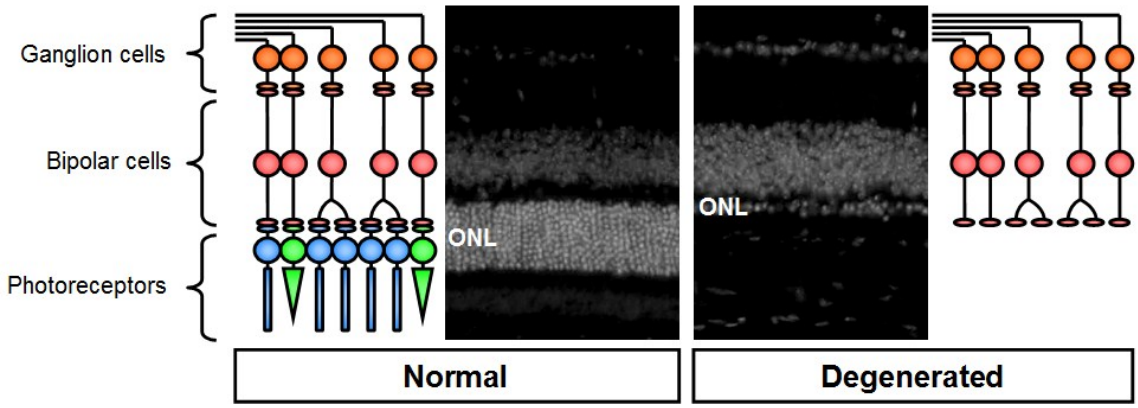

Figure 1.6 Retinal degeneration caused by photoreceptor loss. Loss of photoreceptors in the outer nuclear layer (ONL) in a degenerated *Crx*$^{-/-}$ mouse retina compared to a normal C57Bl/6 mouse retina. The normal retina has an ONL that contains several rows of photoreceptors. The degenerated retina has only one row of photoreceptors.

trait (30 to 40% of cases) or an X-linked trait (5 to 15% of cases) (Hartong et al., 2006). Primary cases of RP are confined to the eye. However, in 20 to 30% of cases, RP is a secondary cause associated with a disease affecting other body systems (Hartong et al., 2006). For example, RP is associated with extraocular abnormalities (hearing loss, cognitive impairment, polydactyly) in Usher syndrome and Bardet-Biedl syndrome (Macrae, 1982).

The early loss of rods is thought to be a minor handicap because with enough illumination these patients are able to retain a fairly normal way of life. It is the eventual secondary degeneration of cone photoreceptors and loss of central vision that has a tremendous negative impact on quality of life. While rod death results from rod-specific genetic mutations, cone loss remains poorly understood. Several mechanisms associated with rod apoptosis have been proposed to explain cone cell death including, deprivation of rod-derived cone viability factor (RdCVF), which has been shown to promote cell survival (Leveillard et al., 2004; Mohand-Said et al., 1998), liberation of toxins, loss of rod-cone gap junctions and oxidative stress (Cronin et al., 2007). In mouse models of RP, the insulin/mTOR pathway has been found to be one of the most affected, thus rod death may be responsible for metabolic changes and cone starvation may account for cell death (Punzo et al., 2009). Therefore, many factors may contribute to non-cell autonomous cone death arising from progressive loss of rods.

1.3 Current and future treatments for retinal degenerative diseases

Currently, existing therapies for retinal degenerative diseases serve to delay disease progression and vision loss. Nutritional supplements such as vitamin A have demonstrated ability slow the rate of retinal degeneration, especially in RP (Berson et al.,

1993). Vascular endothelial growth factor A (VEGF-A) inhibitors have been used to treat exudative AMD by reducing blood vessel growth thereby, slowing progression of the disease. Unfortunately, there is no established treatment to restore vision loss resulting from retinal degeneration. Once the photoreceptors are lost they will not regenerate and vision cannot be improved. A variety of strategies to restore vision are currently being explored and will potentially be used as future therapies, such as gene therapy, visual prostheses, optogenetic therapies and retinal transplantation.

1.3.1 Gene therapy

In diseases such as RP, many of the genetic mutations associated with the disease have been identified. Therefore, it is possible to develop gene therapy approaches to correct these genetic mutations. Gene replacement could be used in recessive conditions to deliver the normal gene to the patient's cells, as they only have copies of the mutant genes. Adeno-associated virus (AAV) gene therapy is studied in many models of retinal diseases, such as AAV-delivery of PDE6α in mouse models of RP (Wert et al., 2013). Furthermore, several gene therapy clinical trials are underway including AAV-delivery of VEGF inhibitors to treat AMD patients (U. S. National Institutes of Health, 2014) and AAV-RPE65 (retinal pigment epithelium-specific protein, 65kDa) treatment of patients with Leber's congenital amaurosis (LCA). LCA patients treated with RPE65 gene replacement therapy showed improvement in vision lasting long-term up to 1.5 years (Bainbridge et al., 2008; Hauswirth et al., 2008; Maguire et al., 2008) .

Other gene therapy methods include ribozyme therapy and RNA interference, which could be useful in autosomal dominant conditions where both normal and abnormal gene products are present. Ribozymes and RNA interference are designed to

destroy the mutant messenger RNA (mRNA) so that the abnormal protein, which is detrimental to photoreceptor survival, is not produced. These strategies may not eliminate all mutant mRNA, however it has been shown that ribozyme therapy reduced mRNA levels sufficiently enough to preserve vision in an RP canine model (Drenser et al., 1998).

Gene therapy is a promising field of study, however there are several disadvantages to this approach. In some cases, vectors may only rescue vision and are unable to preserve photoreceptors (Maguire et al., 2008), thus other treatments would be needed to slow degeneration. In addition, with over 44 different genes causing disease, another disadvantage is different vectors must be created to treat the different cases. Furthermore, while there is knowledge of many causal genes in RP, these genes only account for disease in about half of all patients, indicating that many genes remain to be identified.

1.3.2 Neuroprosthetic devices

Neuroprosthetic devices, or visual prostheses, are devices designed to help patients perceive light without direct stimulation from photons. Instead they use electrical stimulation at different points of the visual pathway. Stimulation can occur at the level of the retina, optic nerve or cerebral cortex (Shintani et al., 2009). External hardware is worn to capture images and transmit the signal to electrodes that are implanted into the targeted area to provide simulation.

Cortical implants demonstrated some success in allowing blind patients to perceive phosphenes, or flashes of light (Bak et al., 1990; Dobelle, 2000; Wyatt & Rizzo, 1996). However, disadvantages of this system include low-resolution imaging, increased risk of seizure due to use of currents in the electrodes, and the invasive nature of

implanting the prosthesis (Shintani et al., 2009). The optic nerve is a more accessible structure than intraocular or intracranial tissues, and optic nerve prostheses have the advantage of being less invasive. However, it does require a healthy optic nerve for proper function. Stimulation of the optic nerve has resulted in some patients being able to perceive coloured phosphenes and aided in localization and discrimination tasks in at least one RP patient (Duret et al., 2006; Veraart et al., 1998).

Retinal prostheses can include either epiretinal or subretinal prostheses. Epiretinal prostheses consist of an external camera and electrodes implanted in the retina. The Argus II Retinal Prosthesis is an epiretinal device with an implant consisting of 60 electrodes and an external eyeglass-mounted camera and processor (Figure 1.7). It has restored perception of light, movement, and shapes, and in some cases, it has allowed once-blind patients to read large print books (Ahuja et al., 2013). In February 2013, the Argus II became the first commercial visual prosthetic device to be approved for use in the United States of America (Steenhuysen, 2013).

Subretinal implants, or microchips, are also being developed that will function without the need for external hardware. A microphotodiode array is implanted, captures light and transforms it into a signal that is transmitted to existing retinal cells. After implantation into blind patients, these microchips containing 1500 microphotodiodes, helped patients locate and recognize objects and shapes, walk in a room freely and read large letters (Zrenner et al., 2011). However, despite the improvements in visual perception, no visual prosthesis has restored "normal" vision.

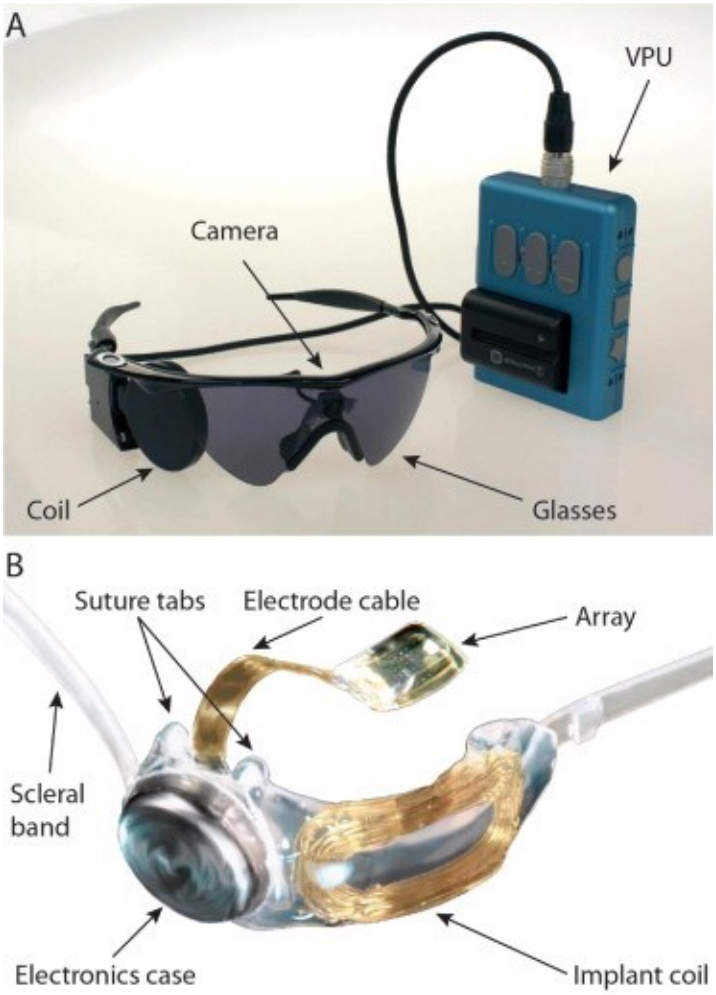

Figure 1.7 The Argus II Retinal Prosthesis. The Argus II consists of (A) an epiretinal prosthesis surgically implanted in the eye and (B) the external hardware. A camera on the glasses captures external images, which are sent to the video processing unit (VPU) to be converted into a signal. The signal is sent wirelessly to the implant where the electrode array stimulates the retina. Reproduced from Humayun et al. (2012) with the permission of Copyright Clearance Center on behalf of Elsevier.

1.3.3 Optogenetics

Optogenetics is a technique that uses light to control neurons that are genetically made photosensistive. In cases of photoreceptor degeneration, it is possible to restore photosensitivity by genetically expressing light-activated cation channels in surviving second order retinal cells. Studies have shown that the algae light-activated channel, channelrhodopsin-2 (ChR2), can be targeted to bipolar cells in mice lacking photoreceptors. Blind mice expressing ChR2 showed some rescue of light sensitivity by responding to light (Bi et al., 2006; Lagali et al., 2008). An advantage to optogenetic approaches is that it avoids issues in immune reactions because it does not involve transplanting cells, tissues or devices into the retina. Therefore, this technique may serve as a therapy help restore light sensitivity. However, the threshold of light intensity to produce a response from ChR2-expressing retinas is high, therefore bright light would be needed to restore light perception. Finally, the success of optogenetics depends on long-term expression of the light-activated channels and survival of the second order neurons in the retina.

1.4 Retinal transplantation therapy

The majority of existing therapies for retinal degeneration serve primarily to delay disease progression, but do not improve visual function. With the exception of visual prostheses and some gene therapy approaches, which are in clinical trials, there is currently no treatment available to actually restore vision. Yet, despite the loss of the photoreceptors in the degenerating ONL, the remaining retinal cells, such as bipolar and ganglion cells, as well as their connections remain intact after photoreceptor death (Shintani et al., 2009). It has been shown that remodelling of inner retinal cells occurs in

later stages of retinal degeneration (Jones et al., 2003; Strettoi & Pignatelli, 2000), however, early on, the "wiring" is preserved and the surviving INL cells are able to transmit a visual signal to the brain (Figure 1.6). Thus, it has been postulated that by replacing the damaged photoreceptors with new cells, they will integrate and form connections with the existing retina, thereby improving visual function.

1.4.1 Transplantation of RPE

As described in Section 1, the RPE is essential for photoreceptor health and function. In diseases where the RPE is affected, secondary photoreceptor loss occurs. Therefore, a great deal of research has focused on RPE replacement using either transplanted stem cells or a monolayer patch as an approach to rescue photoreceptors. In rat models of RPE dysfunction, RPE cell transplantation was able to preserve subretinal anatomy by delaying photoreceptor degeneration (Li & Turner, 1988; Lopez et al., 1989), and improve photoreceptor function (Lund et al., 2001; Sauve et al., 2002).

However, transplanted RPE cells are not able to organize into a proper monolayer and contribute to the blood-retinal barrier. Therefore, research is exploring transplanting sheets of RPE isolated as patches (Seiler & Aramant, 2012). Recently, preclinical work with RPE monolayer patches has also been carried out where the transplanted grafts successfully integrated into host rats, expressed appropriate RPE markers and demonstrated ability to clear away rhodopsin-positive debris (Carr et al., 2009; Vugler et al., 2008). Phase I clinical trials to transplant RPE cells into AMD patients are currently in progress in the United States. Other clinical trials have started in the United Kingdom to investigate transplantation of RPE sheets into patients with RPE tears (Seiler &

Aramant, 2012). However, RPE transplantation can only delay retinal degeneration as long as there are photoreceptors present to rescue.

1.4.2 Retinal transplantation

Because of the dependent relationship between the neural retina and RPE, transplantation of photoreceptors alone will have limited long term effects when the patient has no RPE. Conversely, transplanting RPE alone will have little benefit if there are no photoreceptors to be rescued. Therefore, methods to restore the population of damaged photoreceptors will be essential in treating patients with advanced retinal degeneration. Many different methods of delivering photoreceptors have been considered and investigated, including transplanting retinal sheets, stem cells, and photoreceptor precursors.

1.4.2.1 Transplantation of retinal sheets

Retinal sheets have been extracted as wholemounts or isolated as photoreceptor sheets, then transplanted in the subretinal spaces of rats. Transplanted photoreceptor sheets show poor survival and morphology (Ghosh et al., 1998; Ghosh et al., 1999; Silverman & Hughes, 1989). Meanwhile, whole retinal sheets, both with and without RPE, lead to better transplantation results. Transplanted fetal retinal sheets with their RPE develop a normal lamination pattern and express several components of the visual transduction cascade pathway (Seiler et al., 2010; Seiler et al., 2008; Woch et al., 2001). The transplanted cells were also able to extend processes that appeared to connect with the remaining host retina and restore some visual responses in rat models of retinal degeneration (Seiler & Aramant, 2012; Seiler et al., 2010; Seiler et al., 2008; Woch et al., 2001). Clinical trials have been carried out involving the transplantation of fetal retinal

sheets with RPE into AMD and RP patients (Radtke et al., 2008; Radtke et al., 2002). While the transplanted retinal sheets survived, they showed little success in improving visual function.

1.4.2.2 Transplantation of stem cells

Early work in the field of retinal stem cell transplantation began when it was observed that adult rat hippocampus-derived neural progenitor cells transplanted into neonatal rat retinas were able to survive and migrate into the host retina (Takahashi et al., 1998). However, these non-retina derived stem cells never showed evidence of developing into mature retinal cells, especially photoreceptors, expressing retinal cell markers, making them unsuitable for retinal transplantation (Takahashi et al., 1998).

More recently, interest has shifted to investigating the use of retinal-derived stem cell in transplantation. Transplanted RPCs isolated from embryonic mouse eyes were able to survive and differentiate in the host retina (Canola et al., 2007; Chacko et al., 2000; Qiu et al., 2005). The importance of injection location was also highlighted in these studies, as subretinal injections led to more integration than intravitreal injections (Canola et al., 2007; Sakaguchi et al., 2004). However, drawbacks with RPC transplantations included clumping of the cells and the formation of rosettes subretinally. Additionally, there were low numbers of integrated cells. Finally, there was very little evidence of synaptic connectivity between the transplanted cells and host retina.

1.4.2.3 Transplantation of photoreceptor precursors

In 2006, MacLaren et al. demonstrated the first successful transplantation of rod photoreceptors. They determined that a key factor influencing successful integration was the developmental stage of the donor cells. Whereas prior studies had used stem cells

derived from embryonic mouse retinas, MacLaren et al. hypothesized that photoreceptor precursor cells from a later developmental stage would result in greater success of integration.

To determine the optimal developmental stage for integration, Maclaren et al. dissociated GFP-positive retinal cells from Cba-GFP$^{+/-}$ mice, from embryonic (E) day 11.5 to adult, and transplanted them into the subretinal space of wildtype adult mice (2006). They found that transplanted cells from embryonic and adult donors survived but failed to integrate (MacLaren et al., 2006). The cells from these developmental stages were RPCs or differentiated cells. Meanwhile, cell integration peaked when postnatal (P) day 1 to 7 cells were transplanted (MacLaren et al., 2006). These cells comprised a mixture of proliferating progenitors, post-mitotic rod precursors and differentiated cells. Therefore, increased integration can be correlated to the presence of postmitotic precursor cells in these retinas. To confirm that only post-mitotic cells integrated into the host retina, BrdU-labeling was used to mark mitotic P1 donor cells. BrdU-labeled cells were found only in the subretinal space and none of the BrdU-labeled cells integrated into the recipient retina, indicating that proliferating cells had been transplanted but only post-mitotic cells had integrated (MacLaren et al., 2006).

Since then, the transplantation procedure has been optimized so that donor cells are purified for GFP+ cells by fluorescence activated cell sorting (FACS), cells are delivered to both the superior and inferior recipient retina, and a scleral puncture to the anterior chamber relieves intraocular pressure and reduces reflux of injected cells (Pearson et al., 2012). Rod transplantation integration rates have increased from hundreds of cells to 5000 to 10,000 cells per retina. (Barber et al., 2013; Pearson et al., 2012; Singh

et al., 2013). These integrated cells appear to develop into mature photoreceptors, expressing various arrestins and transducins involved in the visual photocascade and they develop synaptic connections (Pearson et al., 2012).. It has been shown that in models of degenerating retinas, transplantation appears to restore visual function by helping improve scotopic responses, as assessed by electroretinographs (ERGs), optical imaging, and optomotor and watermaze testing (Pearson et al., 2012; Singh et al., 2013). Therefore, retinal transplantation may be a viable treatment for retinal degenerative diseases.

1.4.2.4 Transplantation of cone photoreceptors

Although advances have been made in the field of retinal transplantation, this work has focused primarily on rod photoreceptor transplantation and improvement of scotopic responses. Some attempts have been made to investigate cone transplantation. Transplanting embryonic retinal cells does result in the integration of cells that display cone morphology and express cone markers (Lakowski et al., 2010). However, these studies used a donor cells with a photoreceptor marker that was not cone-specific and was expressed in both rods and cones. Therefore, no study has investigated cone photoreceptor transplantation directly.

1.5 Development of a donor mouse line

The low frequency of cones in the mammalian retina and a lack of cone-specific reporter lines are key limitations to investigating the potential for cone transplantation to improve vision. To overcome these challenges we took advantage of a *Nrl*$^{-/-}$ and a cone gene, Ccdc136, to generate a mouse strain that is enriched for GFP-expressing cone photoreceptors.

1.5.1 *Nrl*$^{-/-}$ mouse

Neural retina leucine zipper (Nrl) is a transcription factor expressed specifically in rod photoreceptors (Swain et al., 2001) that is essential for rod differentiation. Nrl regulates rod-specific gene expression, such as rhodopsin, while simultaneously inhibiting cone photoreceptor development (Mears et al., 2001). The deletion of Nrl in mice results in a complete absence of rod photoreceptors, and instead all rod precursors default to a cone differentiation pathway.

Nrl knock-out (*Nrl*$^{-/-}$) mice do not express rod-specific genes, such as rhodopsin (*Rho*), rod transducin (*Gnat1*) and a rod-specific phosphodiesterase subunit (*Pde6b*). Meanwhile, expression of cone-specific genes, such as S opsin (*Opn1sw*), cone transducin (*Gnat2*) and cone arrestin (*Arr3*), is significantly increased (Mears et al., 2001). The resulting photoreceptors also appear to have a cone-like nuclear morphology (Mears et al., 2001). Furthermore, electrophysiological data demonstrates a change in cone function in *Nrl*$^{-/-}$ retinas (Mears et al., 2001). Retinal function is assessed by electroretinographs (ERGs) which measure the electrical response of a retina to light stimulus. A flash of light will elicit a response comprised of an a-wave and a b-wave. The a-wave is the initial negative electrical response, originating from photoreceptors responding to light stimulus (Perlman, 2014). The b-wave is the subsequent positive electrical response, produced by second order neurons such as bipolar and amacrine cells (Perlman, 2014). ERG analysis shows that *Nrl*$^{-/-}$ retinas exhibit complete loss of rod function and enhanced S cone activity (Mears et al., 2001).

Though it appears that there is a switch from a rod to cone phenotype, the resulting photoreceptors in the *Nrl*$^{-/-}$ mouse are not true cones. Cones synapse with rod

bipolar cells and have reduced flicker responses (a measure of cone recovery time) than wildtype retinas (Daniele et al., 2005). These special photoreceptors have been termed "cods" as cone-rod intermediates. However, they appear and function as cones and are distinct from rods, so they can be considered a species of cone photoreceptor. We believe the *Nrl*$^{-/-}$ mouse is a useful tool to enrich and allow greater access to functional cones.

1.5.2 Coiled-coil domain containing 136

Coiled-coil domain containing 136 (*Ccdc136*) is a 31.3 kb gene on chromosome 7q32.1 (humans) and 6qA3.3 (mouse) (Figure 1.8). It encodes a 1,154 amino acid (134kDa) protein by the same name whose function is unknown. Ccdc136 is predicted to be a single-pass membrane protein but this has not been verified experimentally. It has also been called nasopharyngeal carcinoma-associated gene 6 (NAG6) and is expressed in gastric tissues. It is thought to be a potential tumour suppressor, as it is deleted or significantly downregulated in gastric cancers (Zhang et al., 2004).

Studies in mouse cone-only retinas (*Nrl*$^{-/-}$) and cone-enriched retinas (*Nr2e3*$^{-/-}$) show that *Ccdc136* transcript is highly enriched in these models (Brooks et al., 2011; Corbo & Cepko, 2005; Corbo et al., 2007). In addition to being a cone gene, *Ccdc136* is expressed in a ventral-to-dorsal gradient, comparable to the expression of S opsin (*Opn1sw*). Interestingly, *Ccdc136* is located immediately adjacent to the *Opn1sw* locus, thus similarities in their expression patterns may be related to a possible shared *cis*-regulatory element (Corbo et al., 2007). Because of the cone-restricted expression of *Ccdc136*, this locus might be ideal for driving a cone-specific reporter gene.

1.6 Rational, Hypothesis and Objectives

1.6.1 Rational

Research in retinal cell transplantation has focused primarily on rod photoreceptor transplantation. However, cone degeneration causes the biggest negative impact on vision and quality of life. With the prevalence of AMD increasing as the population ages, therapies for cone degeneration are crucial. If retinal transplantation is to be used as an effective clinical therapy for retinal degenerations, a method of successfully transplanting cones must be explored. Therefore, suitable mouse models must be developed to test cone transplantation and rescue of visual function.

1.6.2 Hypothesis

A *Ccdc136*-GFP mouse on a $Nrl^{-/-}$ background produces a model enriched for GFP-labeled cones that is suitable for investigating cone photoreceptor transplantation.

1.6.3 Objectives

To test this hypothesis, I had the following objectives

1. Generate and characterize *Ccdc136*-GFP mice.
2. Generate and characterize $Nrl^{-/-}$;$Ccdc136^{+/-}$ donor mice.
3. Develop a successful method of transplantation of cone photoreceptors in the degenerating murine retina.

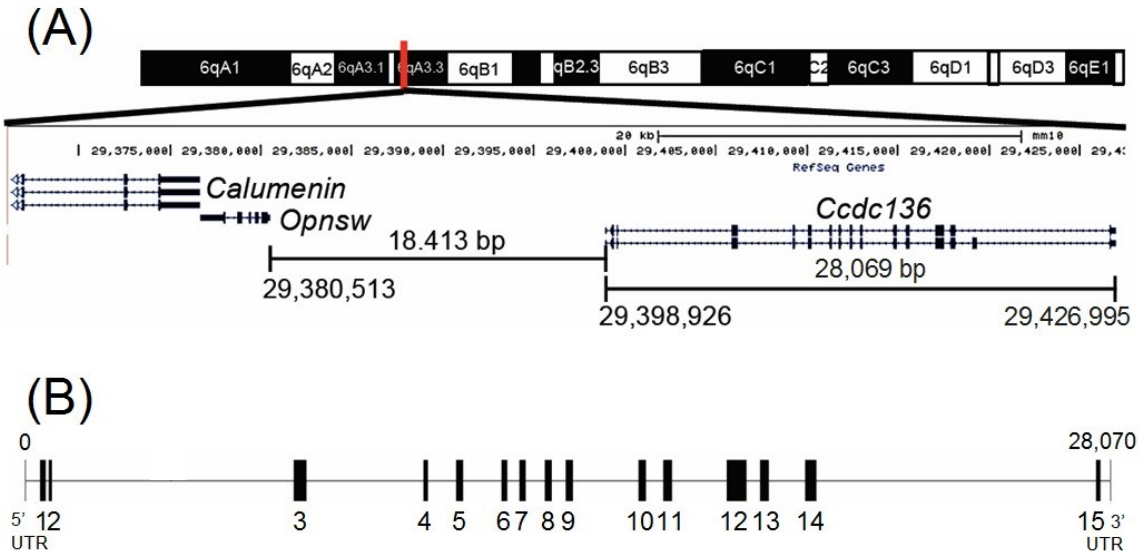

Figure 1.8 The mouse *Ccdc136* locus. (A) Mouse *Ccdc136* is located at 6qA3.3 (human, 7q32.1) on the positive strand, downstream of *Opn1sw*. (B) Mouse *Ccdc136* genomic structure.

Chapter 2. Materials and Methods

2.1 Animals

Animals were maintained under standard laboratory conditions and all procedures were performed in conformity with the University of Ottawa Animal Care and Veterinary Service and the Canadian Council on Animal Care guidelines. The following strains of mice were used: C57BL/6 mice, *Nrl*-EGFP mice where the *Nrl* promoter drives expression of enhanced green fluorescent protein (EGFP) specifically in rod photoreceptors (Akimoto et al., 2006) maintained as a homozygous line, $Nrl^{-/-}$ mice, which have a cone-only retina (Mears et al., 2001) maintained as a homozygous line, $Crx^{-/-}$ mice which fail to develop mature photoreceptors (Furukawa et al., 1999) maintained as a homozygous line, $Ccdc136^{-/-}$ gene trap mice maintained as a homozygous line, and $Nrl^{-/-};Ccdc136^{+/-}$ maintained as a heterozygous line for Ccdc136.

2.2 Genotyping

Mice were genotyped by PCR. Genomic DNA was isolated by incubating tissue from an ear clip in 300µl alkaline lysis buffer (25mM NaOH, 0.2mM EDTA pH 8.0) for 60 minutes at 95°C. Samples were neutralized with 300µl neutralization reagent (40mM Tris-HCl). Genotyping for the wildtype and mutant *Ccdc136* and *Nrl* alleles was performed as follows: 10µl GoTaq (Promega), 1µ each of 15µM forward and reverse primers (Table 2.1), 7µl water, and 1µl DNA. The thermal profile for the PCR reaction was 5 minutes at 94°C followed by 33 cycles of 94°C for 30 seconds, 55°C for 30 seconds and 72°C for 30 seconds. PCR products were run on a 2% agarose gel stained with RedSafe (Froggabio) and visualized using a UV transilluminator. Primers directed against the wild type allele yielded a band size of 405bp (*Ccdc136*) and 244bp (*Nrl*).

Primers directed against the mutant allele yielded a band size of 379bp (*Ccdc136*) and 338bp (*Nrl*).

2.3 Electroretinography[1]

Electroretinogram (ERG) recordings were carried out on $Ccdc136^{+/+}$ (n=6), $Ccdc136^{+/-}$ (n=7), $Ccdc136^{-/-}$ (n=6), $Nrl^{-/-}$ (n=6), $Nrl^{-/-};Ccdc136^{+/+}$ (n=6), $Nrl^{-/-};Ccdc136^{+/-}$ (n=7) and $Nrl^{-/-};Ccdc136^{-/-}$ (n=6) mice. In brief, the mice were dark-adapted for 1 hour before anesthesia with a mixture of ketamine (62.5 mg/kg IP) and xylazine (12.5 mg/kg IP) and the pupils dilated with 1% tropicamide. Body temperature was monitored with a rectal thermometer and maintained at 38°C with a homeothermic electric blanket. Simultaneous bilateral recording was achieved with active gold loop electrodes (placed on each cornea) and a subdermal platinum reference electrode (placed behind each eye); a subdermal ground platinum electrode was placed on the mouse's scruff. Light stimulation (10μs flashes), signal amplification (0.3–300-Hz bandpass), and data acquisition were provided by an electrophysiology system (Espion E2; Diagnosys LLC, Littleton, MA). For each animal, only one eye was considered for statistical comparisons. It corresponded to the eye associated with the dark-adapted b-wave of maximum amplitude.

2.4 Tissue sampling

$Nrl^{-/-};Ccdc136^{+/-}$, $Nrl^{-/-}$, $Ccdc136^{-/-}$, and C57BL/6 eyes were harvested at various stages beginning at embryonic day (E) 13.5 to adult. Mice younger than postnatal day (P) 10 were sacrificed and entire heads with eyes were collected. Mice older than P10 were perfused with 4% paraformaldehyde (PFA) and eyes were marked on their corneas for dorsal orientation with a silver nitrate stick then removed. Tissues were fixed in 4% PFA overnight then cryoprotected overnight in 30% sucrose in phosphate buffered saline

[1] Electroretinogram recordings were performed by Dr. Yves Sauvé (University of Alberta)

Table 2.1 Primer sequences used for genotyping

Primer	**Sequence (5' - 3')**
Ccdc136 wildtype forward	CCGTGGTGGGGGTTGAATCCAA
Ccdc136 wildtype reverse	TGGCAAAGTCATGAAGGGACCACA
Ccdc136 GFP forward	CACATGAAGCAGCACGACTT
Ccdc136 GFP reverse	TGCTCAGGTAGTGGTTGTCG
Nrl wildtype forward	GTGTTCCTTGGCTGGAAAGA
Nrl wildtype reverse	CTGTTCACTGTGGGCTTTCA
Nrl-T[a]	TGAATACAGGGACGACACCA
Nrl-XB[a]	GTTCTAATTCCATCAGAAGCTGAC

[a]*Nrl*-T/XB primers amplify the targeted allele (vector pPNT)

(PBS) (0.14M NaCl, 2.5mM KCl, 0.2M Na_2HPO_4, 0.2M KH_2PO_4). After sinking in sucrose, tissues were equilibrated in 50:50 30% sucrose: OCT (Tissue-Tek) for 1-2 hours, followed by orienting and embedding in plastic molds in sucrose: OCT and frozen. Samples were stored at -80°C. Tissue was sectioned at 12µm onto Superfrost Plus slides (Fisher Scientific) on a CM1850 Cryostat (Leica), air-dried for 1 to 2 hours and stored at -20°C with desiccant.

2.5 Immunohistochemistry

Retinal sections and cells were permeabilized with 70% ethanol for 5 minutes then washed in PBS for 20 minutes. Following an antigen retrieval step (for Chx10, Crx, PKC and Ki67 antibodies), sections were blocked with 50mM Tris buffer (pH 7.4), 10mM lysine, 145mM NaCl and 1% BSA (TBLS; blocking solution) for 1 hour at room temperature. Primary antibodies were diluted in TBLS and sections were incubated with primary antibody solution overnight at 4°C. The primary antibodies used are indicated in Table 2.2. After several washes with PBS, sections were incubated with fluorescent secondary antibody diluted in TBLS for 1 hour at room temperature. Nuclei were counterstained with fluorescent DNA-binding dye, Hoechst (Life Technologies). Sections were washed and glass coverslips were mounted with DAKO mounting media.

Fluorescent images were captured using an Axioimager M1 (Carl Zeiss, Inc.) Confocal images were acquired using a FluoView 1000 confocal microscope (Olympus).

2.7 In situ hybridization

Briefly, DIG-labeled RNA probes were diluted 1:1000 in hybridization buffer (50% formamide, 10% dextran sulfate, 25 lmg/ml yeast RNA, lx Denhardt's and lx salt) that had been denatured for 10 minutes at 70°C. About 100-150µl were added onto the

Table 2.2. List of antibodies used for immunohistochemistry

Antibody (dilution)	Species	Targets	Source (catalog number)
Cone Arrestin (1:1000)	Rabbit	Cone photoreceptors	Millipore (AB15282)
Chx10	Sheep	Bipolar cells	Exalpha (X1179P)
Crx (1:50)	Rabbit	Photoreceptors	
GFP (1:500)	Goat	GFP	Rockland (600-101-215)
Ki67 (1:500)	Rabbit	Proliferating cells	Abcam (AB66155)
M opsin (1:1000)	Rabbit	M cone photoreceptor OS	Millipore (AB5405)
Protein kinase Cα (PKC, 1:1000)	Mouse	Rod bipolar cells	Abcam (AB31)
Peanut agglutinin (PNA, 1:500)	Lectin biotinylated	Cone photoreceptor OS	Vector Laboratories (B-1075)
Recoverin (1:1000)	Rabbit	Photoreceptors and cone bipolar cells	Millipore (AB5585)
Rhodopsin (1:20)	Mouse	Rod photoreceptor OS	Developmental Studies Hybridoma Bank
S opsin (1:100)	Rabbit	S cone photoreceptor OS	Millipore (AB5407)

tissue and glass coverslips were applied. Probes were allowed to hybridize to the tissue overnight at 65°C in a humidified box. Slides were washed for 15 minutes and 30 minutes with wash buffer solution (50% Formamide, lxSSC, 0.1% Tween-20) at 65°C. Slides were then washed 30 minutes with MABT (100mM Maleic acid, 150mM NaCl, 0.1% Tween-20; pH 7.5). Sections were blocked with blocking solution (20% Sheep serum (Sigma) and 2% blocking solution in MABT) for 1 hour at room temperature. Slides were incubated with sheep anti-DIG (diluted 1:1500 in blocking solution) overnight at 4°C in a humidified box.

The following day, slides were washed 4x20 minutes with MABT at room temperature. Then they were incubated 2x10 minutes in staining buffer (100 mM NaCl, 50mM MGC12, 100mM Tris pH 9.5 ad 0.1% Tween-20) before being placed in the dark in staining buffer (100 mM NaCl, 50mM MGC12, 100mM Tris pH 9.5 ad 0.1% Tween-20, tetrazolium chloride (Roche) and 3.5ul/ml 5-bromo-4-choloro-3-indolylphosphate (Roche)) at 37°C until the colour reaction developed. Slides were washed in several times in PBS to stop the color reaction and mounted using 1:1 PBS: glycerol.

2.7 Retinal dissociations

Eyes from donor *Nrl*$^{-/-}$*;Ccdc136*$^{+/-}$ and wildtype C57BL/6 mice at P6 were harvested and dissected to recover the neural retina. Retinas were dissociated in trypsin (Sigma) (5mg/mL, in Ca^{2+}-, Mg^{2+}-free PBS) for 5 minutes at 37°C. Enzymatic activity was stopped with the addition of 20% FBS in CO_2-independent media and the tissues were disrupted by gentle trituration. Cells were centrifuged at 300xG for 5 minutes and resuspended in PBS. Cell viability was assessed using trypan blue and cells were counted using a hemacytometer.

For transplantations, donor cells were prepared from *Nrl*$^{-/-}$;*Ccdc136*$^{+/-}$ and *Nrl*-EGFP mice at P0 and P6. Cells were dissociated with a papain dissociation kit (Worthington Biochemical, UK) according to the manufacturer's directions and resuspended at 200,000cells/µL in Earl's Balanced Salt Solution (EBSS) and kept on ice prior to transplantation.

To analyze cells by immunohistochemistry, a 10µl of cell suspension was streaked onto the slides and was incubated at room temperature for 5 minutes followed by 40 minutes at 37°C. Cells were fixed with 4% PFA for 10 minutes. After several washes in PBS, cells were immunostained and analyzed.

2.8 Subretinal injections

Adult recipient C57Bl/6 or *Crx*$^{-/-}$ mice (4-6 months old) were anesthetised by isoflurane gas inhalation. Eyes were dilated using 1% tropicamide (Mydriacyl, Alcon) drops and 0.5% proparacaine hydrochloride (Alcaine, Alcon) drops were administered as a local anesthetic. A 0.2% hypromellose gel (Genteal, Novartis) was applied to maintain lubrication of the corneas. The left eye of the recipient mouse was gently prolapsed and a scleral puncture was made on the dorsal side directly posterior to the limbus with a V-lance knife. Injections were carried out using a nano-injector (Harvard Apparatus) and performed using a surgical microscope. A 34 gauge blunt-end needle was inserted tangentially through the sclera and across the vitreous to the opposite ventral side and moved into the subretinal space until there was resistance. The needle was retracted slightly and 1uL of cell suspension was injected over the course of 30 seconds. The needle was held in place after injection for 10-20 seconds to allow for equilibration of pressure then slowly retracted. After injection, a coverslip coated with 0.2%

hypromellose gel was placed on top of the cornea providing visualization of the back of the eye and the injection site to ensure subretinal delivery of cells. Right eyes served as untreated controls.

2.9 Tissue processing and cell counts

After 3 weeks, the recipient eyes were harvested and processed according to methods described in Section 2.4. Entire eyes were sectioned in serial sections at 12μm and sections were analyzed using immunohistochemistry. Integrated cells were identified by immunostaining with an anti-GFP antibody. GFP signal was observed through the cell body and inner and outer processes.

Retinal sections were examined using a FluoView 1000 confocal microscope (Olympus). Cells were considered to be integrated if the whole cell body was located in the host ONL, and at least one of the following criteria was additionally observed; cone pedicle, an inner or outer process or IS/OS. The average number of integrated cells per eye was determined by counting all integrated GFP+ cells in alternate sections of each eye and doubling that number. Only animals with successful transplantations, where GFP+ cells were located in the subretinal space, were included in quantitative analysis. If there was evidence of an intravitreal injection, rather than subretinal, or if GFP+ cells were absent from the subretinal space, these animals were defined as an unsuccessful transplant and were omitted from quantitative analysis.

2.10 Image processing, data analysis and statistics

Images of wildtype and mutant retinas were taken at the same exposure at each magnification. In the event that contrast/levels were adjusted, the entire image was

adjusted and both wildtype and mutant retina images were adjusted equally. Images were processed using Photoshop CS4 (Adobe).

Quantification of dissociated cells was performed by counting marker-positive cells and dividing by the total number of cell nuclei (5 images taken per stain with a minimum of 200 total cells counted). All data are presented as mean ± standard error of the mean (SEM). Statistical significance was evaluated using a two-tailed, unpaired Student T-test.

Chapter 3. Results

3.1 *Ccdc136* expression in the adult mouse retina

To assess C*cdc136* expression in cone photoreceptors, *Ccdc136* transcript expression was characterized by *in situ* hybridization on sections of adult wildtype and *Nrl*$^{-/-}$ mouse retinas. C*cdc136* mRNA was expressed in cells in the ONL and INL (Figure 3.1 A, C). In the ONL of wildtype retina, *Ccdc136* expression followed a pattern consistent with cone photoreceptor organization, where cells expressing the transcript were confined to the last few rows on the apical side. In the cone-only *Nrl*$^{-/-}$ retina, *Ccdc136* mRNA was expressed in all cells of the ONL (Figure 3.1 C). Enrichment of *Ccdc136* expression in a cone-enriched model provides further evidence of its expression in cone photoreceptors and as a suitable potential cone marker.

3.2 Generation of *Ccdc136*$^{-/-}$ and *Nrl*$^{-/-}$*;Ccdc136*$^{+/-}$ mice

Ccdc136$^{-/-}$ mice were created using a gene trapped embryonic stem (ES) cell line where a pUPA GFP reporter vector (Centre for Modeling Human Disease, Toronto) was inserted into intron 2 of the *Ccdc136* gene (Figure 3.2 A). Mouse mutants derived from this ES cell line were viable and fertile. Northern blot analysis of adult retina RNA using a full-length *Ccdc136* cDNA probe shows that the full length transcript is reduced in Ccdc136 heterozygous (*Ccdc136*$^{+/-}$) mice and absent in homozygous (*Ccdc136*$^{-/-}$) mice (Figure 3.2 B). *Nrl*$^{-/-}$*;Ccdc136*$^{+/-}$ mice were generated by crossing *Nrl*$^{-/-}$ with *Ccdc136*$^{-/-}$ mice to create *Nrl*$^{+/-}$*/Ccdc136*$^{+/-}$ mice. The *Nrl*$^{+/-}$*/Ccdc136*$^{+/-}$ mice were backcrossed with *Nrl*$^{-/-}$ mice to generate *Nrl*$^{-/-}$*;Ccdc136*$^{+/-}$ mice.

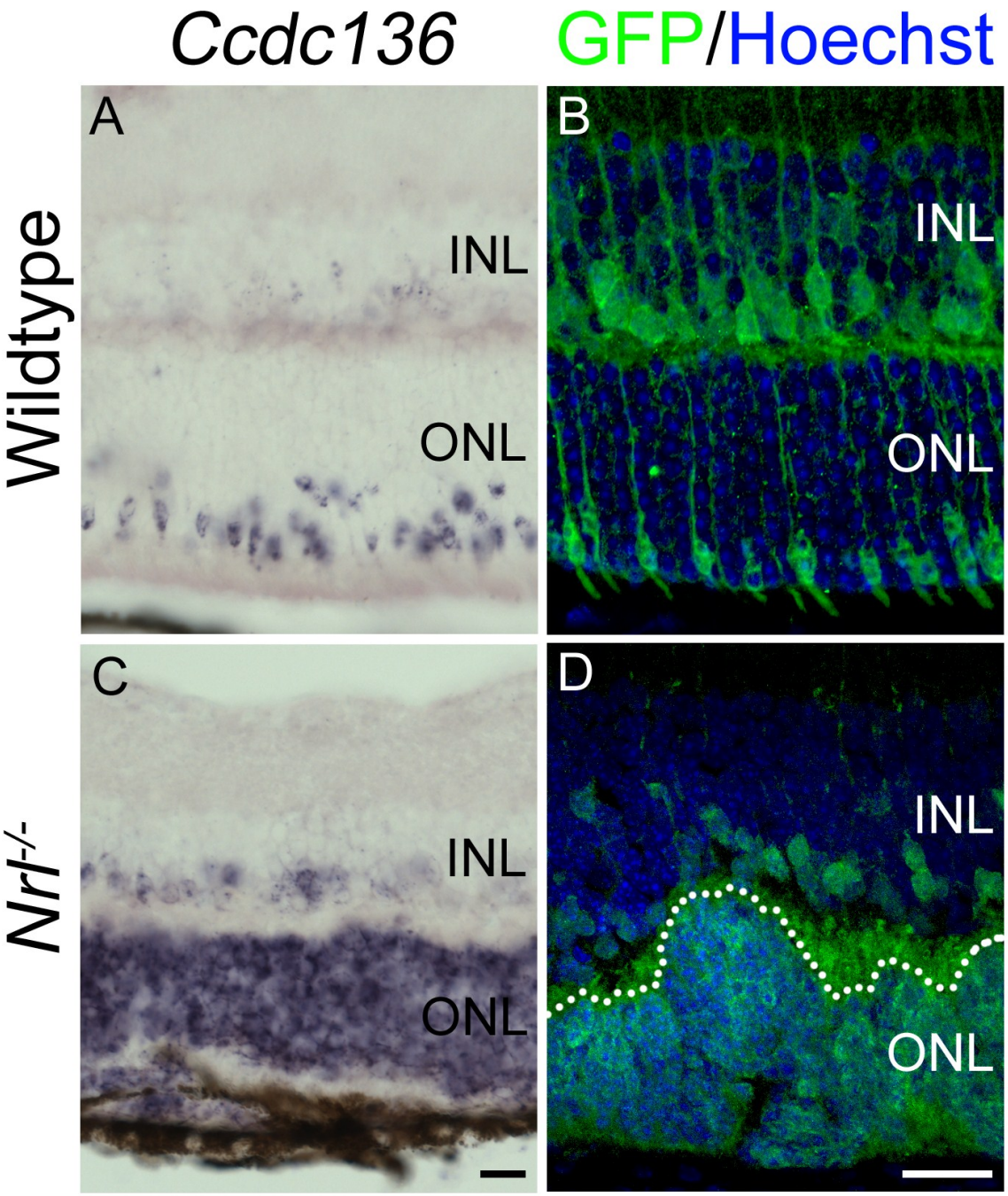

Figure 3.1 Ccdc136 expression in the adult mouse retina. (A, C) *In situ* hybridization for *Ccdc136* expression in wildtype and *Nrl*$^{-/-}$ retinas. (B, D) Immunohistochemistry for GFP reporter (green) in *Ccdc136*$^{-/-}$ and *Nrl*$^{-/-}$*;Ccdc136*$^{+/-}$ retinas. GFP+ cells are found in the INL and ONL. Dashed line indicates the border of the ONL. ONL, outer nuclear layer; INL, inner nuclear layer. Scale bars, 25μm.

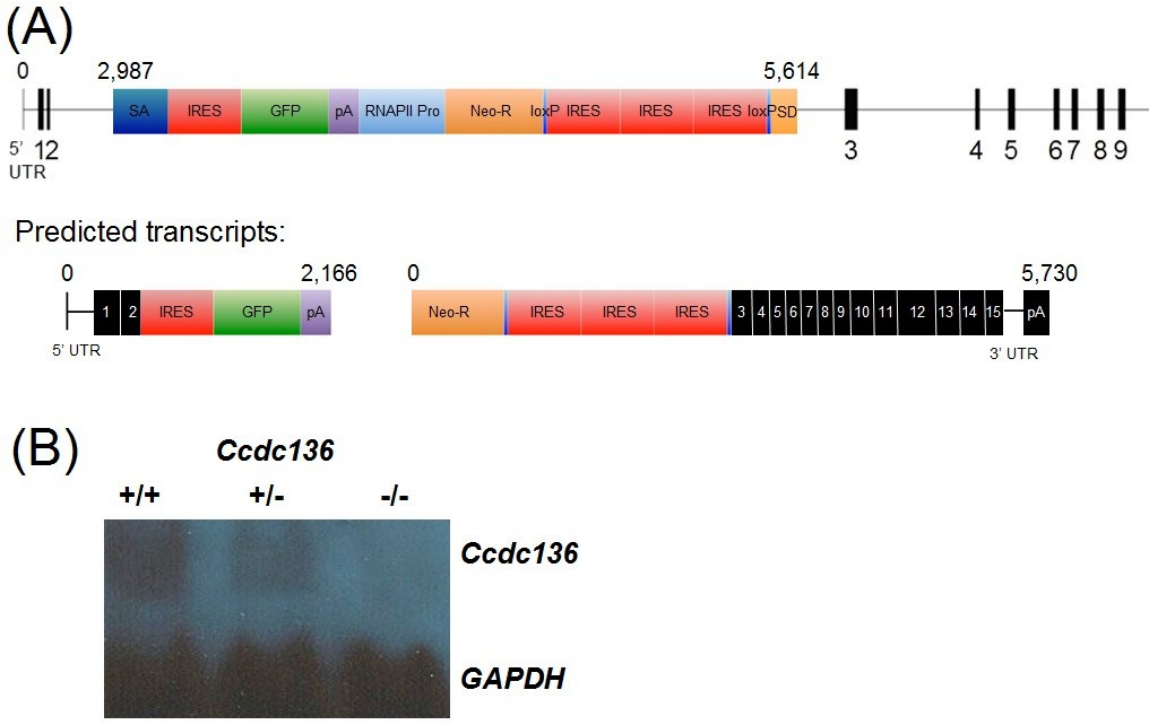

Figure 3.2 Generation of the murine *Ccdc136* gene trap locus. (A) *Ccdc136*-GFP mutant allele, created by gene trap. To create *Ccdc136*-GFP, pUPA has been inserted 2,987 bp into mouse *Ccdc136*. The gene trap locus is predicted to produce two transcripts: a 5' transcript that includes *Ccdc136* exons 1 and 2 fused to IRES and GFP and a 3' transcript that consists of Neo-R, floxed IRES sequences (blue), and *Ccdc136* exons 3 to 15. (B) *Ccdc136* mRNA expression in mice retina wild-type ($^{+/+}$), heterozygous ($^{+/-}$), or homozygous mutant ($^{-/-}$) for Ccdc136. SA, Splice Acceptor; IRES, Internal Ribosome Entry Site; GFP, Green Fluorescent Protein; PA, Poly A; RNAPII Pro, RNA Polymerase II Promoter; Neo-R, Neomycin Resistance; Thin blue segments, LoxP sites; SD, Splice Donor.

3.3 GFP reporter is a cone marker in *Ccdc136*$^{-/-}$ retinas

To characterize the pattern of GFP reporter expression in *Ccdc136*$^{-/-}$, immunohistochemical (IHC) staining was performed on sections of adult *Ccdc136*$^{-/-}$ and *Nrl*$^{-/-}$*;Ccdc136*$^{+/-}$ retinas. The pattern of GFP expression was similar to *Ccdc136* transcript expression in *Ccdc136*$^{-/-}$ retinas on a wildtype and *Nrl*$^{-/-}$ background (Figure 3.1 B, D). In *Ccdc136*$^{-/-}$ retinas, GFP+ cells were located along the apical side of the ONL suggesting the GFP+ cells are cones. In the *Nrl*$^{-/-}$*;Ccdc136*$^{+/-}$ cone-only retinas, all cells of the ONL expressed GFP, again suggesting GFP+ cells are cones. While *Ccdc136* transcript expression was confined to the cell body, GFP signal was observed in the cell body and in apical and basal processes (Figure 3.1).

To confirm the identity of the GFP+ cells as cone photoreceptors, *Ccdc136*$^{-/-}$ retinas were immunostained for GFP and various cone markers. IHC analysis showed co-expression of GFP with the cone markers, cone arrestin (CAr) and peanut agglutinin (PNA) (Figure 3.3). The co-expression was best observed in *Ccdc136*$^{-/-}$ retinas where single GFP+ cells and their co-localization with the various cone markers was easily distinguishable (Figure 3.3). CAr labelled the entire cone photoreceptor and GFP signal co-localized almost entirely with CAr signal, from the synapse and inner process, to the cell body and IS. However, GFP expression did not extend to the cone OS (Figure 3.3 G). PNA labeled cone IS and OS and co-localized with the GFP+ cone IS (Figure 3.3 H).

Furthermore, GFP was expressed in a ventral-to-dorsal gradient (Figure 3.3 I-J, K-L). Expression of GFP was greater in the ventral retina and of *Ccdc136*$^{-/-}$ mice. GFP+ cells remained present in the dorsal retina but exhibited reduced intensity of GFP immunostaining. GFP+ cells also co-localized with graded expression of M and S opsin

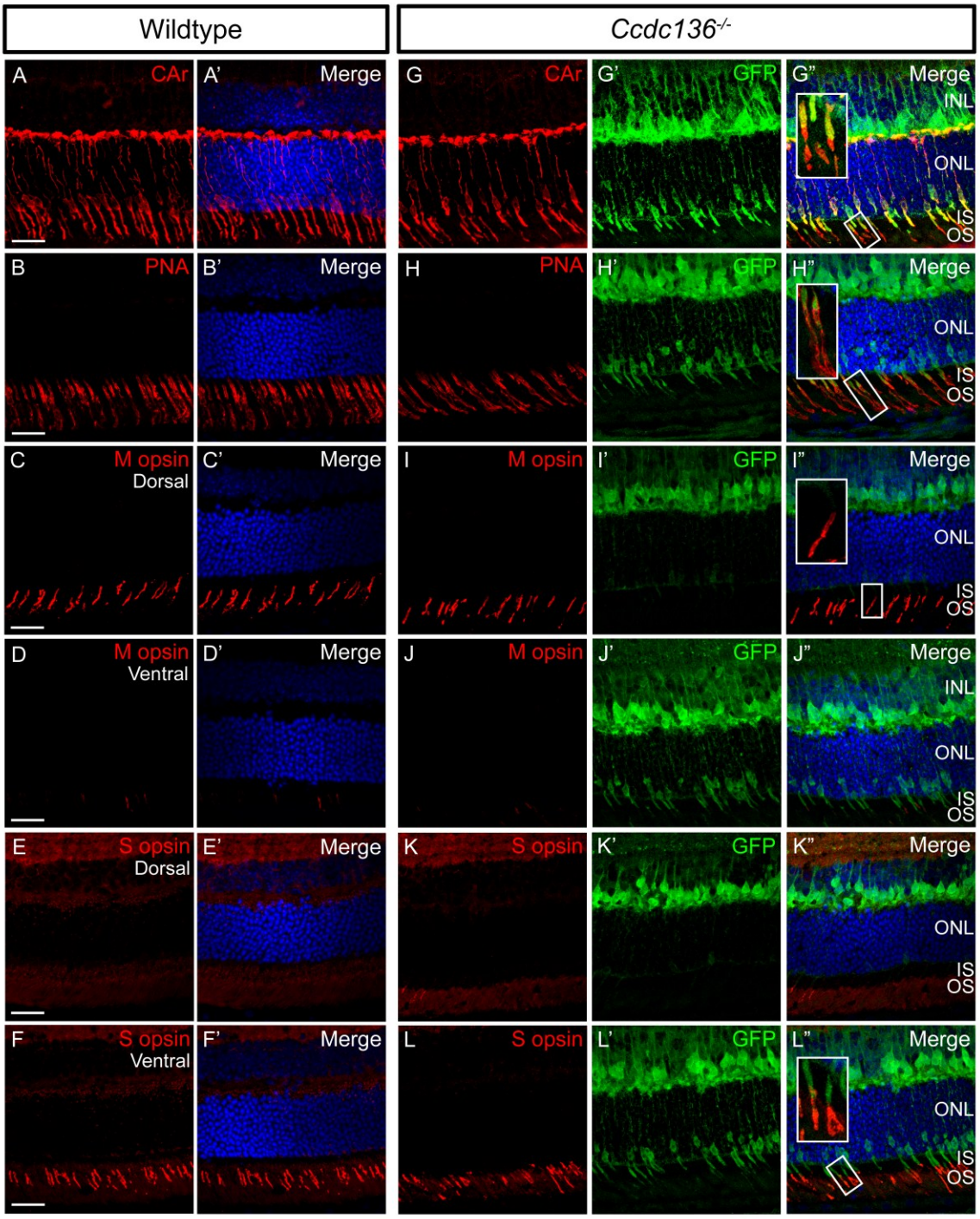
Wildtype
Ccdc136-/-
A
CAr
A'
Merge
G
CAr
G'
GFP
G"
Merge
INL
ONL
IS
OS
B
PNA
B'
Merge
H
PNA
H'
GFP
H"
Merge
ONL
IS
OS
C
M opsin
Dorsal
C'
Merge
I
M opsin
I'
GFP
I"
Merge
ONL
IS
OS
D
M opsin
Ventral
D'
Merge
J
M opsin
J'
GFP
J"
Merge
INL
ONL
IS
OS
E
S opsin
Dorsal
E'
Merge
K
S opsin
K'
GFP
K"
Merge
ONL
IS
OS
F
S opsin
Ventral
F'
Merge
L
S opsin
L'
GFP
L"
Merge
ONL
IS
OS

Figure 3.3 Expression of cone photoreceptor markers in adult (A-F) wildtype and (G-L) *Ccdc136*$^{-/-}$ retinas. (A-L) Target protein immunostaining (red); (G'-L') GFP labelling (green); (A"-L") three-channel merge with Hoechst nuclear stain (blue). (A, G) Cone arrestin is a cone specific marker. (B, H) PNA labels cone outer segments. (C-D, I-J) M opsin labels outer segments of M cones, expressed more in the dorsal than ventral retina. (E-F, K-L) S opsin labels outer segments of S cones, expressed more in the ventral than dorsal retina. Insets show OS of GFP+ cones in *Ccdc136*$^{-/-}$ retina co-expressing cone markers. ONL, outer nuclear layer; INL, inner nuclear layer; OS, outer segments; IS, inner segments. Scale bars, 25μm.

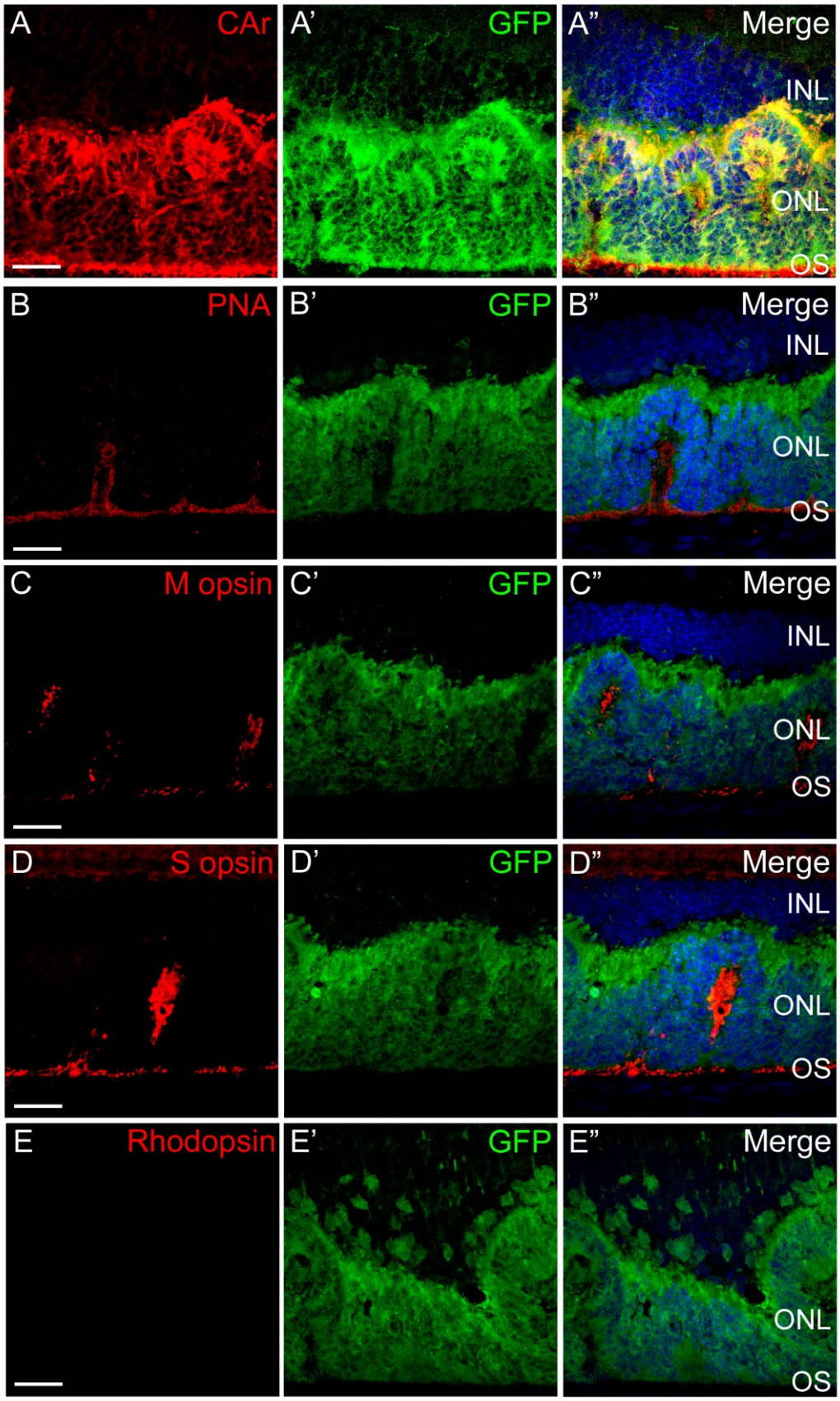
A
CAr
A'
GFP
A"
Merge
INL
ONL
OS
B
PNA
B'
GFP
B"
Merge
INL
ONL
OS
C
M opsin
C'
GFP
C"
Merge
INL
ONL
OS
D
S opsin
D'
GFP
D"
Merge
INL
ONL
OS
E
Rhodopsin
E'
GFP
E"
Merge
ONL
OS

Figure 3.4 Expression of cone photoreceptor markers in adult *Nrl*$^{-/-}$;*Ccdc136*$^{+/-}$ retinas. (A-E) Target protein immunostaining (red); (A'-E') GFP labelling (green); (A"-E") three channel-merge with Hoechst nuclear stain (blue). (A) Cone arrestin (CAr) is a cone specific marker. (B) PNA labels cone outer segments. (C) M opsin labels outer segments of M cones. (D) S opsin labels outer segments of S cones, enriched in *Nrl*$^{-/-}$ retinas. (E) Rhodopsin is a rod photoreceptor marker. ONL, outer nuclear layer; INL, inner nuclear layer; OS, outer segments. Scale bars, 25μm.

positive cells (Figure 3.3 I-L). M and S opsins labelled M and S cones OS, respectively. GFP co-localization with S opsin was observed easily due to high intensity staining of both markers in the ventral retina (Figure 3.3 L). However, cones with low GFP expression co-localized with M opsin in the dorsal retina (Figure 3.3 I). Therefore, GFP is a cone marker that is expressed in both M and S cones. It is important to note that loss of Ccdc136 did not appear to affect cone protein expression, localization and cone morphology.

Finally, to examine whether loss of Ccdc136 affected *Nrl*$^{-/-}$ cones in the transplantation donor mouse line, *Nrl*$^{-/-}$*;Ccdc136*$^{+/-}$ retinas were also double-stained for GFP and cone markers. In *Nrl*$^{-/-}$*;Ccdc136*$^{+/-}$ retinas the co-expression of GFP and CAr is easily observed in cell bodies (Figure 3.4 A). However, OS in *Nrl*$^{-/-}$ mice are stunted (Mears et al., 2001) making it difficult to observe GFP co-localization with cone outer segment markers, such as PNA, M opsin and S opsin. Yet, these cone markers are expressed, confirming the identity of these cells as cone photoreceptors (Figure 3.4 B-D). Furthermore, *Nrl*$^{-/-}$*;Ccdc136*$^{+/-}$ retinas fail to express the rod photoreceptor marker, rhodopsin (Figure 3.4 E). Therefore, the donor mice lack rod photoreceptors and instead have an overabundance of GFP-tagged cone photoreceptors.

3.4 GFP reporter is expressed in rod bipolar cells in *Ccdc136*$^{-/-}$ retinas

While the GFP reporter labels cone photoreceptors in the ONL, it also labels a subset of cells in the INL of adult *Ccdc136*$^{-/-}$ and *Nrl*$^{-/-}$*;Ccdc136*$^{+/-}$ retinas (Figure 3.1 B, D). Thus, Ccdc136 expression is not restricted to cone photoreceptors in the retina. Immunostaining with the rod bipolar cell marker, protein kinase C (PKC), shows co-localization with GFP+ cells in adult *Ccdc136*$^{-/-}$ and *Nrl*$^{-/-}$*;Ccdc136*$^{+/-}$ retinas (Figure 3.5).

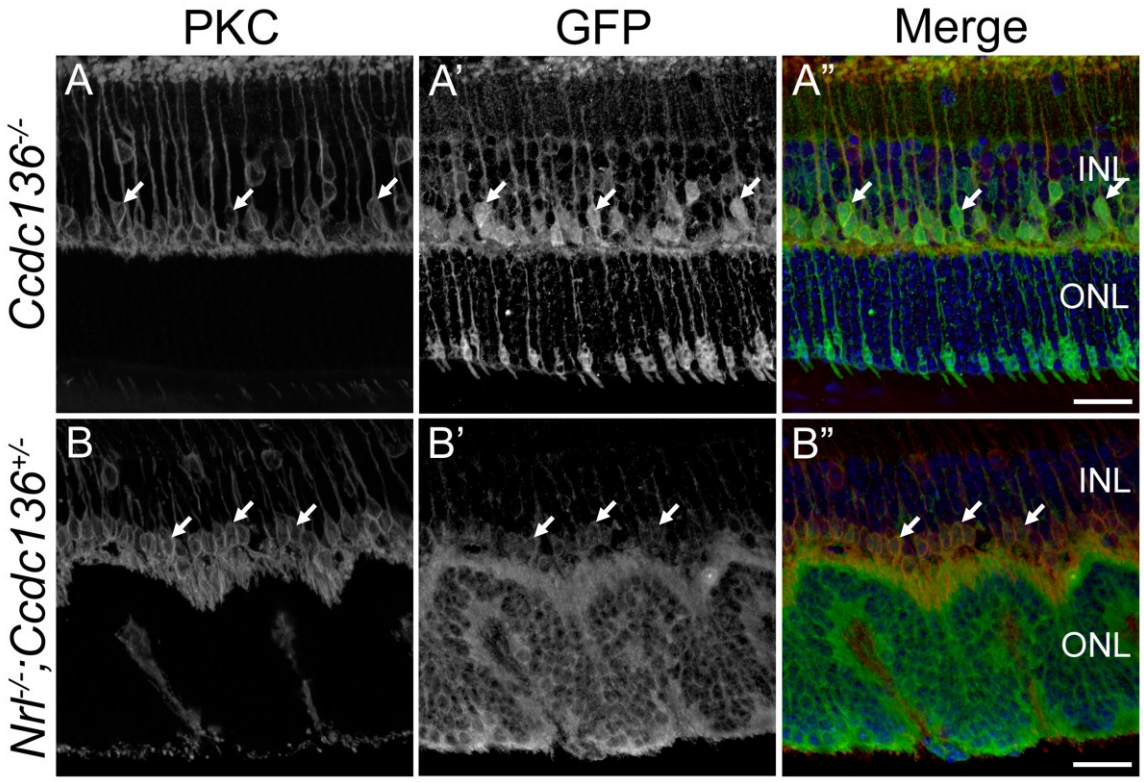

Figure 3.5 Expression of PKC in adult *Ccdc136*$^{-/-}$ and *Nrl*$^{-/-}$*;Ccdc136*$^{+/-}$ retinas. GFP+ cells in the INL co-localize with the rod bipolar cell marker, PKC. (A-B) PKC immunostaining (red); (A'-B') GFP labelling (green); (A"-B") three-channel merge with Hoechst nuclear stain (blue). ONL, outer nuclear layer; INL, inner nuclear layer. Scale bars, 25μm.

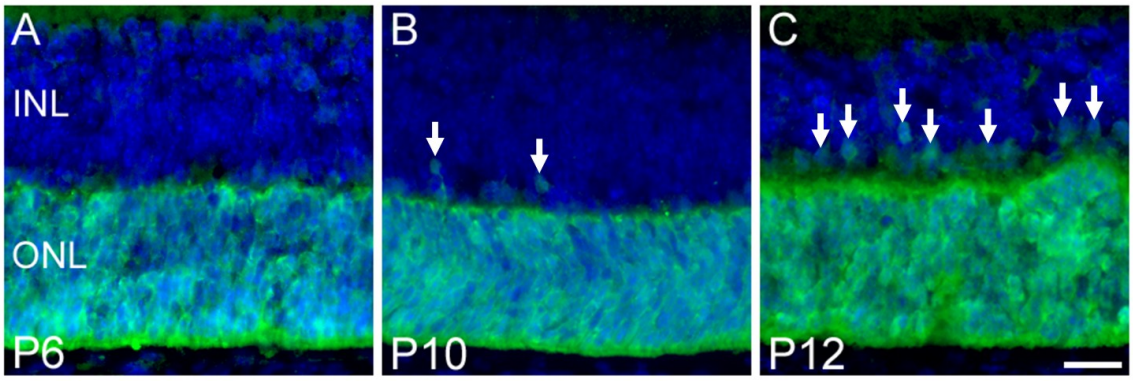

Figure 3.6 Expression of GFP in the INL of postnatal *Nrl*$^{-/-}$;*Ccdc136*$^{+/-}$ retinas. GFP+ cells in INL (arrows) begin to appear at (B) P10 and (C) P12 retinas. ONL, outer nuclear layer; INL, inner nuclear layer. Scale bar, 25μm.

Since the GFP reporter is not cone specific, problems may arise in transplanting GFP+ cells, which also include a portion of bipolar cells.

However, based on previous studies on rod transplantation optimal integration is observed with donor cells that are at a post-mitotic precursor stage (MacLaren et al., 2006). In *Nrl*$^{-/-}$*;Ccdc136*$^{+/-}$ retinas, the cone precursor population peaks at P1 to P6 as retinal histogenesis follows a rod developmental pathway (Oh et al., 2007). IHC analysis of *Nrl*$^{-/-}$*;Ccdc136*$^{+/-}$ retinas revealed that GFP+ cells in the INL develop after P6 (Figure 3.6), which is beyond the stage at which the donor cone precursor cells would be harvested for transplantation studies. Therefore, while GFP+ bipolar cells represent a factor to consider during analysis of transplanted eyes, they do not appear to be a problem at transplantation donor age.

3.5 *Nrl*$^{-/-}$*;Ccdc136*$^{+/-}$ mice have functional cone photoreceptors

Loss of Ccdc136 has the potential of affecting the function of the cells in which it is normally expressed. To examine whether Ccdc136 loss impacts cone photoreceptor function, electroretinograph (ERG) responses were recorded to compare retinal function between *Ccdc136*$^{-/-}$ mice on wildtype and *Nrl*$^{-/-}$ backgrounds. Both scotopic (rod dependent) and photopic (cone dependent) responses were examined.

Ccdc136$^{+/-}$ and *Ccdc136*$^{-/-}$ mice showed normal scotopic responses (Figure 3.7 A-B). Mice on a *Nrl*$^{-/-}$ background showed virtually no scotopic response at a low stimulus (Figure 3.7 C-D), which is characteristic of a retina lacking rods. At higher light stimuli, *Nrl*$^{-/-}$ and *Nrl*$^{-/-}$*;Ccdc136*$^{+/-}$ mice showed some response but had lower amplitudes compared to mice on a wildtype background. This slight scotopic response may be due to

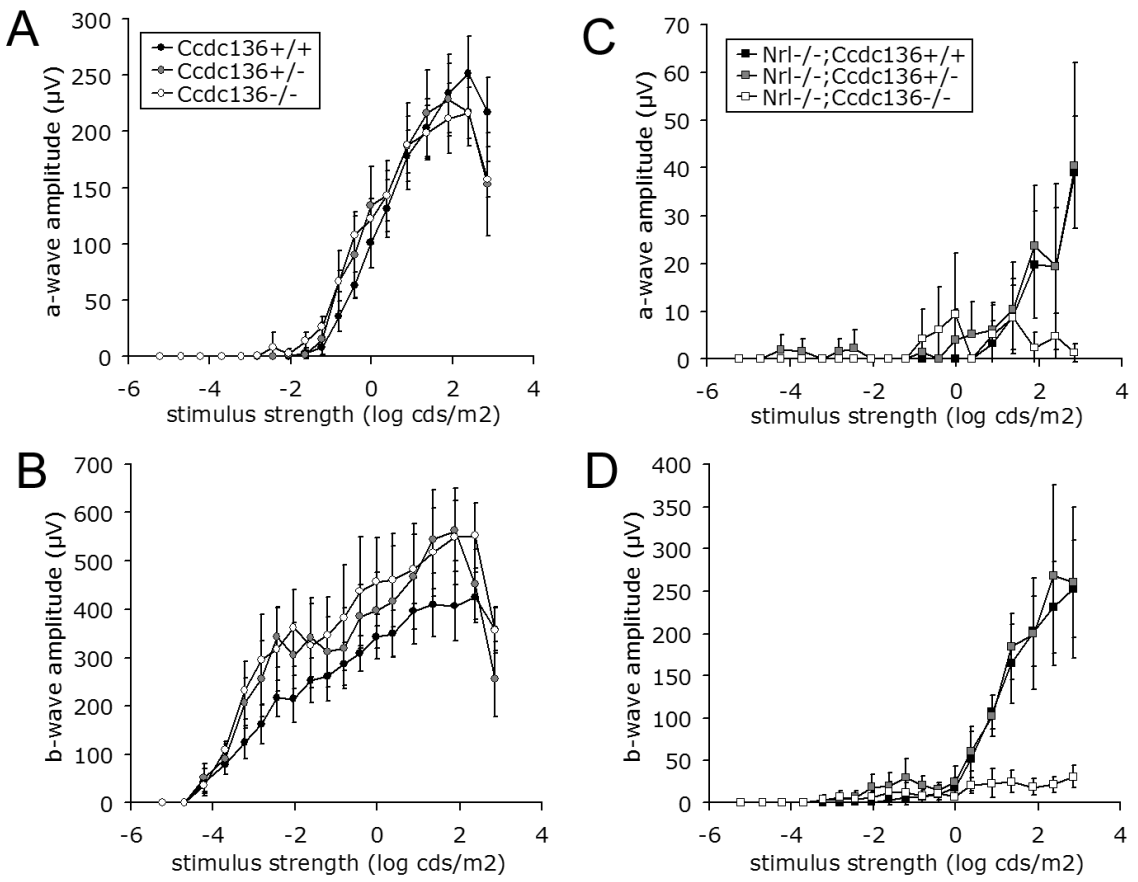

Figure 3.7 Comparison of ERG scotopic (rod-dependent) responses in *Ccdc136*$^{-/-}$ mice on (A-B) wildtype and (C-D) *Nrl*$^{-/-}$ backgrounds. Average values for each step are presented for scotopic a waves (A, C) and b waves (B, D) for mice of the indicated genotypes. *Ccdc136*$^{+/+}$ (n=6), *Ccdc136*$^{+/-}$ (n=7), *Ccdc136*$^{-/-}$ (n=6), *Nrl*$^{-/-}$*;Ccdc136*$^{+/+}$ (n=6), *Nrl*$^{-/-}$*;Ccdc136*$^{+/-}$ (n=7) and *Nrl*$^{-/-}$*;Ccdc136*$^{-/-}$ mice (n=6).

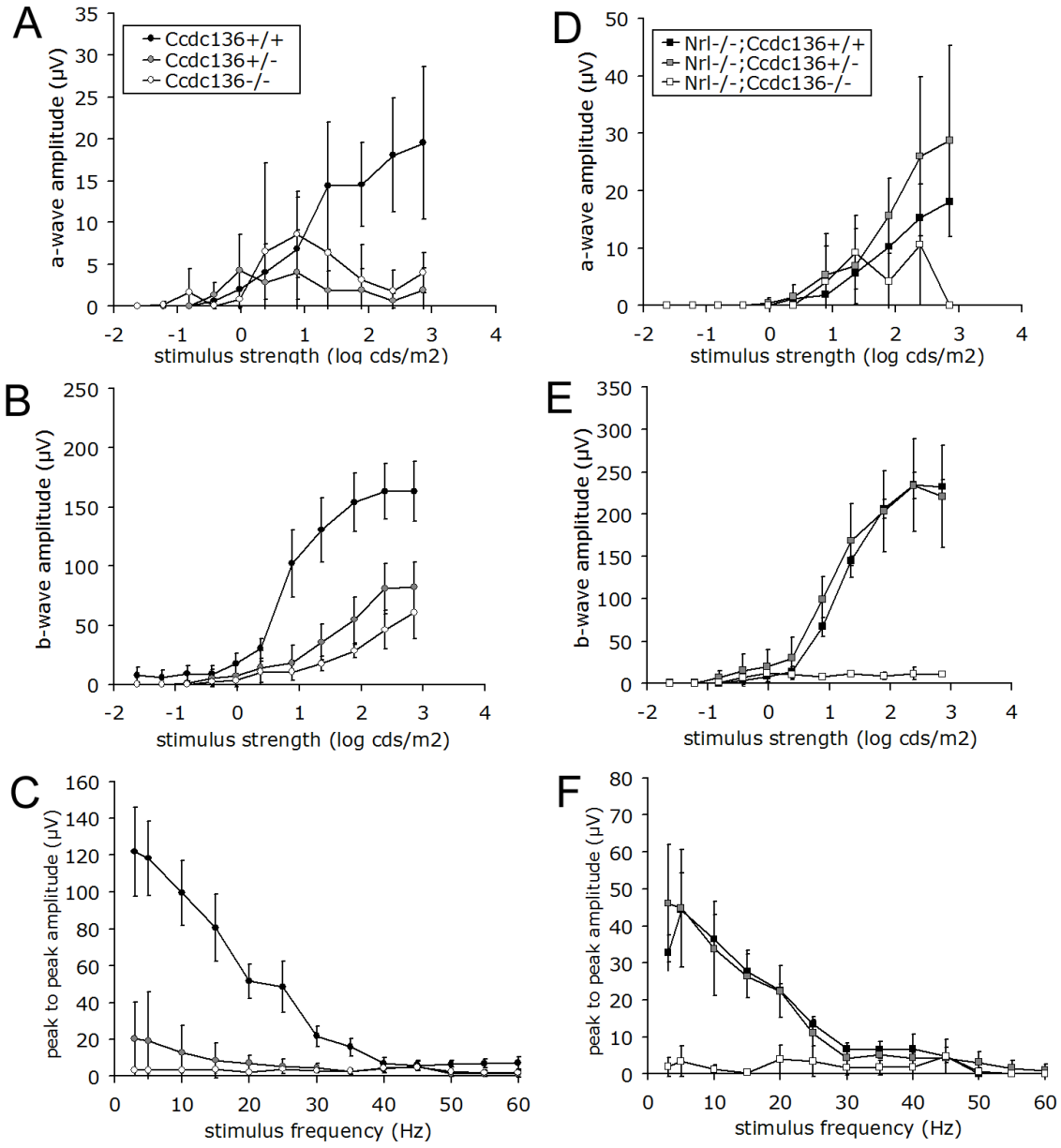

Figure 3.8 Comparison of ERG photopic (cone-dependent) responses in *Ccdc136*$^{-/-}$ mice on (A-C) wildtype and (D-F) *Nrl*$^{-/-}$ backgrounds. Average values for each step are presented for photopic a waves (A), b waves (B, D), and flicker frequency series (A) for mice of the indicated genotypes. *Ccdc136*$^{+/+}$ (n=6), *Ccdc136*$^{+/-}$ (n=7), *Ccdc136*$^{-/-}$ (n=6), *Nrl*$^{-/-}$*/Ccdc136*$^{+/+}$ (n=6), *Nrl*$^{-/-}$*;Ccdc136*$^{+/-}$ (n=7) and *Nrl*$^{-/-}$*/Ccdc136*$^{-/-}$ mice (n=6).

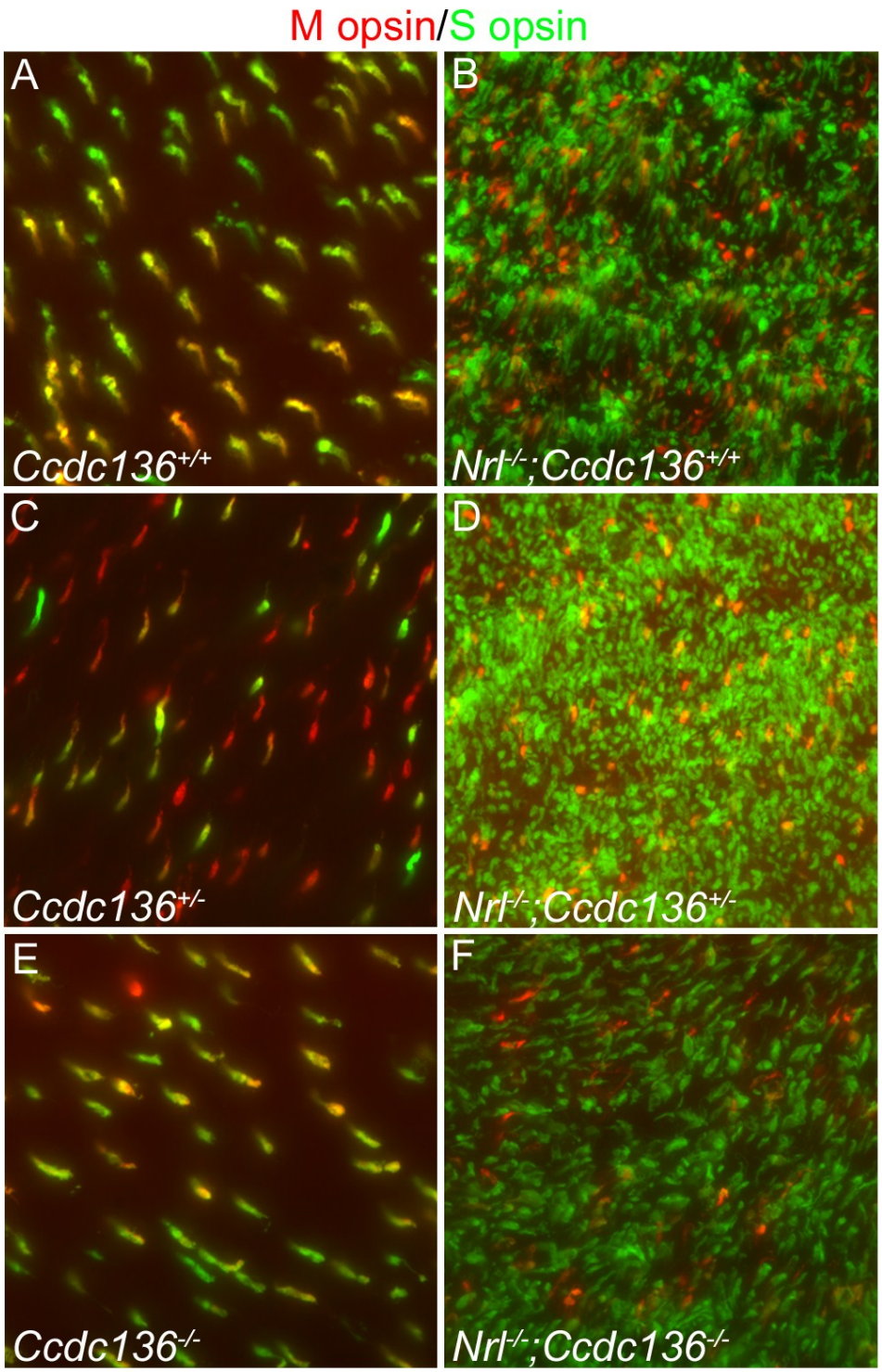

Figure 3.9 Expression of M and S opsin in retinal flatmounts from electroretinograph analyzed mice. IHC analysis for M opsin (red) and S opsin (green) shows cone outer segments (OS) in *Ccdc136*$^{-/-}$ retinas on a wildtype background (A, C, E) or on a *Nrl*$^{-/-}$ background (B, D, F).

a large number of cone photoreceptors responding to higher levels of stimulus in the *Nrl*$^{-/-}$ mice.

Meanwhile, photopic responses were significantly reduced in *Ccdc136*$^{+/-}$ and *Ccdc136*$^{-/-}$ mice relative to wildtype mice, indicating a loss of cone function (Figure 3.8 A-C). *Nrl*$^{-/-}$*Ccdc136*$^{-/-}$ also had significant reduction in photopic response (Figure 3.8 D-F). Loss of photopic vision was not due to cone photoreceptor degeneration as shown by presence of M and S opsin expressing cones in wholemount retinas from the mice that underwent ERG analysis (Figure 3.9).

Interestingly, the photopic response of *Nrl*$^{-/-}$*;Ccdc136*$^{+/-}$ donor mice was indistinguishable from *Nrl*$^{-/-}$ mice (Figure 3.8 D-F). *Nrl*$^{-/-}$*;Ccdc136*$^{+/-}$ showed an increased photopic response (Figure 3.8 D-E). Their flicker responses appear delayed (Figure 3.8 F), but this is characteristic of *Nrl*$^{-/-}$ mice. Therefore, Ccdc136 has no effect on rod function but is required for normal cone function. Furthermore, the rescue of cone function in the *Nrl*$^{-/-}$*;Ccdc136*$^{+/-}$ mice suggests a possible interaction between *Nrl* and *Ccdc136* genes may exist (see Appendix 1). Ultimately, the *Nrl*$^{-/-}$*;Ccdc136*$^{+/-}$ mice to be used as the transplantation donor model do have cone function despite loss of Ccdc136.

3.6 Dissociated *Nrl*$^{-/-}$*;Ccdc136*$^{+/-}$ cells have a large population of GFP+ cone precursors

As described above, donor cells used in transplantations integrate most efficiently when they are at the post-mitotic precursor stage (P1 to P6). To characterize the population of donor cells, P6 *Nrl*$^{-/-}$*;Ccdc136*$^{+/-}$ retinas were enzymatically dissociated and analyzed for various retinal cell markers. At P6, 60.1% (± 2.6%) of the dissociated retinal cells expressed GFP (Figure 3.10). By examining the GFP+ population of cells, none of

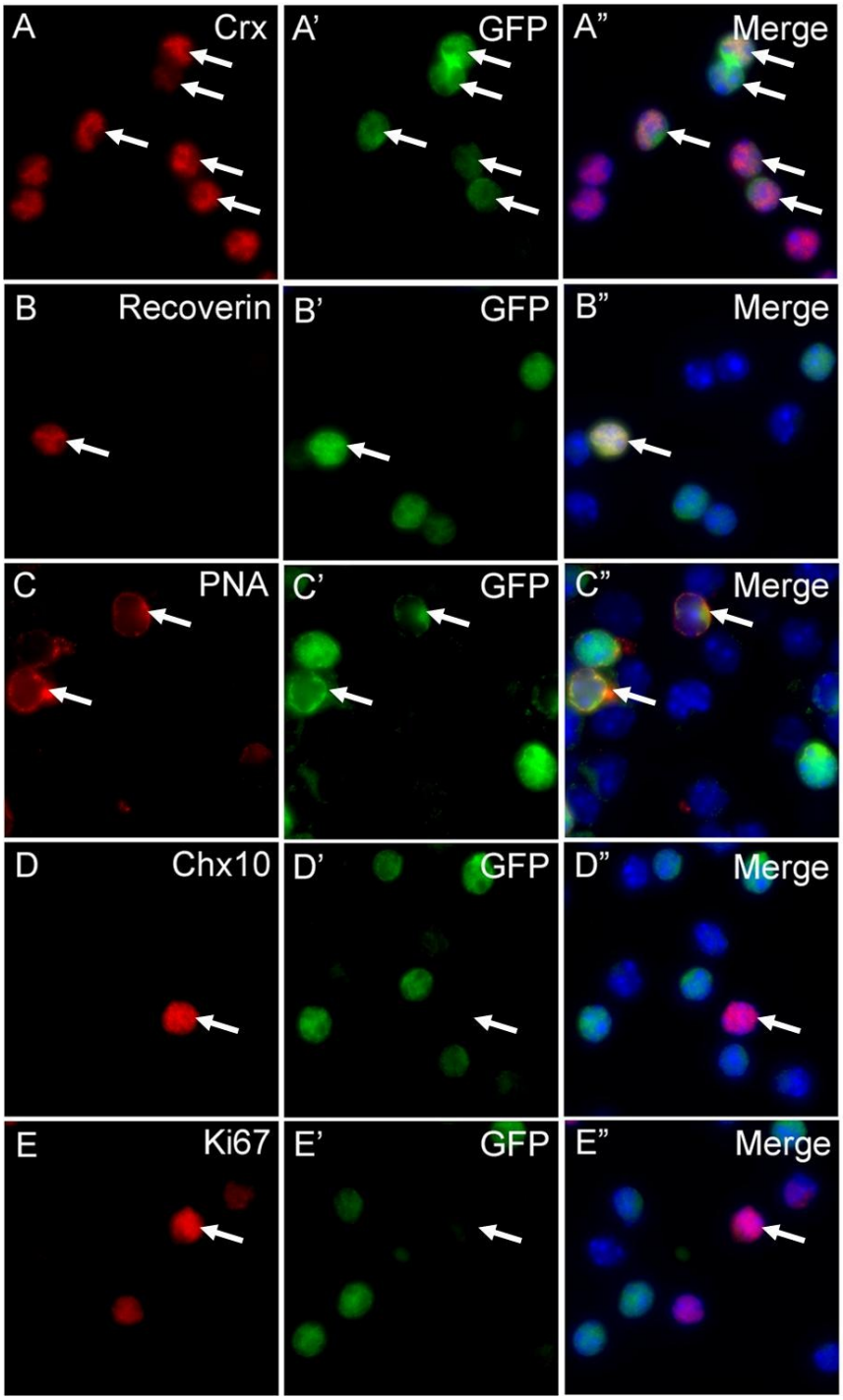

Figure 3.10 Expression of cell markers in P6 *Nrl*$^{-/-}$*;Ccdc136*$^{+/-}$ dissociated cells. (A-E) Target protein immunostaining (red); (A'-E') GFP labelling (green); (A"-E") three-channel merge with Hoechst nuclear stain (blue). (A-B) Crx and recoverin are photoreceptor markers. (C) PNA is a cone specific marker. (D) Chx10 is a bipolar marker. (E) Ki67 is a proliferation marker.

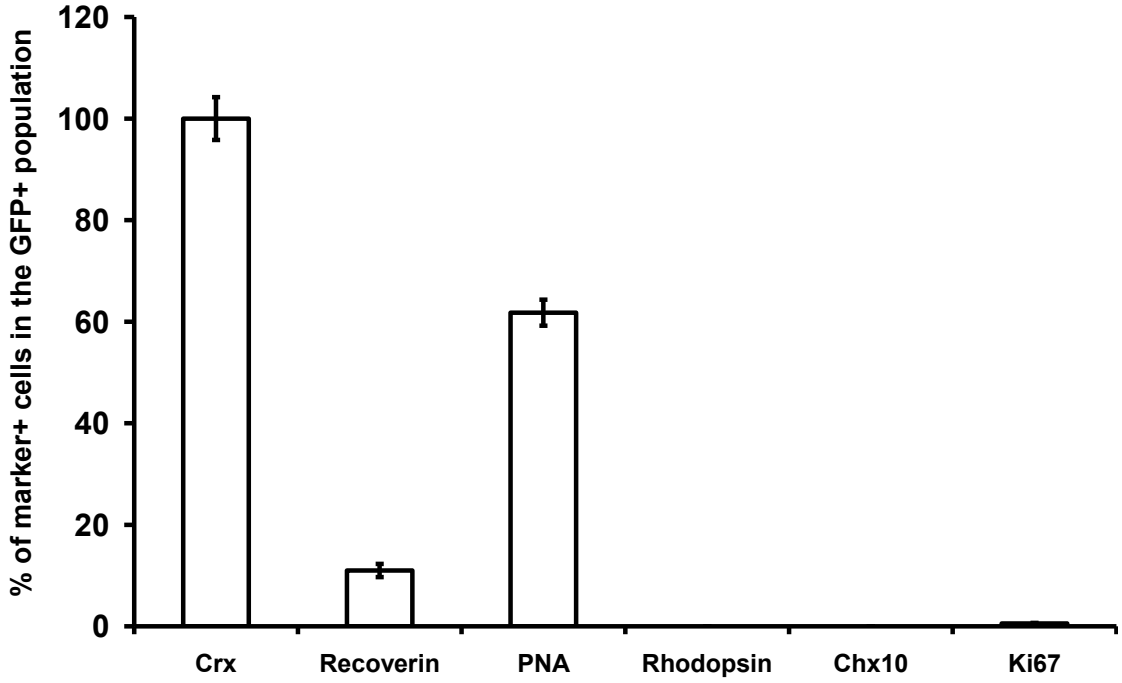

Figure 3.11 Percentage of cells showing positive immunostaining for indicated cell markers in the GFP+ cell population of P6 *Nrl*$^{-/-}$*Ccdc136*$^{+/-}$ retinas. Cells were dissociated by papain treatment and immunostained for the marker and GFP. Five fields of view were taken for each condition containing at least 200 cells/view. Cells were counted and expressed as a proportion of the GFP+ve cells. Bars represent mean + SEM (n=3).

these cells expressed either the pan-bipolar cell marker, Chx10 or the rod marker, rhodopsin (Figure 3.11). While the proliferation marker, Ki67, was expressed in only 0.5% GFP+ cells, 100% of GFP+ cells also expressed the photoreceptor marker Crx (Figure 3.11). Crx expression and absence of Ki67 expression indicates nearly all GFP+ cells post-mitotic photoreceptors at P6. Furthermore, about 10.9% of GFP+ cells co-expressed the photoreceptor marker recoverin (Figure 3.10), further confirming their identity as developing photoreceptors. More importantly, 61.8% of GFP+ cells expressed the cone specific marker, PNA (Figure 3.11). Other cone markers, such as M and S opsin, were not detectable at P6. PNA expression indicates that a large portion of donor cells are committed to a cone photoreceptor fate and absence of opsin expression indicates that cells are not yet mature photoreceptors. Therefore, a large proportion of GFP+ cells to be transplanted are post-mitotic cone precursors.

3.7 Transplantation of *Nrl*-EGFP rod precursors into adult recipient retinas

As a control to optimize the injection procedure, I transplanted rods from *Nrl*-EGFP mice, the donor mouse line used in many rod transplantation studies (Barber et al., 2013; Pearson et al., 2012; Singh et al., 2013). P4 *Nrl*-EGFP retinal cells were transplanted into 4 to 6 month adult recipient C57Bl/6, $Crx^{-/-}$ and $Nrl^{-/-}$ mice and retinas were harvested at 3 weeks. Transplantation was successful when cells were delivered to the subretinal space and was unsuccessful if no GFP+ cells were found in the subretinal space. Successful transplantations were observed in 6 of the total 13 transplanted mice. When all transplanted mice were included, including unsuccessful transplanations, numbers of integrated cells ranged from 24 to 244 cells/eye between the different recipient lines (Figure 3.12), averaging approximately 100 integrated cells/eye overall

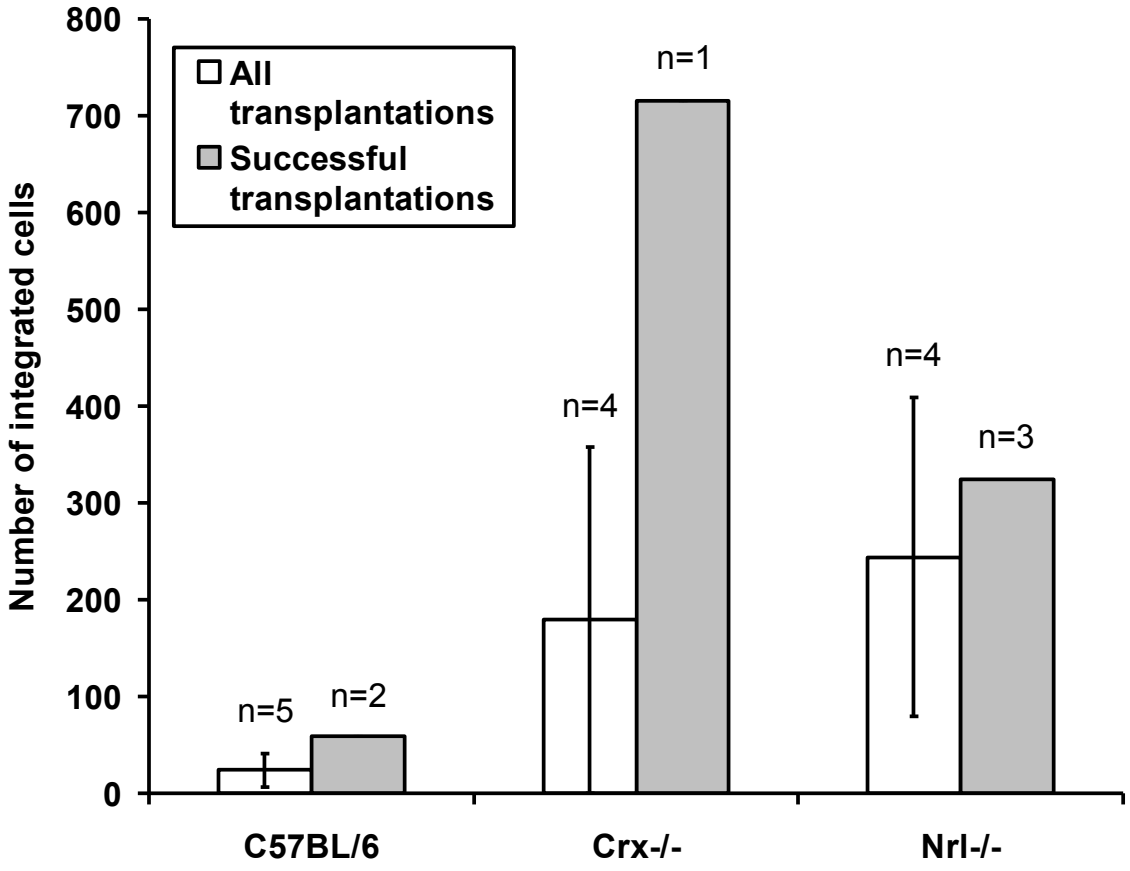

Figure 3.12 Number of integrated P4 *Nrl*-EGFP cells in recipient retinas. White bars indicate mean number of transplanted integrated cells for all transplanted mice ± SEM (C57BL/6, n=5; *Crx*$^{-/-}$, n=4, *Nrl*$^{-/-}$, n=4). Gray bars indicate mean number of integrated cells for successful transplantations only (C57BL/6, n=2; *Crx*$^{-/-}$, n=1; *Nrl*$^{-/-}$, n=3).

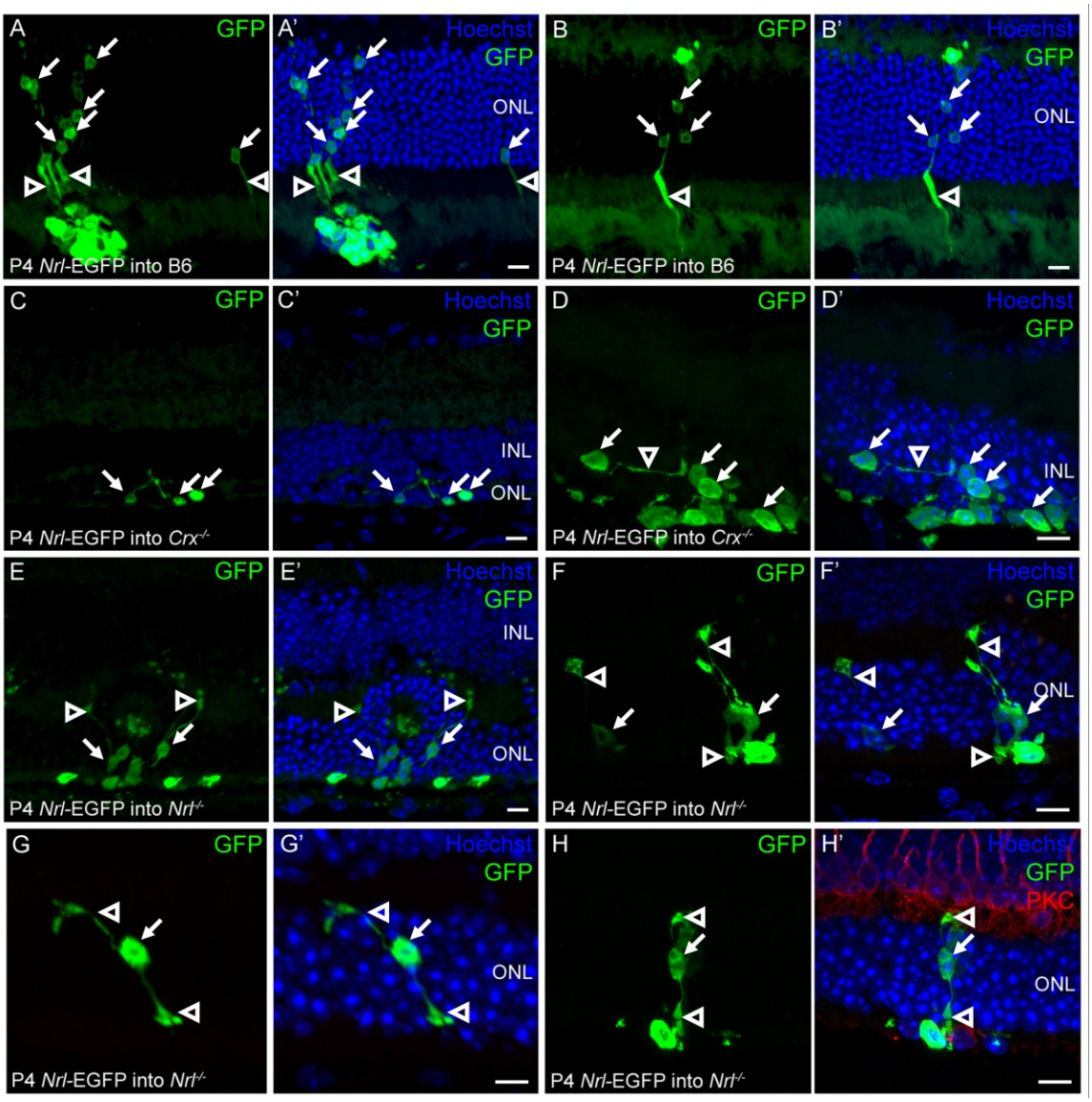

Figure 3.13 Integration of P4 Nrl-EGFP cells into adult recipient eyes. Low- (A, C, E) and high-magnification (B, D, F-H) images of P4 GFP+ cells integrating into C57BL/6, *Crx*$^{-/-}$ and *Nrl*$^{-/-}$ retinas. Arrows indicate cell body in host ONL, open arrowheads indicate a process. (H) Inner process of integrated cell extends to OPL synaptic layer, marked by PKC+ (red) dendrites of bipolar cells. ONL, outer nuclear layer; INL, inner nuclear layer; OPL, outer plexiform layer. Scale bars, 10μm.

(n=13 eyes). If only the successful transplantations were considered, integrated cells range between 59 to 716 cells/eye between the recipient lines, averaging 300 integrated cells/eye (n=6 eyes).

After 3 weeks, GFP+ cells had migrated into the host ONL in clusters. In C57BL/6 and *Nrl*$^{-/-}$ recipients, integrated cells formed apical and basal processes spanning the ONL (Figure 3.13 A-B, E-H). It also appeared that integrated cells had inner processes with terminals located in the IPL, where they may have synapsed with PKC+ bipolar cells in INL (Figure 3.13 H).

In *Nrl*$^{-/-}$ recipients, fewer than 5% of integrated cells appeared to be oriented laterally, due to the disorganization and rosettes in the ONL of *Nrl*$^{-/-}$ mice (Figure 3.13 E). In *Crx*$^{-/-}$ recipients, GFP+ cells also migrated into the host retina but did not extend well-formed processes, likely due to extreme degeneration *Crx*$^{-/-}$ retinas (Figure 3.13 C-D). Often, these recipient retinas had an ONL comprised of only one or two rows of nuclei (Figure 3.13 C) while others lacked an ONL completely (Figure 3.13 D). Therefore, the GFP+ cells integrated directly into the recipient INL (Figure 3.13 D). Despite this severe retinal degeneration, it did appear as if the transplanted cells did extend processes laterally (Figure 3.13 C-D).

3.8 Transplantation of *Nrl*$^{-/-}$*;Ccdc136*$^{+/-}$ cone precursors into adult recipient retinas

To assess integration of cones, P1 or P6 *Nrl*$^{-/-}$*;Ccdc136*$^{+/-}$ cells were transplanted into 2 to 10 month adult C57Bl/6 and *Crx*$^{-/-}$ recipient mice. After 3 weeks post transplantation, P6 donor cells exhibited low integration rates and poor morphology in adult recipient retinas (Figure 3.14). Donor cells were typically located in large aggregates in the subretinal space (Figure 3.14 A). Of the rare cells that were detected in

the host ONL, only GFP+ cell bodies were observed and rarely did cells exhibit apical or basal processes. In successfully transplanted C57Bl/6 (n=5) and *Crx*$^{-/-}$ (n=5) mice, a range of 100 to 600 cells integrated per eye (Figure 3.16).

Meanwhile, P1 *Nrl*$^{-/-}$*;Ccdc136*$^{+/-}$ donor cells appeared to migrate into the host ONL in clusters. Compared with P6 donors, integrated cells from P6 donors exhibited improved morphology with evidence of apical and basal processes in C57Bl/6 recipient retinas (Figure 3.15 A-B). In *Crx*$^{-/-}$ recipients, P1 GFP+ cells migrated into the host retina, however, they did not exhibit proper morphology. The P1 cells extended lateral processes that were not oriented properly along the apical basal axis of the host retina (Figure 3.15 C). Similar to the integrated *Nrl*-EGFP cells, *Nrl*$^{-/-}$*;Ccdc136*$^{+/-}$ cells migrated into the *Crx*$^{-/-}$ INL (Figure 3.15 C), likely due to the degeneration of the ONL in these retinas.

In C57Bl/6 recipients, IHC staining revealed examples of P1 cells that co-localized with the cone marker, PNA (Figure 3.15 D), indicating that they developed into cones with OS. However, other cell markers, such as M and S opsin, were not detected in integrated cells, indicating that they may not be producing the protein components necessary to convert light energy into a signal or may not be fully differentiating into cone photoreceptors. In successfully transplanted C57Bl/6 (n=5) and *Crx*$^{-/-}$ (n=5) mice, range of 100 to 300 cells integrated per eye (Figure 3.16).

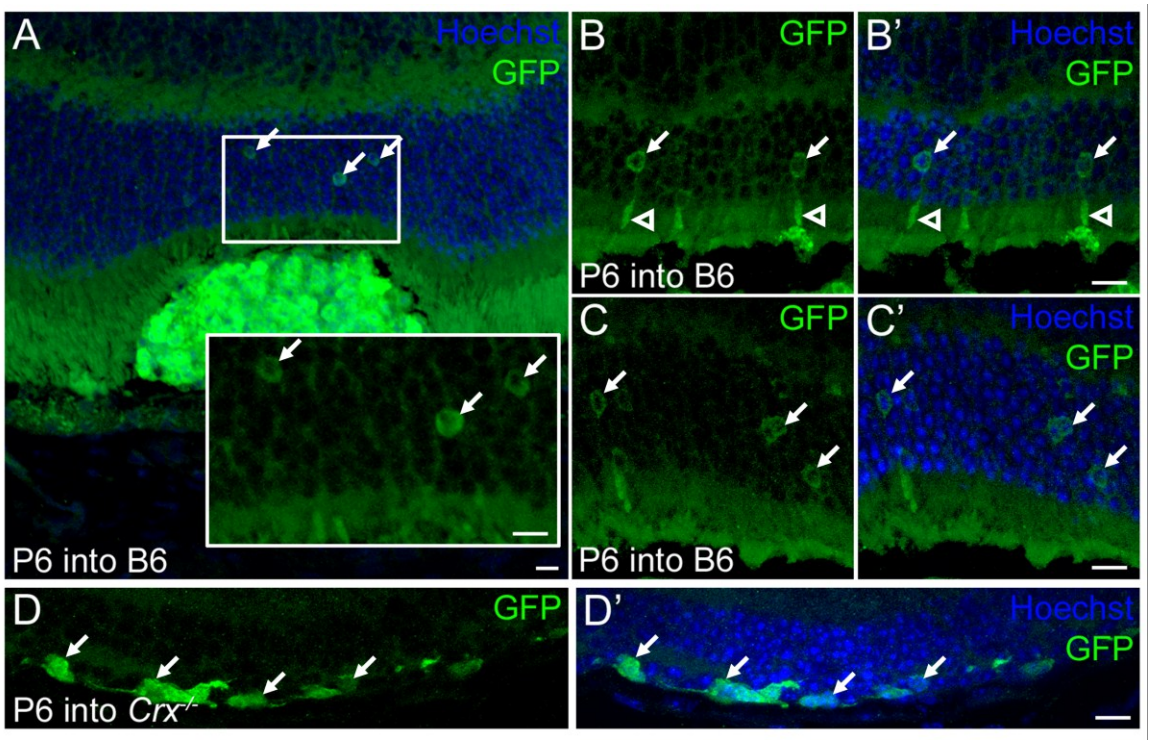

Figure 3.14 Integration of P6 *Nrl*$^{-/-}$;*Ccdc136*$^{+/-}$ cells into adult recipient eyes. (A) Low-magnification image of P6 cells into C57Bl/6 retinas. Inset shows a high magnification. High-magnification images of P6 cells integrated into (B-C) C57BL/6 retinas and (D) *Crx*$^{-/-}$ retinas. Arrows indicate GFP+ cell body, open arrowheads indicate a formed process. Scale bars, 10μm.

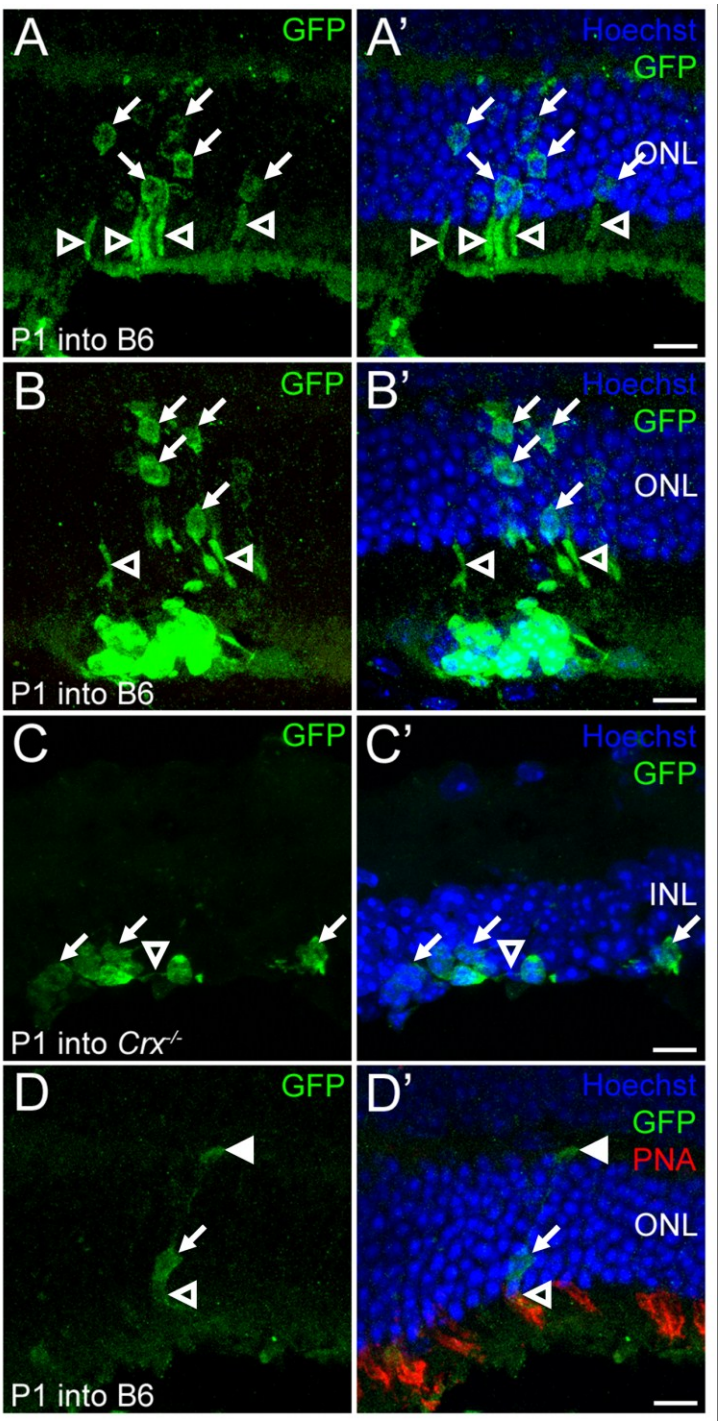

Figure 3.15. Integration of P1 *Nrl*$^{-/-}$*;Ccdc136*$^{+/-}$ cells into adult recipient eyes. GFP+ cells (green) integrate into ONL in (A-B, D) C57Bl/6 and (C) *Crx*$^{-/-}$ recipients. (D) A GFP+ cell co-localizes with the cone marker, PNA (red). Arrows indicate cell body in host ONL, open arrowheads indicate an outer process, closed arrowheads indicate a cone pedicle. ONL, outer nuclear layer; INL, inner nuclear layer. Scale bars, 10μm.

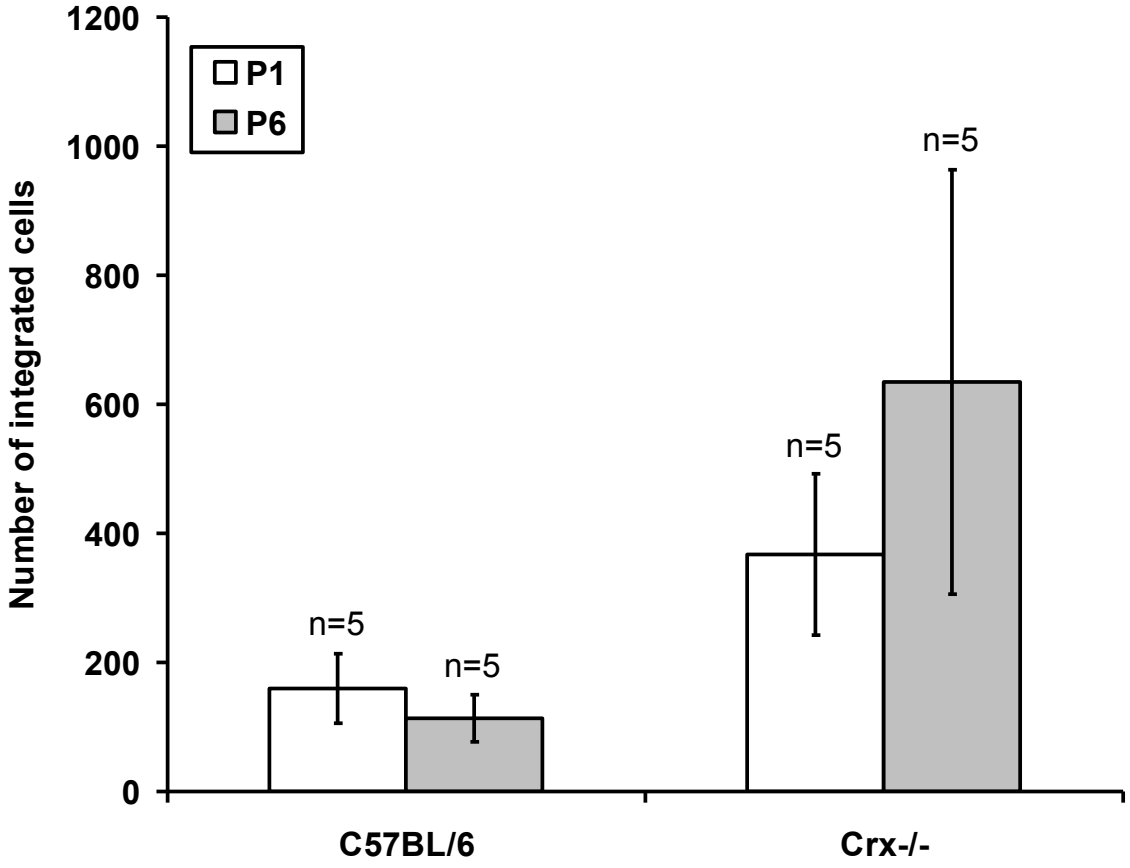

Figure 3.16 Number of integrated *Nrl*$^{-/-}$*;Ccdc136*$^{+/-}$ cells in each recipient eye. White bars indicate mean number of P1 integrated cells ± SEM. Gray bars indicate mean number of P6 integrated cells ± SEM. Values include integrated cells from successful transplantations only. C57BL/6, n=5; *Crx*$^{-/-}$, n=5.

Chapter 4. Discussion

The objective of this study was to develop a cone-reporter mouse model, characterize its suitability for cone transplantation and investigate cone photoreceptor transplantation to the retina. Currently, there is a lack of reliable cone-specific genetic markers to identify donor cells and allow for tracking after transplantation. Cone markers are often promoted by cone-specific phototransduction proteins that are not expressed until later stages. For example, transgenic mice expressing Cre recombinase under the human red/green pigment (HRGP) promotor exhibit Cre reporter activity specifically in M opsin-expressing cones (Le et al., 2004). However, expression does not initiate until P7-10 (Le et al., 2004). This is unsuitable for transplantations because donor cells must be acquired at the post-mitotic precursor stage (<P6). Other cone-specific genes that may be targeted, like thyroid hormone receptor β2 (TRβ2), are expressed early (E11) but expression declines after P10 (Ng et al., 2009). Again, this is unsuitable because donor cells must have a marker that allows for tracking several weeks post injection.

The identification of a novel cone gene, Ccdc136, allowed us to generate a Ccdc136-GFP reporter mouse line which we crossed onto an *Nrl*$^{-/-}$ background to provide us with a cone-enriched retina mouse model. *Ccdc136*$^{-/-}$ mice showed GFP reporter expression in cone but not rod photoreceptors, and also rod bipolar cells. At stages suitable for donor transplantation (P0-P6), *Nrl*$^{-/-}$*;Ccdc136*$^{+/-}$ mice expressed GFP in only cone photoreceptor precursors. Donor cells were used in transplantation studies and integration was observed in adult mouse retinas.

4.1 Ccdc136 is a marker of cone but not rod photoreceptors

This analysis shows that Ccdc136 is marker for cones. In adult wildtype retinas, Ccdc136 transcript is present in cone photoreceptors and is enriched in the cone-only *Nrl*$^{-/-}$ retinas. In adult *Ccdc136*$^{-/-}$ mice, the GFP reporter is expressed in cone photoreceptors as confirmed by co-localization with cone arrestin, PNA, M and S opsin expression. The GFP signal is observed throughout the cone cell, in the cell body and inner and outer processes. However, it is not observed in cone OS, possibly because reporter GFP protein is generated in the cell body and is not properly transported through the narrow cilium to the OS. Despite the loss of Ccdc136, cone protein expression and localization is comparable to wildtype cones.

By crossing the *Ccdc136*$^{-/-}$ mice onto an *Nrl*$^{-/-}$ background, enrichment of cone photoreceptors is observed. GFP is found in all cells in the ONL and is found to co-localize with cone markers. Rhodopsin is not expressed in *Nrl*$^{-/-}$*;Ccdc136*$^{+/-}$ retinas, confirming them as a cone-only model. This model appears suitable for cone transplantation studies as it has a large population of GFP labelled cones.

4.2 Ccdc136 is a marker of rod bipolar cells

Ccdc136 is not a cone-specific marker, labelling rod bipolar cells in addition to cones. In adult *Ccdc136*$^{-/-}$ and *Nrl*$^{-/-}$*;Ccdc136*$^{+/-}$ retinas, GFP+ cells co-localize with the rod bipolar marker, PKC. The concern here is that GFP+ rod bipolar cells may be transplanted with the GFP+ cones, particularly if donor cells are not enriched for cone precursors. Since the ultimate goal is to restore cone function in degenerating retinas, any GFP+ bipolar cell integration may interfere with evaluation of cone integration and vision rescue. Fortunately, in *Nrl*$^{-/-}$*;Ccdc136*$^{+/-}$ retinas at donor age of P6 or younger, GFP+ cells

are only found in the ONL as cone photoreceptors precursors and not in the INL. In fact, GFP+ rod bipolar cells do not begin to develop until P10. Therefore, at the time of transplantation, only GFP+ cells of photoreceptor identity exist. This does not exclude the possibility that transplanted GFP-negative bipolar cell precursors may develop into GFP+ bipolar cells in the recipient mouse retina. To address this concern, GFP+ integrated cells should be examined for co-expression of bipolar cell markers in transplanted retinas. To avoid the GFP+ bipolar cell issue, cells that give rise to bipolar cells can be reduced from the donor cells by sorting to enrich GFP+ cones prior to transplantation.

4.3 Donor *Nrl*$^{-/-}$;*Ccdc136*$^{+/-}$ cells have a large population of cone precursors

Rod transplantation studies have demonstrated that donor cells from both embryonic (progenitor cells) and adult retinas (mature, differentiated cells) do not integrate successfully (MacLaren et al., 2006). Instead, photoreceptors integrate best when post-mitotic precursors are transplanted. In wildtype mouse retinas, cone photoreceptor development begins early at E11 and rod development takes place over embryonic to postnatal stages, but peaks post-natally (Young, 1985). In *Nrl*$^{-/-}$ retinas, cone development takes place differently than in wildtype retinas. Endogenous cone photoreceptors development takes place as described. Early on, some RPCs commit to cone precursor fate to develop into M and S cones. However, the difference lies in the precursors destined to become rod photoreceptors. Nrl expression is necessary to direct post-mitotic photoreceptor precursors to the rod fate while also inhibiting cone developement. In the absence of Nrl, it is believed that the production of photoreceptor precursor development is normal but the fate of these cells is driven towards cones

instead of rods (Hao et al., 2012; Oh et al., 2007). Therefore, in *Nrl*$^{-/-}$ mice the majority of cones develop post-natally.

In P6 *Nrl*$^{-/-}$*;Ccdc136*$^{+/-}$, 60% of donor cells express GFP. These cells are post-mitotic, as confirmed by lack of co-localization with Ki67. Furthermore, all GFP+ cells express Crx, which is a transcription factor which is present in post-mitotic photoreceptor precursors (Swaroop et al., 2010). However, some Crx+ cells are GFP negative, indicating some photoreceptor precursor cells do not express GFP. This suggests Ccdc136, reported by GFP expression, is not initiated until after Crx expression. When comparing GFP expression in P6 versus adult retinal cells, the proportion of GFP+ cells increases from about 60% to about 75% (see Appendix 3). Furthermore, not all GFP+ cells express cone markers at P6. Over half of the GFP+ cells also express PNA, identifying them as being committed to a cone photoreceptor fate. However, none of the GFP+ cells express mature cone proteins, such as M or S opsin. Therefore, Ccdc136 is expressed at a developmental stage some point after cell cycle exit in photoreceptor precursors but prior to expression of mature cone proteins. Overall, this analysis shows donor retinas have a population of GFP+ post-mitotic photoreceptor precursors, destined to become cone photoreceptors.

4.4 *Nrl*$^{-/-}$*;Ccdc136*$^{+/-}$ mice have functional cone photoreceptors

The ultimate goal of cone transplantation is to restore photopic vision in the degenerating retina. Thus, it is important that the donor mice have functioning cone photoreceptors. ERGs responses show that *Ccdc136*$^{+/-}$ and *Ccdc136*$^{-/-}$ mice exhibit a significant reduction in cone-mediated vision. *Nrl*$^{-/-}$*Ccdc136*$^{-/-}$ mice also have significantly reduced photopic responses. Since wholemount IHC analysis of retinas from

the same mice that underwent ERG confirmed the presence of M and S opsin expressing cones, this specific loss of the photopic ERG is not secondary to cone degeneration.

While loss of Ccdc136 does not alter expression of cone arrestin and M and S opsin (Figure 3.3), further investigation has revealed that there is a significant reduction in Pde6c protein levels in *Ccdc136*$^{-/-}$ mice, as demonstrated by IHC (see Appendix 2). Pde6c is a protein component in the phototransduction cascade and is essential for cone function. Mutations in *PDE6C* in humans cause achromatopsia, a condition associated with profound cone-dependent vision loss (Chang et al., 2009; Thiadens et al., 2009). Therefore, loss of cone response in *Ccdc136*$^{-/-}$ mice is associated with loss of Pde6c, suggesting that Ccdc136 may be involved in Pde6c regulation. The mechanism of this regulation, whether it be at the transcriptional or posttranscriptional level, is the subject of ongoing investigation.

In contrast, *Nrl*$^{-/-}$*;Ccdc136*$^{+/-}$ donor mice appear to have a rescue in photopic vision, as ERG responses were identical to *Nrl*$^{-/-}$ mice. The rescue in visual function in *Nrl*$^{-/-}$*;Ccdc136*$^{+/-}$ mice is associated with the presence of Pde6c staining, which has the same staining intensity as in *Nrl*$^{-/-}$ mice. The rescue of cone function in the *Nrl*$^{-/-}$*;Ccdc136*$^{+/-}$ mice suggests that an interaction between *Nrl* and *Ccdc136* genes may exist (See Appendix 1). Regardless of the mechanism behind this interaction, *Nrl*$^{-/-}$*;Ccdc136*$^{+/-}$ donor mice do have functioning cones that may be used to restore cone vision in transplantation studies.

4.5 *Nrl*-EGFP rod precursors successfully integrate into adult retinas

One of the most challenging aspects of the transplantation procedure is injection technique and successful delivery of cells to the subretinal space. To optimise this

procedure, *Nrl*-EGFP donor cells were used, as they are known to successfully integrate into adult mouse retinas (Barber et al., 2013; Pearson et al., 2012; Singh et al., 2013).

A caveat in this analysis was that because this was performed as a pilot study only a limited number of mice were transplanted (n=13). However, transplantations were successful in about 50% of injected mice, where *Nrl*-EGFP cells were delivered to the subretinal space of the recipient mouse. The donor cells behaved as predicted by migrating into the host ONL and extending processes. An average of 300 cells integrated per eye was observed. Variability in integration rates was high, with numbers of integrated cells ranging from as few as 59 cells per eye up to 716 cells per eye. While there were not enough successfully transplanted mice to determine statistical significance in integration rates between recipient mouse lines, these numbers are comparable to initial studies of rod transplantation, where the range was reported to be 200-800 cells integrating per eye (MacLaren et al., 2006). By replicating these results, it can be concluded that my injection technique successfully delivers cells to the subretinal space allowing for integration into adult retinas.

4.6 *Nrl*$^{-/-}$;*Ccdc136*$^{+/-}$ cone precursors successfully integrate into adult retinas

The *Nrl*$^{-/-}$;*Ccdc136*$^{+/-}$ donor cells were transplanted to the retina using an identical method as reported for rods. *Nrl*$^{-/-}$;*Ccdc136*$^{+/-}$ donor cells were observed to integrate into the host retinas numbers similar to that reported for rods (100-600 cells per eye). Morphology of integrated cells appears to improve with a younger donor age. Nearly all integrated P1 donor cells extended processes while P6 donor cells were rarely observed to have extended processes. Occasionally, P1 cells were found to co-localize with the cone marker, PNA. However, none of the integrated cells expressed M or S opsin, which are

necessary for cone function, indicating they had not fully differentiated into cone photoreceptors or they were not able to produce the appropriate proteins to their OS necessary for phototransduction.

Given that GFP+ integrated cells were observed without PNA expression, it must be considered that they may not be cones. It is possible that they may be bipolar cells, which have turned on GFP as they developed in the host retina. This is unlikely as integrated cell morphology does not resemble a bipolar cell with dendrites and no PKC+ cells were found in the host ONL. It is also possible that once integrated, the host retina promotes development of the *Nrl*$^{-/-}$*;Ccdc136*$^{+/-}$ cells into rod photoreceptors. In C57Bl/6 recipients, the integrated cells are observed throughout different rows of the host ONL, as rods would be, and are not confined exclusively to the apical side where cones are typically be found. Rod markers on integrated cells cannot be examined in C57Bl/6 recipients because of the interference with signal from the endogenous host rods, which would make it difficult to confirm cell fate after integration. It is also difficult to analyze integrated cells in *Crx*$^{-/-}$ recipients because they lack the retinal structure for integrated cells to display proper morphology. Therefore, a different recipient model may be necessary to investigate cone transplantation and their fate after integration.

In terms of integration rates, there were only a small number of successful transplantations with a high degree of variability in the number of engrafted cells, similar to *Nrl*-EGFP transplantations. Therefore, I cannot conclude whether there is a significant difference in integration rates between C57Bl/6 and *Crx*$^{-/-}$ recipients. Although due to the extreme degeneration of the ONL in *Crx*$^{-/-}$ mice, it does appear that donor cells incorporate into these retinas more readily. Likewise, I cannot confirm whether recipient

age impacts integration. Both young and old recipients were used, however, due to the variability in integration rates, no significant difference was found in age of recipient. Despite these constraints, this analysis has given a baseline integration rate (in the hundreds of cells), which we can use to further optimise cone transplantation.

4.7 Future directions

This analysis showed that the *Nrl*$^{-/-}$*;Ccdc136*$^{+/-}$ mouse line has a retina enriched with functional GFP labelled cones making it suitable donor line for investigating cone transplantation. Admittedly, *Nrl*$^{-/-}$ cones are not perfect; the Nrl$^{-/-}$ background creates cods instead of true cones. Therefore, while these cells are suitable for proof-of-concept cone transplantation studies, endogenous cones would be ideal donor cells. Unfortunately, while the *Ccdc136*$^{-/-}$ mice have endogenous GFP labelled cones, the gene trap of this locus results in loss of cone function. GFP+ cells from *Ccdc136*$^{-/-}$ mice would not be suitable for transplantation studies as these cells would not restore cone response in degenerating retinas. However, *Ccdc136* is a reliable cone-specific genetic marker because it is expressed at early stages (E13) and continues to be expressed in adult retinas. To take advantage of this gene, a mouse model could be generated with co-expression of *Ccdc136* and a reporter gene using a bicistronic vector, preventing disruption of *Ccdc136* and cone dysfunction.

Integration was observed in this study, yet integration rates for both rods and cones remain low with only a few hundred cells integrating from the 200,000 cells that were transplanted (0.1% of cells integrate). However, cone transplantation is being investigated with the ultimate goal of restoring cone vision in degenerating retinas. It is unknown how many cones will be needed to integrate to recover vision. In rod transplantation studies, approximately 10,000 integrated rods can restore vision in

recipient mice that lack rod function (Pearson et al., 2012). Restoration of cone vision may be attained with fewer integrated cells as normal retinas function with only 3% cones. The human foveal pit contains 20,000 cones (Curcio et al., 1990), therefore, in clinical applications, this may be a number to target. Regardless, increasing efficiency of integration rates is necessary before rescue in vision can be tested.

Increasing integration efficiency may be achieved by targeting barriers at the different steps of integration. When donor cells are transplanted, they must survive in the environment of the recipient eye. It is possible to increase survival of transplanted cells using X-linked inhibitor of apoptosis (XIAP) as adjunctive therapy (Yao et al., 2011). Immune suppression of recipients has also led to an increase in transplanted cell survival (West et al., 2010).

The transplanted cells must then separate from the rest of the injected cells in the subretinal space. Based on my injections, it appears that unsorted *Nrl*$^{-/-}$*;Ccdc136*$^{+/-}$ cells remain in large aggregates and organize into rosette structures within these aggregates, especially P6 donor cells. This observation suggests that these cells prefer to form connections with the cells surrounding them then to migrate into a foreign host retina. I hypothesize that by injecting a homogenous population photoreceptor precursors, this aggregation may be avoided. In fact, one of the most promising methods to increase integration rates appears to be cell sorting. By enriching the photoreceptor precursor population based on fluorescence of reporter proteins, such as GFP, or based on surface antigens, significant increases in integration are observed (Eberle et al., 2011; Lakowski et al., 2010; Lakowski et al., 2011). Preliminary results demonstrate GFP+ *Nrl*$^{-/-}$*;Ccdc136*$^{+/-}$ cells can be quantified by flow cytometry. Approximately 55-60% of cells

are GFP+ supporting the quantification from immunostaining data (compared to 60%) (see Appendix 3). Furthermore, *Nrl*$^{-/-}$*;Ccdc136*$^{+/-}$ GFP+ cells can be successfully enriched using FACS (>97% GFP+) (See Appendix 3). Therefore, the effects of cell sorting on integration will be evaluated in future transplantation experiments.

Another barrier in donor cell migration into the host retina is the outer limiting membrane (OLM). The OLM is a physical barrier on the apical side of the ONL comprised of adherens junctions between photoreceptors and Müller glia (Omri et al., 2010). Methods to increase the efficiency of photoreceptor integration may lie in targeting the OLM. Disruption of this barrier using pharmacological agents or by disrupting adherens junction proteins significantly increases integration rates (Pearson et al., 2010; West et al., 2008). It is important to note that the C57Bl/6 mice used in this study had compromised OLM integrity. The C57Bl/6N (Charles River) substrain used contains the retinal degeneration 8 (*rd8*) mutation which affects the Crumbs Homolog 1 (*Crb1*) gene (Mattapallil et al., 2012). *Crb1* encodes the Crb1 protein involved in adherens junctions and mutations in this gene cause disruptions in the OLM (Mattapallil et al., 2012), suggesting C57Bl/6N mice should show improved integration rates. However, as previously stated, integration rates were too variable to draw any conclusions.

Furthermore, numbers of integrated cells are only one issue to consider. Another important factor is that integrated cells must also mature into functional cones in the host retina. *Nrl*$^{-/-}$*;Ccdc136*$^{+/-}$ cells have shown potential of maturing into cones after integration. However, to recover vision, cells must mature into cones with the proper protein components for phototransduction, such as cone-specific opsins, transducin, and

phosphodiesterase. Cone cell differentiation could be promoted with the addition of various growth factors. Addition of thyroid hormone to dissociated rat retinal cell cultures resulted in larger proportions of cone cells generated (Kelley et al., 1995). Therefore, thyroid hormone may be injected with donor cells to help promote cone development.

Chapter 5. General conclusions

In Canada, retinal degenerative diseases are the leading cause of blindness. Prevalence of these diseases, such as AMD, is increasing with the aging population. Therefore, this study sought to develop a cone-reporter mouse model to investigate cone transplantation. Ccdc136 was determined to be a cone marker. In mice *Ccdc136*$^{-/-}$ and *Nrl*$^{-/-}$*;Ccdc136*$^{+/-}$ mice, the GFP reporter is expressed in cones but not rod photoreceptors. GFP+ bipolar cells are also found in adult retinas, but not at donor age. *Nrl*$^{-/-}$*;Ccdc136*$^{+/-}$ mice have an enrichment of GFP-labelled cone photoreceptors, which are functional despite loss of Ccdc136, making them a suitable donor model for cone transplantation. When transplanted, cone precursors integrate into adult mouse retinas in numbers comparable to rod transplantations. P1 donor cells also show potential of maturing into cone photoreceptors. This study provides a baseline rate of integration which can be optimized to increase numbers of integrating cells. Ultimately, once consistently high integration of cone photoreceptors is achieved, restoration of vision may be tested by electrophysiological and behavioural tests.

REFERENCES

Abugreen, S., Muldrew, K. A., Stevenson, M. R., VanLeeuwen, R., DeJong, P. T., & Chakravarthy, U. (2003). CNV subtype in first eyes predicts severity of ARM in fellow eyes. *Br J Ophthalmol, 87*(3), 307-311.

Ahuja, A. K., Yeoh, J., Dorn, J. D., Caspi, A., Wuyyuru, V., McMahon, M. J., . . . Dacruz, L. (2013). Factors Affecting Perceptual Threshold in Argus II Retinal Prosthesis Subjects. *Transl Vis Sci Technol, 2*(4), 1. doi: 10.1167/tvst.2.4.1

Akimoto, M., Cheng, H., Zhu, D., Brzezinski, J. A., Khanna, R., Filippova, E., . . . Swaroop, A. (2006). Targeting of GFP to newborn rods by Nrl promoter and temporal expression profiling of flow-sorted photoreceptors. *Proc Natl Acad Sci U S A, 103*(10), 3890-3895. doi: 10.1073/pnas.0508214103

Ali, R. R., & Sowden, J. C. (2011). Regenerative medicine: DIY eye. *Nature, 472*(7341), 42-43. doi: 10.1038/472042a

Arditi, A., & Rosenthal, B. (1998). *Developing an objective definition of visual impairment.* Paper presented at the Vision '96: International Low Vision Conference, Madrid, Spain.

Bainbridge, J. W., Smith, A. J., Barker, S. S., Robbie, S., Henderson, R., Balaggan, K., . . . Ali, R. R. (2008). Effect of gene therapy on visual function in Leber's congenital amaurosis. *N Engl J Med, 358*(21), 2231-2239. doi: 10.1056/NEJMoa0802268

Bak, M., Girvin, J. P., Hambrecht, F. T., Kufta, C. V., Loeb, G. E., & Schmidt, E. M. (1990). Visual sensations produced by intracortical microstimulation of the human occipital cortex. *Med Biol Eng Comput, 28*(3), 257-259.

Barber, A. C., Hippert, C., Duran, Y., West, E. L., Bainbridge, J. W., Warre-Cornish, K., . . . Pearson, R. A. (2013). Repair of the degenerate retina by photoreceptor transplantation. *Proc Natl Acad Sci U S A, 110*(1), 354-359. doi: 10.1073/pnas.1212677110

Bassett, E. A., & Wallace, V. A. (2012). Cell fate determination in the vertebrate retina. *Trends Neurosci, 35*(9), 565-573. doi: 10.1016/j.tins.2012.05.004

Berson, E. L., Rosner, B., Sandberg, M. A., Hayes, K. C., Nicholson, B. W., Weigel-DiFranco, C., & Willett, W. (1993). A randomized trial of vitamin A and vitamin E supplementation for retinitis pigmentosa. *Arch Ophthalmol, 111*(6), 761-772.

Bi, A., Cui, J., Ma, Y. P., Olshevskaya, E., Pu, M., Dizhoor, A. M., & Pan, Z. H. (2006). Ectopic expression of a microbial-type rhodopsin restores visual responses in mice with photoreceptor degeneration. *Neuron, 50*(1), 23-33. doi: 10.1016/j.neuron.2006.02.026

Bok, D. (1993). The retinal pigment epithelium: a versatile partner in vision. *J Cell Sci Suppl, 17*, 189-195.

Boughman, J. A., Conneally, P. M., & Nance, W. E. (1980). Population genetic studies of retinitis pigmentosa. *Am J Hum Genet, 32*(2), 223-235.

Bowmaker, J. K., & Dartnall, H. J. (1980). Visual pigments of rods and cones in a human retina. *J Physiol, 298*, 501-511.

Brooks, M. J., Rajasimha, H. K., Roger, J. E., & Swaroop, A. (2011). Next-generation sequencing facilitates quantitative analysis of wild-type and Nrl($^{-/-}$) retinal transcriptomes. *Mol Vis, 17*, 3034-3054.

Canola, K., Angenieux, B., Tekaya, M., Quiambao, A., Naash, M. I., Munier, F. L., . . . Arsenijevic, Y. (2007). Retinal stem cells transplanted into models of late stages of retinitis pigmentosa preferentially adopt a glial or a retinal ganglion cell fate. *Invest Ophthalmol Vis Sci, 48*(1), 446-454. doi: 10.1167/iovs.06-0190

Carr, A. J., Vugler, A., Lawrence, J., Chen, L. L., Ahmado, A., Chen, F. K., . . . Coffey, P. J. (2009). Molecular characterization and functional analysis of phagocytosis by human embryonic stem cell-derived RPE cells using a novel human retinal assay. *Mol Vis, 15*, 283-295.

Chacko, D. M., Rogers, J. A., Turner, J. E., & Ahmad, I. (2000). Survival and differentiation of cultured retinal progenitors transplanted in the subretinal space of the rat. *Biochem Biophys Res Commun, 268*(3), 842-846. doi: 10.1006/bbrc.2000.2153

Chang, B., Grau, T., Dangel, S., Hurd, R., Jurklies, B., Sener, E. C., . . . Wissinger, B. (2009). A homologous genetic basis of the murine cpfl1 mutant and human

achromatopsia linked to mutations in the PDE6C gene. *Proc Natl Acad Sci U S A, 106*(46), 19581-19586. doi: 10.1073/pnas.0907720106

Corbo, J. C., & Cepko, C. L. (2005). A hybrid photoreceptor expressing both rod and cone genes in a mouse model of enhanced S-cone syndrome. *PLoS Genet, 1*(2), e11. doi: 10.1371/journal.pgen.0010011

Corbo, J. C., Myers, C. A., Lawrence, K. A., Jadhav, A. P., & Cepko, C. L. (2007). A typology of photoreceptor gene expression patterns in the mouse. *Proc Natl Acad Sci U S A, 104*(29), 12069-12074. doi: 10.1073/pnas.0705465104

Cronin, T., Leveillard, T., & Sahel, J. A. (2007). Retinal degenerations: from cell signaling to cell therapy; pre-clinical and clinical issues. *Curr Gene Ther, 7*(2), 121-129.

Curcio, C. A., Sloan, K. R., Kalina, R. E., & Hendrickson, A. E. (1990). Human photoreceptor topography. *J Comp Neurol, 292*(4), 497-523. doi: 10.1002/cne.902920402

Daniele, L. L., Lillo, C., Lyubarsky, A. L., Nikonov, S. S., Philp, N., Mears, A. J., . . . Pugh, E. N., Jr. (2005). Cone-like morphological, molecular, and electrophysiological features of the photoreceptors of the Nrl knockout mouse. *Invest Ophthalmol Vis Sci, 46*(6), 2156-2167. doi: 10.1167/iovs.04-1427

Dobelle, W. H. (2000). Artificial vision for the blind by connecting a television camera to the visual cortex. *ASAIO J, 46*(1), 3-9.

Drenser, K. A., Timmers, A. M., Hauswirth, W. W., & Lewin, A. S. (1998). Ribozyme-targeted destruction of RNA associated with autosomal-dominant retinitis pigmentosa. *Invest Ophthalmol Vis Sci, 39*(5), 681-689.

Duret, F., Brelen, M. E., Lambert, V., Gerard, B., Delbeke, J., & Veraart, C. (2006). Object localization, discrimination, and grasping with the optic nerve visual prosthesis. *Restor Neurol Neurosci, 24*(1), 31-40.

Eberle, D., Schubert, S., Postel, K., Corbeil, D., & Ader, M. (2011). Increased integration of transplanted CD73-positive photoreceptor precursors into adult mouse retina. *Invest Ophthalmol Vis Sci, 52*(9), 6462-6471. doi: 10.1167/iovs.11-7399

Farrar, G. J., Kenna, P. F., & Humphries, P. (2002). On the genetics of retinitis pigmentosa and on mutation-independent approaches to therapeutic intervention. *EMBO J, 21*(5), 857-864. doi: 10.1093/emboj/21.5.857

Fine, S. L., Berger, J. W., Maguire, M. G., & Ho, A. C. (2000). Age-related macular degeneration. *N Engl J Med, 342*(7), 483-492. doi: 10.1056/NEJM200002173420707

Foster, R. G., Provencio, I., Hudson, D., Fiske, S., De Grip, W., & Menaker, M. (1991). Circadian photoreception in the retinally degenerate mouse (rd/rd). *J Comp Physiol A, 169*(1), 39-50.

Foundation Fighting Blindness (2014). Retinitis Pigmentosa ~ Overview. Retrieved April 28, 2014, 2014, from http://www.ffb.ca/eye_conditions/rp_center.html

Fu, Y., & Yau, K. W. (2007). Phototransduction in mouse rods and cones. *Pflugers Arch, 454*(5), 805-819. doi: 10.1007/s00424-006-0194-y

Fuhrmann, S., Levine, E. M., & Reh, T. A. (2000). Extraocular mesenchyme patterns the optic vesicle during early eye development in the embryonic chick. *Development, 127*(21), 4599-4609.

Furukawa, T., Morrow, E. M., Li, T., Davis, F. C., & Cepko, C. L. (1999). Retinopathy and attenuated circadian entrainment in Crx-deficient mice. *Nat Genet, 23*(4), 466-470. doi: 10.1038/70591

Ghosh, F., Arner, K., & Ehinger, B. (1998). Transplant of full-thickness embryonic rabbit retina using pars plana vitrectomy. *Retina, 18*(2), 136-142.

Ghosh, F., Juliusson, B., Arner, K., & Ehinger, B. (1999). Partial and full-thickness neuroretinal transplants. *Exp Eye Res, 68*(1), 67-74. doi: 10.1006/exer.1998.0582

Hageman, G. S. (2011). *Webvision* H. Kolb, R. Nelson, E. Fernandez & B. Jones (Eds.), *The Organization of the Retina and Visual System* Retrieved from http://webvision.med.utah.edu/book/

Haim, M. (2002). Epidemiology of retinitis pigmentosa in Denmark. *Acta Ophthalmol Scand Suppl*(233), 1-34.

Hao, H., Kim, D. S., Klocke, B., Johnson, K. R., Cui, K., Gotoh, N., . . . Swaroop, A. (2012). Transcriptional regulation of rod photoreceptor homeostasis revealed by in vivo NRL targetome analysis. *PLoS Genet, 8*(4), e1002649. doi: 10.1371/journal.pgen.1002649

Hartong, D. T., Berson, E. L., & Dryja, T. P. (2006). Retinitis pigmentosa. *Lancet, 368*(9549), 1795-1809. doi: 10.1016/S0140-6736(06)69740-7

Hauswirth, W. W., Aleman, T. S., Kaushal, S., Cideciyan, A. V., Schwartz, S. B., Wang, L., . . . Jacobson, S. G. (2008). Treatment of leber congenital amaurosis due to RPE65 mutations by ocular subretinal injection of adeno-associated virus gene vector: short-term results of a phase I trial. *Hum Gene Ther, 19*(10), 979-990. doi: 10.1089/hum.2008.107

Hendrickson, A., Bumsted-O'Brien, K., Natoli, R., Ramamurthy, V., Possin, D., & Provis, J. (2008). Rod photoreceptor differentiation in fetal and infant human retina. *Exp Eye Res, 87*(5), 415-426. doi: 10.1016/j.exer.2008.07.016

Humayun, M. S., Dorn, J. D., de Cruz, L., Dagnelie, G., Sahel, J. A., Stanga, P. E., . . . Greenberg, R. J. (2012). Interim results from the international trial of Second Sight's visual prosthesis. *Opthalmology, 119*(4), 779-788. doi: 10.1016/j.ophtha.2011.09.028

Jia, L., Oh, E. C., Ng, L., Srinivas, M., Brooks, M., Swaroop, A., & Forrest, D. (2009). Retinoid-related orphan nuclear receptor RORbeta is an early-acting factor in rod photoreceptor development. *Proc Natl Acad Sci U S A, 106*(41), 17534-17539. doi: 10.1073/pnas.0902425106

Jones, B. W., Watt, C. B., Frederick, J. M., Baehr, W., Chen, C. K., Levine, E. M., . . . Marc, R. E. (2003). Retinal remodeling triggered by photoreceptor degenerations. *J Comp Neurol, 464*(1), 1-16. doi: 10.1002/cne.10703

Kelley, M. W., Turner, J. K., & Reh, T. A. (1995). Ligands of steroid/thyroid receptors induce cone photoreceptors in vertebrate retina. *Development, 121*(11), 3777-3785.

Koike, C., Nishida, A., Ueno, S., Saito, H., Sanuki, R., Sato, S., . . . Furukawa, T. (2007). Functional roles of Otx2 transcription factor in postnatal mouse retinal development. *Mol Cell Biol, 27*(23), 8318-8329. doi: 10.1128/MCB.01209-07

Kolb, H. (2011). *Webvision* H. Kolb, R. Nelson, E. Fernandez & B. Jones (Eds.), *The Organization of the Retina and Visual System* Retrieved from http://webvision.med.utah.edu/book/

Lagali, P. S., Balya, D., Awatramani, G. B., Munch, T. A., Kim, D. S., Busskamp, V., . . . Roska, B. (2008). Light-activated channels targeted to ON bipolar cells restore visual function in retinal degeneration. *Nat Neurosci, 11*(6), 667-675. doi: 10.1038/nn.2117

Lakowski, J., Baron, M., Bainbridge, J., Barber, A. C., Pearson, R. A., Ali, R. R., & Sowden, J. C. (2010). Cone and rod photoreceptor transplantation in models of the childhood retinopathy Leber congenital amaurosis using flow-sorted Crx-positive donor cells. *Hum Mol Genet, 19*(23), 4545-4559. doi: 10.1093/hmg/ddq378

Lakowski, J., Han, Y. T., Pearson, R. A., Gonzalez-Cordero, A., West, E. L., Gualdoni, S., . . . Sowden, J. C. (2011). Effective transplantation of photoreceptor precursor cells selected via cell surface antigen expression. *Stem Cells, 29*(9), 1391-1404. doi: 10.1002/stem.694

Le, Y. Z., Ash, J. D., Al-Ubaidi, M. R., Chen, Y., Ma, J. X., & Anderson, R. E. (2004). Targeted expression of Cre recombinase to cone photoreceptors in transgenic mice. *Mol Vis, 10*, 1011-1018.

Leveillard, T., Mohand-Said, S., Lorentz, O., Hicks, D., Fintz, A. C., Clerin, E., . . . Sahel, J. A. (2004). Identification and characterization of rod-derived cone viability factor. *Nat Genet, 36*(7), 755-759. doi: 10.1038/ng1386

Li, L. X., & Turner, J. E. (1988). Inherited retinal dystrophy in the RCS rat: prevention of photoreceptor degeneration by pigment epithelial cell transplantation. *Exp Eye Res, 47*(6), 911-917.

Lopez, R., Gouras, P., Kjeldbye, H., Sullivan, B., Reppucci, V., Brittis, M., . . . Goluboff, E. (1989). Transplanted retinal pigment epithelium modifies the retinal degeneration in the RCS rat. *Invest Ophthalmol Vis Sci, 30*(3), 586-588.

Lu, A., Ng, L., Ma, M., Kefas, B., Davies, T. F., Hernandez, A., . . . Forrest, D. (2009). Retarded developmental expression and patterning of retinal cone opsins in hypothyroid mice. *Endocrinology, 150*(3), 1536-1544. doi: 10.1210/en.2008-1092

Lund, R. D., Adamson, P., Sauve, Y., Keegan, D. J., Girman, S. V., Wang, S., . . . Greenwood, J. (2001). Subretinal transplantation of genetically modified human cell lines attenuates loss of visual function in dystrophic rats. *Proc Natl Acad Sci U S A, 98*(17), 9942-9947. doi: 10.1073/pnas.171266298

MacLaren, R. E., Pearson, R. A., MacNeil, A., Douglas, R. H., Salt, T. E., Akimoto, M., . . . Ali, R. R. (2006). Retinal repair by transplantation of photoreceptor precursors. *Nature, 444*(7116), 203-207. doi: 10.1038/nature05161

Macrae, W. G. (1982). Retinitis pigmentosa in Ontario - a survey. *Birth Defects Orig Artic Ser, 18*(6), 175-185.

Maguire, A. M., Simonelli, F., Pierce, E. A., Pugh, E. N., Jr., Mingozzi, F., Bennicelli, J., . . . Bennett, J. (2008). Safety and efficacy of gene transfer for Leber's congenital amaurosis. *N Engl J Med, 358*(21), 2240-2248. doi: 10.1056/NEJMoa0802315

Marc, R. E., Jones, B. W., Watt, C. B., & Strettoi, E. (2003). Neural remodeling in retinal degeneration. *Prog Retin Eye Res, 22*(5), 607-655.

Marieb, E. N., & Hoehn, K. (2007) *Human Anatomy & Physiology* (7th ed. ed.). San Francisco: Pearson Education, Inc.

Mattapallil, M. J., Wawrousek, E. F., Chan, C. C., Zhao, H., Roychoudhury, J., Ferguson, T. A., & Caspi, R. R. (2012). The Rd8 mutation of the Crb1 gene is present in vendor lines of C57BL/6N mice and embryonic stem cells, and confounds ocular induced mutant phenotypes. *Invest Ophthalmol Vis Sci, 53*(6), 2921-2927. doi: 10.1167/iovs.12-9662

Mears, A. J., Kondo, M., Swain, P. K., Takada, Y., Bush, R. A., Saunders, T. L., . . . Swaroop, A. (2001). Nrl is required for rod photoreceptor development. *Nat Genet, 29*(4), 447-452. doi: 10.1038/ng774

Mitton, K. P., Swain, P. K., Chen, S., Xu, S., Zack, D. J., & Swaroop, A. (2000). The leucine zipper of NRL interacts with the CRX homeodomain. A possible mechanism of transcriptional synergy in rhodopsin regulation. *J Biol Chem, 275*(38), 29794-29799. doi: 10.1074/jbc.M003658200

Mohand-Said, S., Deudon-Combe, A., Hicks, D., Simonutti, M., Forster, V., Fintz, A. C., . . . Sahel, J. A. (1998). Normal retina releases a diffusible factor stimulating cone

survival in the retinal degeneration mouse. *Proc Natl Acad Sci U S A, 95*(14), 8357-8362.

National Coalition for Vision Health (2007). Foundations for a Canadian Vision Health Strategy.

Ng, L., Ma, M., Curran, T., & Forrest, D. (2009). Developmental expression of thyroid hormone receptor beta2 protein in cone photoreceptors in the mouse. *Neuroreport, 20*(6), 627-631. doi: 10.1097/WNR.0b013e32832a2c63

Nishida, A., Furukawa, A., Koike, C., Tano, Y., Aizawa, S., Matsuo, I., & Furukawa, T. (2003). Otx2 homeobox gene controls retinal photoreceptor cell fate and pineal gland development. *Nat Neurosci, 6*(12), 1255-1263. doi: 10.1038/nn1155

Oh, E. C., Khan, N., Novelli, E., Khanna, H., Strettoi, E., & Swaroop, A. (2007). Transformation of cone precursors to functional rod photoreceptors by bZIP transcription factor NRL. *Proc Natl Acad Sci U S A, 104*(5), 1679-1684. doi: 10.1073/pnas.0605934104

Omri, S., Omri, B., Savoldelli, M., Jonet, L., Thillaye-Goldenberg, B., Thuret, G., . . . Behar-Cohen, F. (2010). The outer limiting membrane (OLM) revisited: clinical implications. *Clin Ophthalmol, 4*, 183-195.

Osterberg, G. (1935). Topography of the layer of rods and cones in the human retina. *Acta Ophthal Suppl, 6*, 1–103.

Pauleikhoff, D., Harper, C. A., Marshall, J., & Bird, A. C. (1990). Aging changes in Bruch's membrane. A histochemical and morphologic study. *Ophthalmology, 97*(2), 171-178.

Pearson, R. A., Barber, A. C., Rizzi, M., Hippert, C., Xue, T., West, E. L., . . . Ali, R. R. (2012). Restoration of vision after transplantation of photoreceptors. *Nature, 485*(7396), 99-103. doi: 10.1038/nature10997

Pearson, R. A., Barber, A. C., West, E. L., MacLaren, R. E., Duran, Y., Bainbridge, J. W., . . . Ali, R. R. (2010). Targeted disruption of outer limiting membrane junctional proteins (Crb1 and ZO-1) increases integration of transplanted photoreceptor precursors into the adult wild-type and degenerating retina. *Cell Transplant, 19*(4), 487-503. doi: 10.3727/096368909X486057

Perlman, I. (2014). *Webvision* H. Kolb, R. Nelson, E. Fernandez & B. Jones (Eds.), *The Electroretinogram: ERG* Retrieved from http://webvision.med.utah.edu/book/electrophysiology/the-electroretinogram-erg/

Punzo, C., Kornacker, K., & Cepko, C. L. (2009). Stimulation of the insulin/mTOR pathway delays cone death in a mouse model of retinitis pigmentosa. *Nat Neurosci, 12*(1), 44-52. doi: 10.1038/nn.2234

Qiu, G., Seiler, M. J., Mui, C., Arai, S., Aramant, R. B., de Juan, E., Jr., & Sadda, S. (2005). Photoreceptor differentiation and integration of retinal progenitor cells transplanted into transgenic rats. *Exp Eye Res, 80*(4), 515-525. doi: 10.1016/j.exer.2004.11.001

Radtke, N. D., Aramant, R. B., Petry, H. M., Green, P. T., Pidwell, D. J., & Seiler, M. J. (2008). Vision improvement in retinal degeneration patients by implantation of retina together with retinal pigment epithelium. *Am J Ophthalmol, 146*(2), 172-182. doi: 10.1016/j.ajo.2008.04.009

Radtke, N. D., Seiler, M. J., Aramant, R. B., Petry, H. M., & Pidwell, D. J. (2002). Transplantation of intact sheets of fetal neural retina with its retinal pigment epithelium in retinitis pigmentosa patients. *Am J Ophthalmol, 133*(4), 544-550.

Sakaguchi, D. S., Van Hoffelen, S. J., Theusch, E., Parker, E., Orasky, J., Harper, M. M., . . . Young, M. J. (2004). Transplantation of neural progenitor cells into the developing retina of the Brazilian opossum: an in vivo system for studying stem/progenitor cell plasticity. *Dev Neurosci, 26*(5-6), 336-345. doi: 10.1159/000082275

Sauve, Y., Girman, S. V., Wang, S., Keegan, D. J., & Lund, R. D. (2002). Preservation of visual responsiveness in the superior colliculus of RCS rats after retinal pigment epithelium cell transplantation. *Neuroscience, 114*(2), 389-401.

Science, P. (2014). Fovea (Vol. 2014).

Seiler, M. J., & Aramant, R. B. (2012). Cell replacement and visual restoration by retinal sheet transplants. *Prog Retin Eye Res, 31*(6), 661-687. doi: 10.1016/j.preteyeres.2012.06.003

Seiler, M. J., Aramant, R. B., Thomas, B. B., Peng, Q., Sadda, S. R., & Keirstead, H. S. (2010). Visual restoration and transplant connectivity in degenerate rats implanted

with retinal progenitor sheets. *Eur J Neurosci, 31*(3), 508-520. doi: 10.1111/j.1460-9568.2010.07085.x

Seiler, M. J., Thomas, B. B., Chen, Z., Wu, R., Sadda, S. R., & Aramant, R. B. (2008). Retinal transplants restore visual responses: trans-synaptic tracing from visually responsive sites labels transplant neurons. *Eur J Neurosci, 28*(1), 208-220. doi: 10.1111/j.1460-9568.2008.06279.x

Shintani, K., Shechtman, D. L., & Gurwood, A. S. (2009). Review and update: current treatment trends for patients with retinitis pigmentosa. *Optometry, 80*(7), 384-401. doi: 10.1016/j.optm.2008.01.026

Silverman, M. S., & Hughes, S. E. (1989). Transplantation of photoreceptors to light-damaged retina. *Invest Ophthalmol Vis Sci, 30*(8), 1684-1690.

Singh, M. S., Charbel Issa, P., Butler, R., Martin, C., Lipinski, D. M., Sekaran, S., . . . MacLaren, R. E. (2013). Reversal of end-stage retinal degeneration and restoration of visual function by photoreceptor transplantation. *Proc Natl Acad Sci U S A, 110*(3), 1101-1106. doi: 10.1073/pnas.1119416110

Steenhuysen, J. (2013). FDA approves first retinal implant for rare eye disease, *Reuters*. Retrieved from http://www.reuters.com/article/2013/02/14/us-secondsight-fda-eyeimplant-idUSBRE91D1AK20130214

Steinberg, R. H., Fisher, S. K., & Anderson, D. H. (1980). Disc morphogenesis in vertebrate photoreceptors. *J Comp Neurol, 190*(3), 501-508. doi: 10.1002/cne.901900307

Strauss, O. (2005). The retinal pigment epithelium in visual function. *Physiol Rev, 85*(3), 845-881. doi: 10.1152/physrev.00021.2004

Strauss, O. (2011). *Webvision* H. Kolb, R. Nelson, E. Fernandez & B. Jones (Eds.), *The Organization of the Retina and Visual System* Retrieved from http://webvision.med.utah.edu/book/

Strettoi, E., & Pignatelli, V. (2000). Modifications of retinal neurons in a mouse model of retinitis pigmentosa. *Proc Natl Acad Sci U S A, 97*(20), 11020-11025. doi: 10.1073/pnas.190291097

Sunness, J. S. (1999). The natural history of geographic atrophy, the advanced atrophic form of age-related macular degeneration. *Mol Vis, 5*, 25.

Swain, P. K., Hicks, D., Mears, A. J., Apel, I. J., Smith, J. E., John, S. K., . . . Swaroop, A. (2001). Multiple phosphorylated isoforms of NRL are expressed in rod photoreceptors. *J Biol Chem, 276*(39), 36824-36830. doi: 10.1074/jbc.M105855200

Swaroop, A., Kim, D., & Forrest, D. (2010). Transcriptional regulation of photoreceptor development and homeostasis in the mammalian retina. *Nat Rev Neurosci, 11*(8), 563-576. doi: 10.1038/nrn2880

Takahashi, M., Palmer, T. D., Takahashi, J., & Gage, F. H. (1998). Widespread integration and survival of adult-derived neural progenitor cells in the developing optic retina. *Mol Cell Neurosci, 12*(6), 340-348. doi: 10.1006/mcne.1998.0721

Thiadens, A. A., den Hollander, A. I., Roosing, S., Nabuurs, S. B., Zekveld-Vroon, R. C., Collin, R. W., . . . Klaver, C. C. (2009). Homozygosity mapping reveals PDE6C mutations in patients with early-onset cone photoreceptor disorders. *Am J Hum Genet, 85*(2), 240-247. doi: 10.1016/j.ajhg.2009.06.016

Turner, D. L., & Cepko, C. L. (1987). A common progenitor for neurons and glia persists in rat retina late in development. *Nature, 328*(6126), 131-136. doi: 10.1038/328131a0

Turner, D. L., Snyder, E. Y., & Cepko, C. L. (1990). Lineage-independent determination of cell type in the embryonic mouse retina. *Neuron, 4*(6), 833-845.

U. S. National Institutes of Health. (2014). Safety and Efficacy Study of rAAV.sFlt-1 in Patients With Exudative Age-Related Macular Degeneration (AMD). Retrieved April 27, 2014, 2014, from http://clinicaltrials.gov/ct2/show/NCT01494805

Veraart, C., Raftopoulos, C., Mortimer, J. T., Delbeke, J., Pins, D., Michaux, G., . . . Wanet-Defalque, M. C. (1998). Visual sensations produced by optic nerve stimulation using an implanted self-sizing spiral cuff electrode. *Brain Res, 813*(1), 181-186.

Vugler, A., Carr, A. J., Lawrence, J., Chen, L. L., Burrell, K., Wright, A., . . . Coffey, P. (2008). Elucidating the phenomenon of HESC-derived RPE: anatomy of cell

genesis, expansion and retinal transplantation. *Exp Neurol, 214*(2), 347-361. doi: 10.1016/j.expneurol.2008.09.007

Wallace, V. A. (2011). Concise review: making a retina--from the building blocks to clinical applications. *Stem Cells, 29*(3), 412-417. doi: 10.1002/stem.602

Wert, K. J., Davis, R. J., Sancho-Pelluz, J., Nishina, P. M., & Tsang, S. H. (2013). Gene therapy provides long-term visual function in a pre-clinical model of retinitis pigmentosa. *Hum Mol Genet, 22*(3), 558-567. doi: 10.1093/hmg/dds466

West, E. L., Pearson, R. A., Barker, S. E., Luhmann, U. F., Maclaren, R. E., Barber, A. C., . . . Ali, R. R. (2010). Long-term survival of photoreceptors transplanted into the adult murine neural retina requires immune modulation. *Stem Cells, 28*(11), 1997-2007. doi: 10.1002/stem.520

West, E. L., Pearson, R. A., Tschernutter, M., Sowden, J. C., MacLaren, R. E., & Ali, R. R. (2008). Pharmacological disruption of the outer limiting membrane leads to increased retinal integration of transplanted photoreceptor precursors. *Exp Eye Res, 86*(4), 601-611. doi: 10.1016/j.exer.2008.01.004

Wetts, R., & Fraser, S. E. (1988). Multipotent precursors can give rise to all major cell types of the frog retina. *Science, 239*(4844), 1142-1145.

Woch, G., Aramant, R. B., Seiler, M. J., Sagdullaev, B. T., & McCall, M. A. (2001). Retinal transplants restore visually evoked responses in rats with photoreceptor degeneration. *Invest Ophthalmol Vis Sci, 42*(7), 1669-1676.

World Health Organization (2014). Causes of blindness and visual impairment. Retrieved April 10, 2014, 2014, from http://www.who.int/blindness/causes/en/

Wright, A. F., Chakarova, C. F., Abd El-Aziz, M. M., & Bhattacharya, S. S. (2010). Photoreceptor degeneration: genetic and mechanistic dissection of a complex trait. *Nat Rev Genet, 11*(4), 273-284. doi: 10.1038/nrg2717

Wyatt, J., & Rizzo, J. (1996). Ocular implants for the blind *Spectrum, IEEE, 33*(5), 47-53. doi: 10.1109/6.490056

Yao, J., Feathers, K. L., Khanna, H., Thompson, D., Tsilfidis, C., Hauswirth, W. W., . . . Zacks, D. N. (2011). XIAP therapy increases survival of transplanted rod

precursors in a degenerating host retina. *Invest Ophthalmol Vis Sci, 52*(3), 1567-1572. doi: 10.1167/iovs.10-5998

Young, R. W. (1971). The renewal of rod and cone outer segments in the rhesus monkey. *J Cell Biol, 49*(2), 303-318.

Young, R. W. (1976). Visual cells and the concept of renewal. *Invest Ophthalmol Vis Sci, 15*(9), 700-725.

Young, R. W. (1985). Cell differentiation in the retina of the mouse. *Anat Rec, 212*(2), 199-205. doi: 10.1002/ar.1092120215

Zhang, X. M., Sheng, S. R., Wang, X. Y., Bin, L. H., Wang, J. R., & Li, G. Y. (2004). Expression of tumor related gene NAG6 in gastric cancer and restriction fragment length polymorphism analysis. *World J Gastroenterol, 10*(9), 1361-1364.

Zrenner, E., Bartz-Schmidt, K. U., Benav, H., Besch, D., Bruckmann, A., Gabel, V. P., . . . Wilke, R. (2011). Subretinal electronic chips allow blind patients to read letters and combine them to words. *Proc Biol Sci, 278*(1711), 1489-1497. doi: 10.1098/rspb.2010.1747

Appendix I: Interaction between *Nrl* and *Ccdc136* causing rescue of rosettes in *Nrl*$^{-/-}$ mice

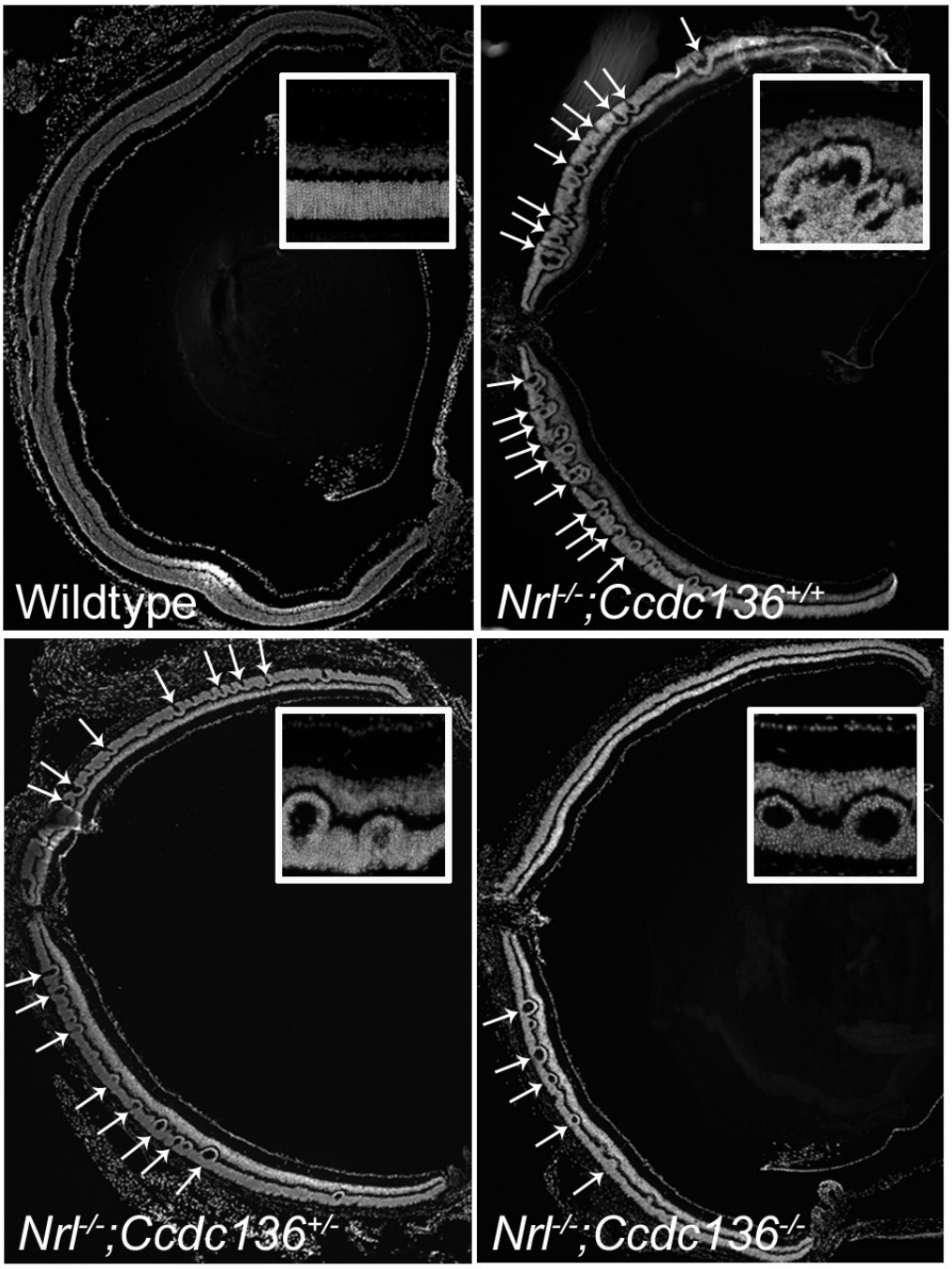

Figure 1 Rosettes in adult *Ccdc136*$^{-/-}$ retinas on a *Nrl*$^{-/-}$ background. Sections of whole retinas. Wildtype retina shows normal morphology. Rosettes (arrowheads) are seen in the *Nrl*$^{-/-}$*;Ccdc136*$^{+/+}$, *Nrl*$^{-/-}$*;Ccdc136*$^{+/-}$ and *Nrl*$^{-/-}$*;Ccdc136*$^{-/-}$ retinas. Insets show high magnification of rosettes.

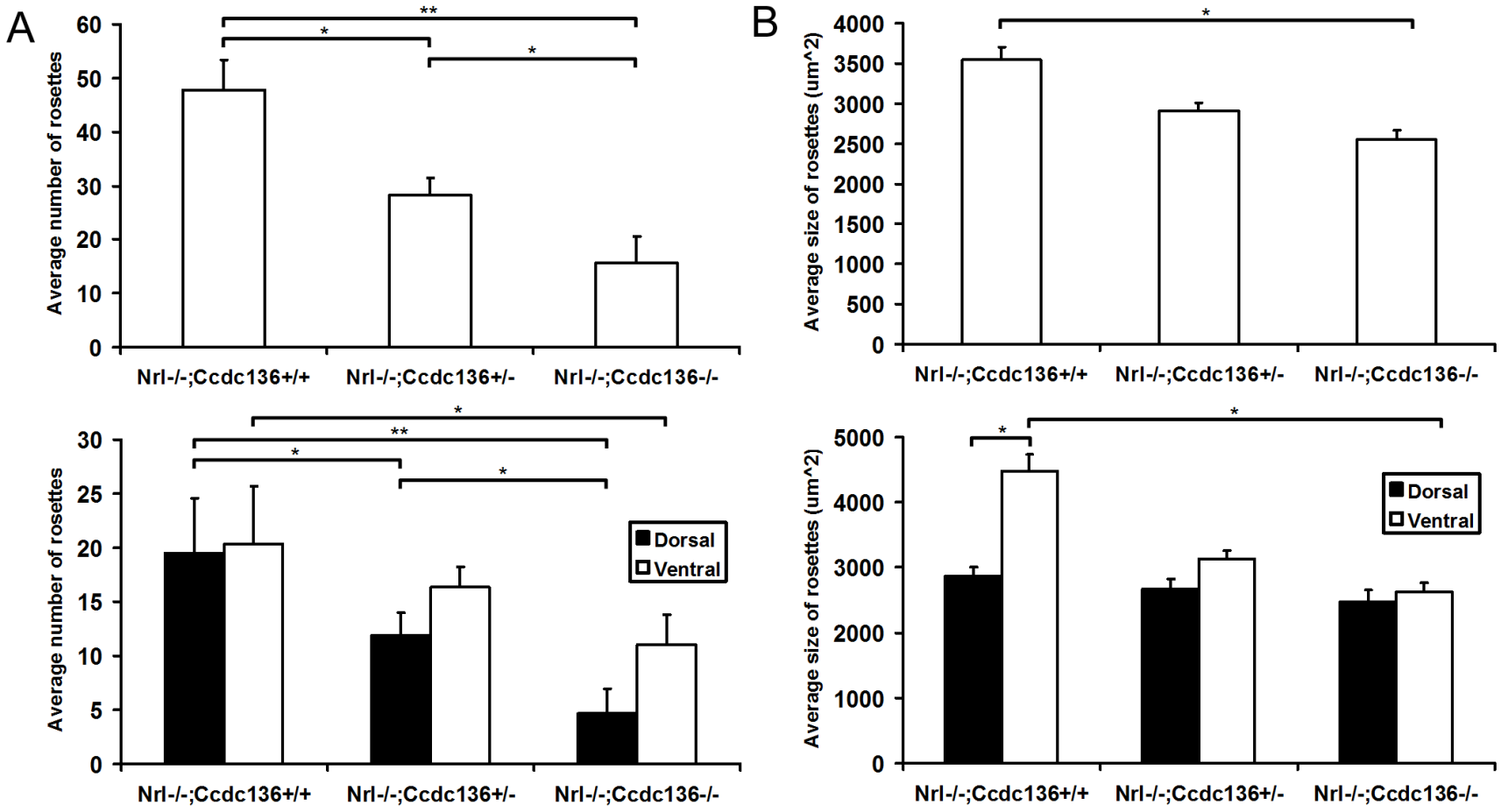
A
B
Average number of rosettes
Average size of rosettes (um^2)
Nrl-/-;Ccdc136+/+
Nrl-/-;Ccdc136+/-
Nrl-/-;Ccdc136-/-
Dorsal
Ventral
*
**

Figure 2 Quantification of rosettes in adult *Ccdc136*$^{-/-}$ retinas on a *Nrl*$^{-/-}$ background Rosette number (A) and size (B) in sections taken at the level of the optic nerve head. Counts from entire retina (top) and dorsal versus ventral retina (bottom). Counts are average values ± SEM. sample size, n=5 for each genotype; *, $p<0.05$; **, $p<0.01$.

Appendix II: Loss of Ccdc136 leads to downregulation of PDE6C

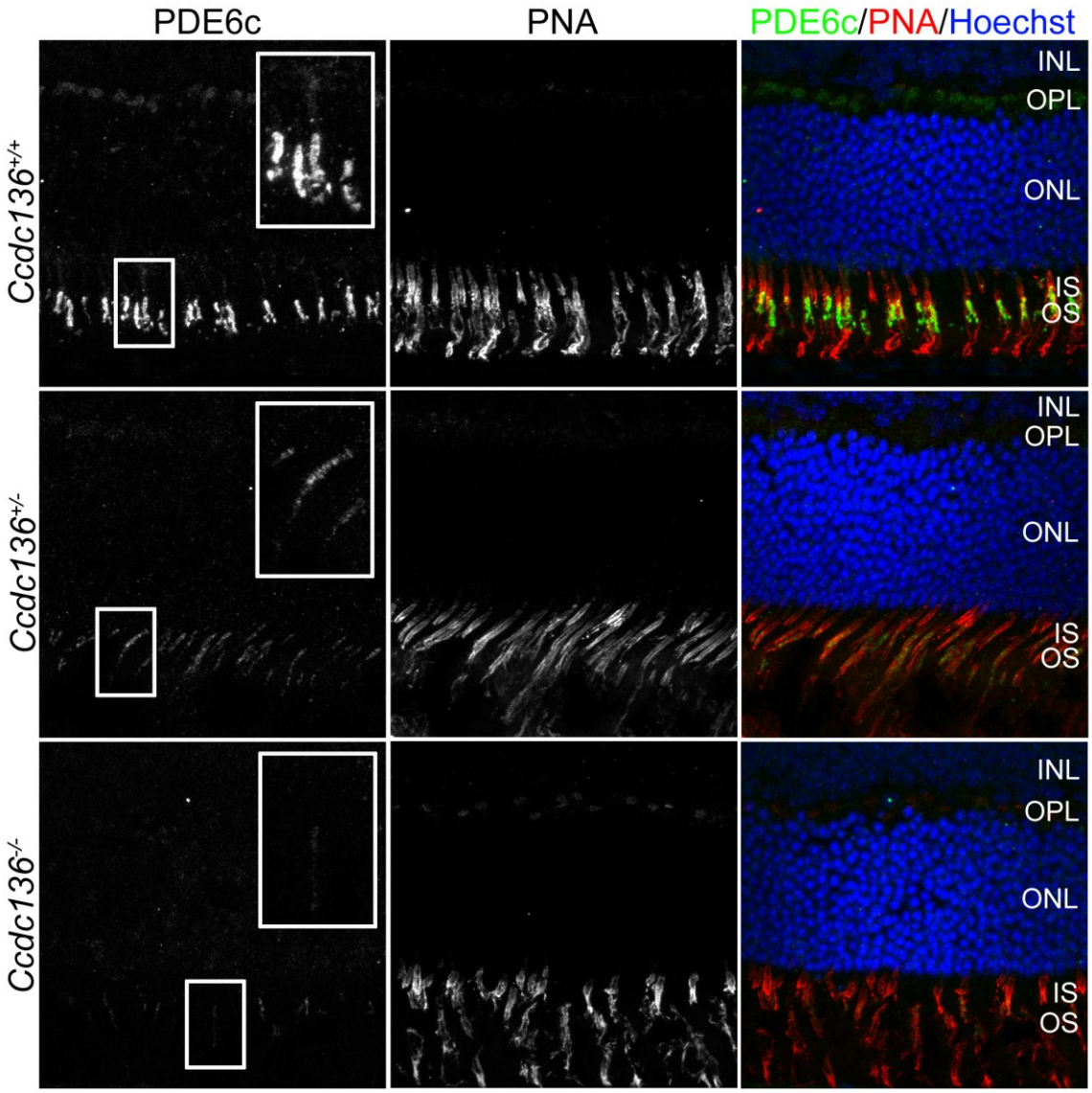

Figure 1 Expression of PDE6c in *Ccdc136*$^{-/-}$ retinas. IHC analysis for PDE6c and PNA expression in retinas of mice of the indicated genotypes. Note the localization of PDE6c to the OS and PNA to IS and OS in cones. Insets show higher magnification images of OS. Merge shows PDE6c (green), PNA (red) and Hoechst nuclear stain (blue). INL, inner nuclear layer; OPL, outer plexiform layer; ONL, outer nuclear layer; IS, inner segments; OS, outer segments.

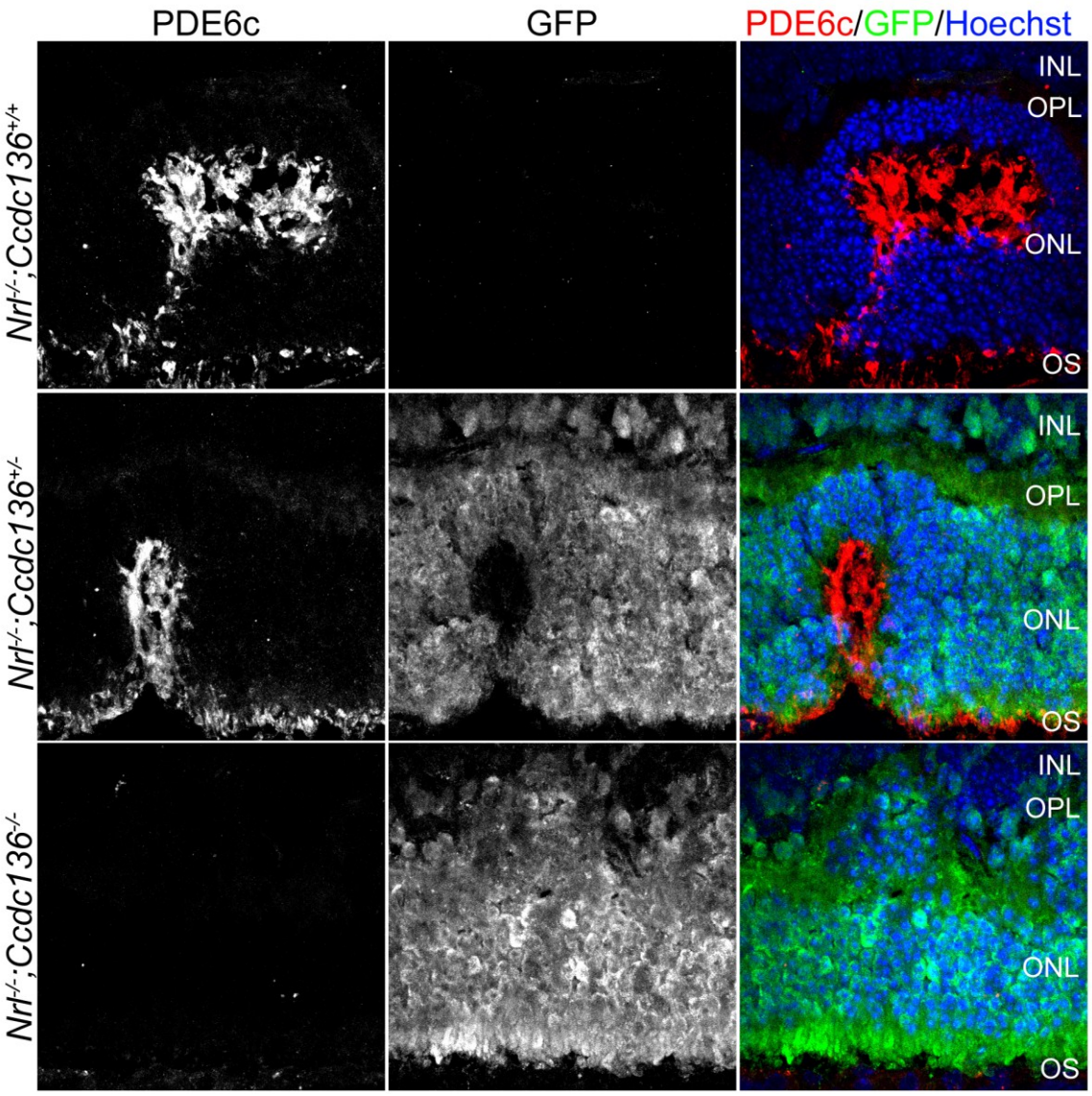

Figure 2 Expression of PDE6c in *Ccdc136*$^{-/-}$ retinas on an *Nrl*$^{-/-}$background. IHC analysis for PDE6c and GFP expression in retinas of mice of the indicated genotypes. Merge shows PDE6c (green), PNA (red) and Hoechst nuclear stain (blue). INL, inner nuclear layer; OPL, outer plexiform layer; ONL, outer nuclear layer; IS, inner segments; OS, outer segments.

Appendix III: Flow cytometric analysis of *Nrl*$^{-/-}$;*Ccdc136*$^{+/-}$ cells

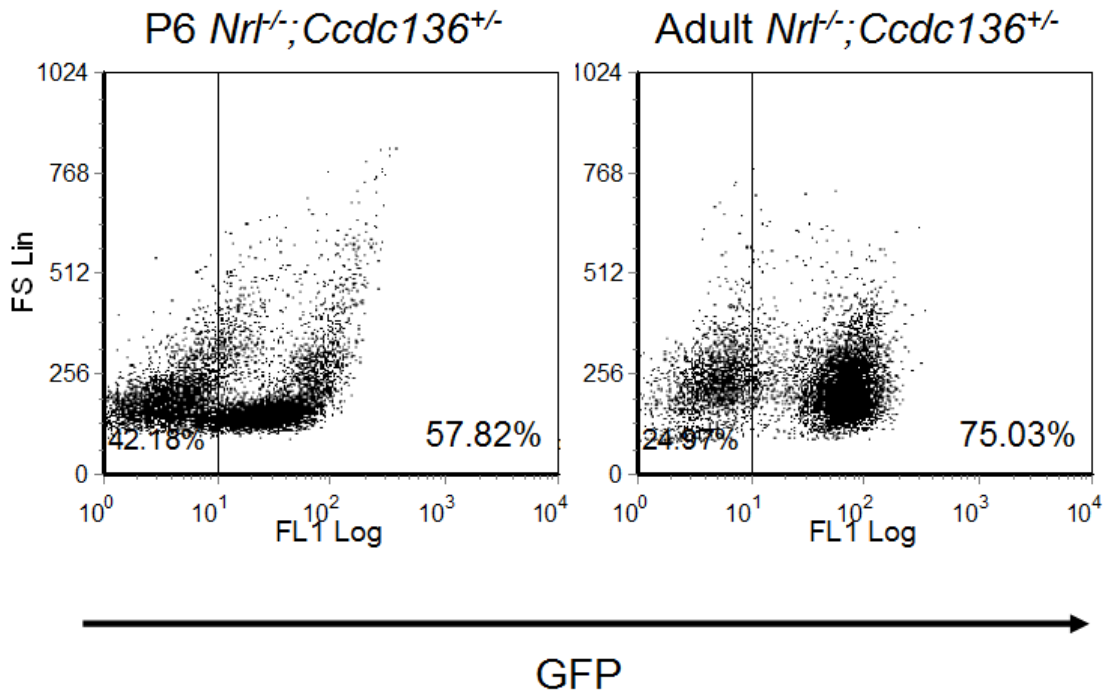

Figure 1 Flow cytometric analysis of GFP expression in P6 and adult *Nrl*$^{-/-}$;*Ccdc136*$^{+/-}$ donor cells. Representative dot plot patterns of GFP+ cells. Vertical lines mark the detection threshold for GFP signal. Right hand quadrants indicate percentage of total cells that are GFP+.

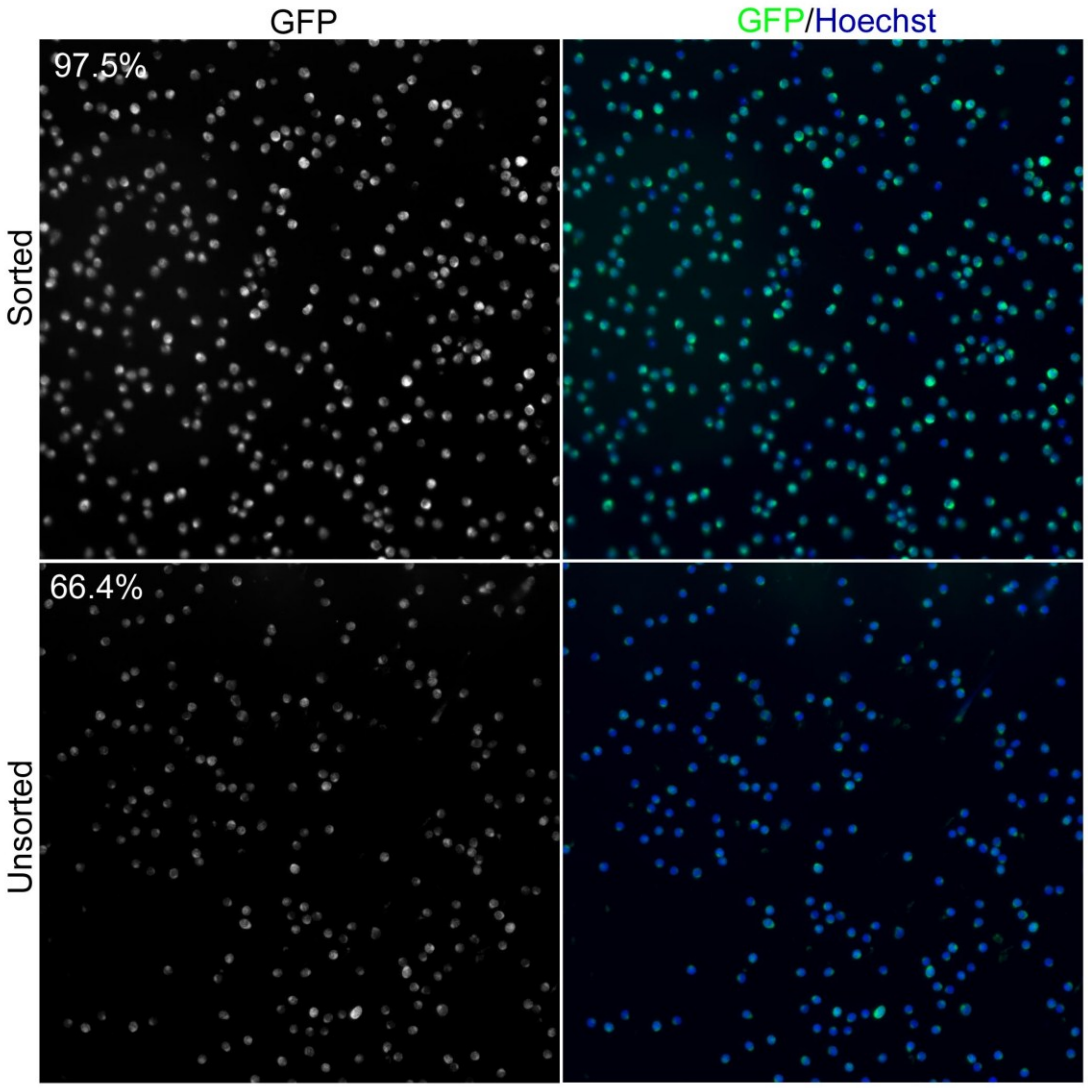

Figure 2 GFP+ cells enriched by fluorescence activated cell sorting (FACS) in P8 *Nrl*$^{-/-}$*;Ccdc136*$^{+/-}$ cells.